All Dissertations   Dissertations

12-1993

Modeling of Algal Productivity and Diel Oxygen Profiles in the Partitioned Aquaculture System

Caye M. Drapcho
Clemson University, cdrapch@clemson.edu

Recommended Citation

December 9, 1993

To the Graduate School:

This dissertation entitled "Modeling of Algal Productivity and Diel Oxygen Profiles in the Partitioned Aquaculture System" and written by Caye M. Drapcho is presented to the Graduate School of Clemson University. I recommend that it be accepted in partial fulfillment of the requirements for the degree of Doctor of Philosophy with a major in Agricultural Engineering.

_____

Dissertation Advisor

We have reviewed this dissertation
and recommend its acceptance:

_____

_____

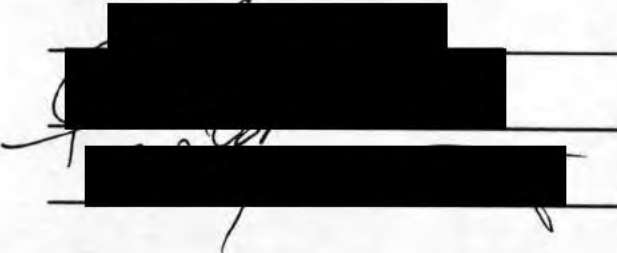Accepted for the Graduate School:

_____

MODELING OF ALGAL PRODUCTIVITY AND DIEL OXYGEN PROFILES

IN THE PARTITIONED AQUACULTURE SYSTEM

_____

A Dissertation

Presented to

the Graduate School of

Clemson University

_____

In Partial Fulfillment

of the Requirements for the Degree

Doctor of Philosophy

Agricultural Engineering

_____

by

Caye M. Drapcho

December 1993

ABSTRACT

Fish production in pond culture systems is often limited by the dissolved oxygen (DO) concentration. Algal biomass and productivity, which greatly impact the DO concentration, are difficult to control in traditional pond systems. The Partitioned Aquaculture System (PAS) was designed to increase fish production by managing algal productivity and DO through control of algal cell retention time, water depth, and mixing. The objectives of this study were 1) to determine impact of culture conditions on algal productivity, 2) develop a model of algal productivity and diel DO levels, and 3) to predict the maximum fish production attainable with the PAS.

For this study, algal cell retention time was controlled through continuous discharge of the culture. Algal productivity was calculated from algal biomass (measured with 0.45 µm filters), retention time and water depth. Oxygen production and respiration rates were measured using in-pond incubations.

Algal species composition was dependent on the inorganic carbon content of the culture water. The algal culture was comprised primarily of blue-green algae (*Cyanophyta*) at 0.7 mmol/l/d inorganic carbon addition rate, and green algae (*Chlorophyta*) at 1.1 and 1.8 mmol/l/d addition rates.

Algal productivity was 1.2 times greater for the 1.1 and 1.8 rates than for the 0.7 mmol/l/d inorganic carbon addition rate; 1.2 times greater for the 0.34 m than the 0.66 m water depth; 1.5 times greater for the 0.125 m/s than for the 0.0313 and 0.0625 m/s water velocity; and 1.3 times greater for the 1.2 day than the 2.5 day retention time.

Maximum oxygen production rates of 0.11 and 0.12 mg O_2/mg TSS/hr were achieved for blue-green and green algal cultures, respectively. Maximum DO concentrations of 25 - 30 mg/l were routinely observed.

The algal productivity and DO model constructed for the PAS incorporates an inhibitory light model for light-limited algal growth and the Monod model for carbon- and nitrogen-limited growth. Steady state and dynamic simulations of the DO profile as a function of the design and environmental conditions closely matched the observed values. Maximum fish production of 10,000 kg/ha is predicted for light-limited cultures in the PAS operated at 0.0313 m/s water velocity, 20 hour retention time and 0.6 m water depth.

ACKNOWLEDGEMENTS

I would like to express my appreciation to my advisor, Dr. David Brune, for his guidance in this research and for his part in making my graduate work rewarding and enjoyable. I would like to thank the members of my committee, Dr. A. Ray Abernathy, Dr. John Collier, and Dr. Arnie Eversole, for their advice, insights and review of my dissertation. I would also like to thank Mr. Scott Davis for the algal identification work and for assisting with the construction and maintenance of the research system.

Finally, I would like to offer a special thanks to my parents, Cyril and Catherine Drapcho, my family, and my friend, Tony Ambrose, for all of their encouragement and support.

TABLE OF CONTENTS

Table of Contents (Continued)

Table of Contents (Continued)

LIST OF TABLES

List of Tables (Continued)

LIST OF FIGURES

List of Figures (continued)

CHAPTER I

INTRODUCTION

Conventional catfish culture in the United States is characterized by extensive pond systems in which minimal control of algal biomass or algal productivity is attempted or achieved. Algal growth in these systems occurs primarily as result of nutrient inputs from fish metabolic wastes and decay of uneaten fish food. Fish production is often dependent on the minimum dissolved oxygen (DO) concentration in the pond. The minimum DO which typically occurs in the early morning is caused primarily by the combined respiration of fish and algae. Also, sudden degeneration of a mature, dense algal bloom in a pond can result in severe DO depletions and fish mortality. Factors that affect the DO concentration in a pond include photosynthetic oxygen production, phytoplankton respiration and decay, fish respiration, fish waste production, and surface reaeration. Management of these factors could increase the oxygen available for fish respiration and therefore increase the fish production.

In ponds, the average algal cell retention time may be on the order of several days (Brune et al., 1994), since the only removal of algal biomass occurs through cell decay, settling of algae to the sediments, and grazing by zooplankton. As the cell retention time increases, the average algal growth rate decreases and the rate of oxygen production decreases. Therefore, the amount of oxygen consumed by algal respiration and decay may equal the amount of oxygen produced by photosynthesis in pond culture systems. Management of the algal growth rate and biomass could greatly improve the oxygen

dynamics and increase the fish capacity of the pond. To achieve a positive net oxygen production as a result of photosynthesis, the algal growth rate must be increased and the standing crop decreased through the control of algal cell retention time. This goal would be difficult to achieve in a traditional pond setting. Therefore, the Partitioned Aquaculture System (PAS) was designed to enable control of both algal biomass and growth rate through control of cell retention time, mixing level and water depth. In this system, the fish would be housed in cages in tanks separate from the algae culture tanks (Figure 1). Low head circulators would be used to mix the water in the algal culture basin and to keep the algae suspended. Oxygenated water from the algal culture basin would flow to the fish culture tank to supply dissolved oxygen to the fish and to flush dissolved nutrients from the tank. The oxygen-depleted but nutrient-rich water from the fish culture tank would be pumped to the algal basin where the nutrients would be utilized by the algae for growth. Supplemental inorganic nutrients could be added directly to the algal basin to raise the nutrient addition to achieve the desired algal productivity level. Algal cell retention time would be controlled through discharging a portion of the culture continuously, employing a cell separation technique and returning the water flow back to the culture, or by utilizing filter-feeding organisms in the fish culture tank to graze on the algal culture.

This system would have several advantages over conventional pond culture. The primary advantage would be the projected increased fish production that could be achieved. In addition, if biomass separation or filter feeding organisms were used to remove algal biomass, the water flow would be returned to the culture and freshwater would be required only to replace water lost through evaporation and seepage and to fill
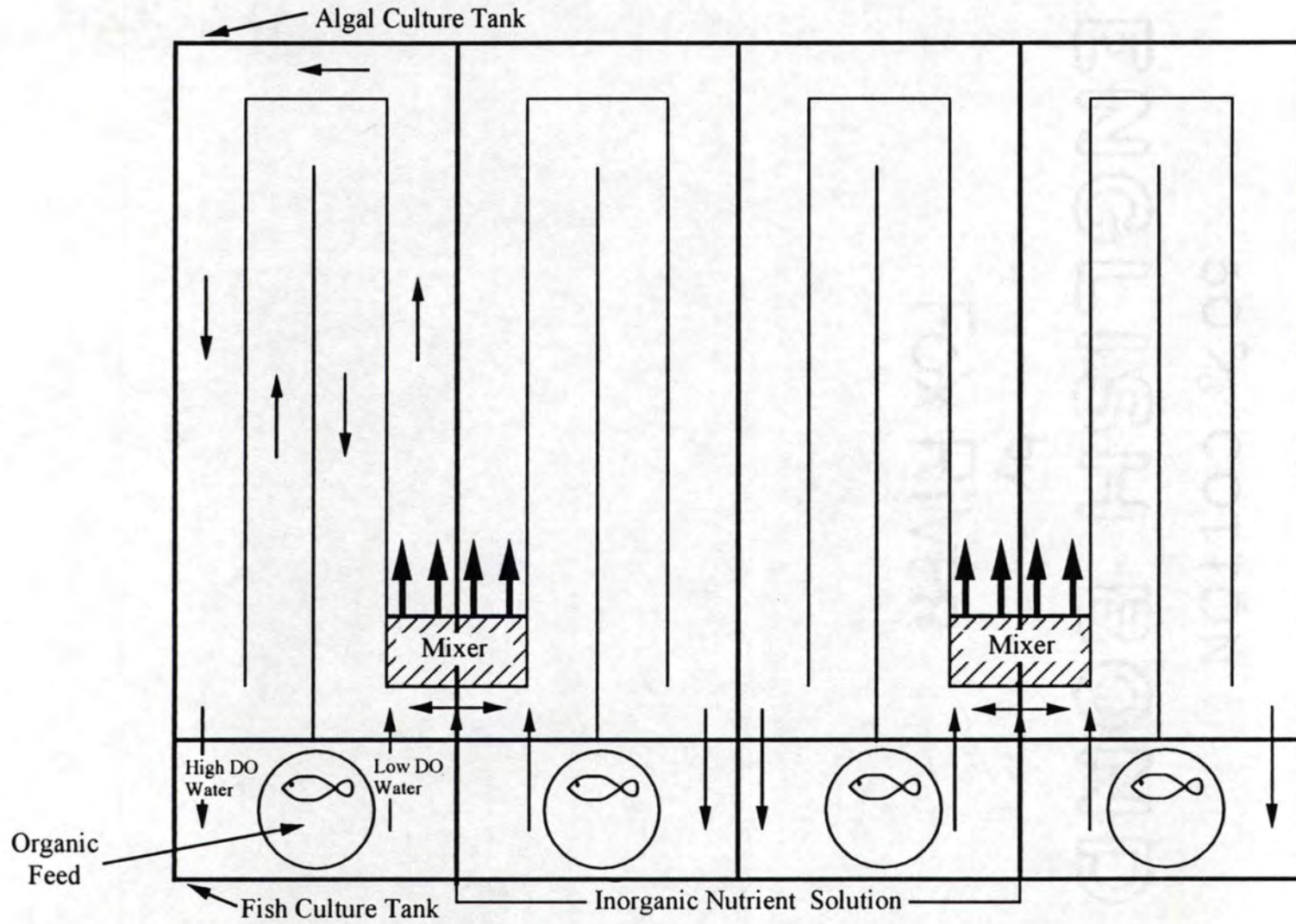
Figure 1. Schematic of Partitioned Aquaculture System

the pond initially. Finally, the discharge of aquacultural effluents containing nitrogen and phosphorus compounds and algal biomass would be avoided if the system were operated as a closed system; instead, the nutrients would be utilized by the algal culture.

The goal of this research was to investigate the potential for increasing fish production in a pond culture system by increasing the photosynthetic oxygen production through management of phytoplankton growth and productivity. The specific objectives were as follows:

1. To determine the impact of the design variables of retention time, water depth, inorganic carbon addition rate and mixing level on algal productivity and oxygen production in a field-scale aquacultural system.

2. To develop a model of algal productivity and diel DO profile as a function of the design variables and the environmental variables of solar radiation, temperature and wind.

3. To determine the optimal operating conditions to maximize DO production for increased fish yields.

Experimental Plan

The experimental plan consisted of the six phases listed below:

Phase I.   Construction of the experimental system;

Phase II.   determination of physical parameters, such as hydraulic characteristics and oxygen transfer coefficient;

Phase III.   determination of biological parameters such as algal productivity, oxygen production and respiration rates for use in predictive model;

Phase IV.   development of predictive model to simulate algal productivity and DO profiles as a function of design and environmental variables;

Phase V.   calibration and verification of model; and

Phase VI.   simulations of maximum PAS productivity.

CHAPTER II

THEORETICAL BASIS

Redfield et al. (1963) determined the C:N:P ratio of marine phytoplankton to be 106:16:1 on a molar basis. Stumm and Morgan (1962) utilized the Redfield ratio to develop the stoichiometric relationship for photosynthesis and the reverse process of respiration (Equation 1);

$$106CO_2 + 16NO_3^- + HPO_4^{2-} + 122H_2O + 18H^+ \rightarrow C_{106}H_{263}O_{110}N_{16}P + 138O_2 \,. (1)$$
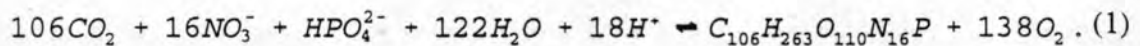
This relationship yields the predictive ratios of 3.47 g O_2 produced per g of carbon fixed through photosynthesis, 1.24 g O_2 produced per g of algal biomass (dry weight) produced and 0.358 g C fixed per g of algal biomass produced. However, during cell respiration and decay Equation 1 proceeds in the reverse direction and 3.47 g of O_2 will be required per g of algal carbon oxidized.

The growth of algae in a typical catfish pond occurs as essentially a batch culture (Brune, 1994) since the only removal of active algal biomass occurs through settling of the algae, grazing by zooplankton and algal decay. Batch cultures experience four distinct phases: I) initiation or lag phase; II) exponential growth phase; III) maximum stationary phase; and IV) death phase. Algal biomass increases exponentially during phase II, reaches a maximum during phase III and decreases during phase IV. The net algal growth rate and net oxygen production rate are therefore greater than zero during phase II, equal to zero during phase III and less than zero during phase IV as oxygen is

consumed by the decay of algal cells. As the algal cells decay, nutrients will be released back in to the culture medium and phase I will be re-initiated. Thus, algal growth and oxygen production in pond culture systems cycle between the four phases if not managed in some way.

In addition, settling of algal biomass and grazing of phytoplankton biomass by zooplankton may cause sudden decreases in algal biomass in aquaculture ponds. Both algal settling rates and zooplankton growth and grazing rates have been found to increase as algal density increases (Brune, 1994). Therefore, sudden declines in algal biomass often occur in batch algal cultures due to decay, settling or grazing.

The batch growth of algae in fish.ponds negatively affects the DO profile in two ways. First, dense algal cultures in the stationary or zero net growth phase consume large amounts of oxygen at night due to respiration, causing the DO profile to decline. Secondly, the sudden 'crashes' of algal biomass consume large amounts of oxygen due to decay of the algal biomass.

Continuous culture of algae by comparison is carried out by removing, or wasting, a portion of the algal biomass continuously. The mass balance of algal biomass can be expressed as follows:

$$V\frac{dX}{dt} = QX_o - Q_wX - (Q-Q_w)X \pm \sum rV \qquad (2)$$

where

V = algal culture tank volume, l;

X = algal biomass concentration, mg/l;

t = time, hr;

Q, Q_w = influent and wastage flow rate respectively, l/hr;

$(Q-Q_w)$ = main effluent flow, l/hr;

X_o, X = algal TSS in influent flow and tank, mg/l; and

$\Sigma \dot{r}$ = all rates involving algal biomass occurring within tank, mg/l/hr.

If biomass wasting occurs solely though the effluent flow, the influent flow rate is equal to the wastage flow rate, and the hydraulic retention time (volume/flow rate) and cell retention times (volume/wastage flow rate) are equal. Therefore, assuming X_o is zero and algal decay and loss rates are neglible, Equation 2 simplifies to

$$\frac{dX}{dt} = -\frac{Q}{V}X + \mu X \tag{3}$$

or

$$\frac{dX}{dt} = -\frac{X}{\tau} + \mu X \tag{4}$$

where

μ = algal specific growth rate, hr^{-1}; and

τ = hydraulic retention time, h.

At steady-state, the diel-averaged algal biomass concentration is constant. Therefore, $dX/dt \equiv 0$, and Equation 4 simplifies to

$$\mu X = \frac{X}{\tau} \tag{5}$$

or

$$\mu = \frac{1}{\tau} \ . \tag{6}$$

Equation 6 states that at steady state, the algal growth rate must equal $1/\tau$. Therefore, the algal growth rate can be controlled through control of the retention time. If the retention time is decreased, the diel-averaged algal growth rate will increase, thus increasing the oxygen production rate. Further, the steady state algal biomass level of both nutrient and light-limited cultures decreases as the retention time is decreased, so

that the DO consumed through algal respiration will decrease as retention time decreases. The result is that for pond aquacultural systems, decreasing the algal cell retention time through algal culture discharge, algal cell separation or algal harvesting with filter feeding fish will cause an increase in the algal growth rate and the net oxygen production rate. In addition, as the diel-averaged algal biomass decreases with decreasing retention time, biomass stability will improve by reducing the effects of algal settling and grazing rates on the biomass.

CHAPTER III

EXPERIMENTAL APPARATUS

Culture Tanks

The experimental system was constructed at the Clemson Aquaculture Facility on the Clemson University campus during the period August 1988 to June 1990. The system consists of four sets of fish and algal culture tanks (Figure 1). The tanks were built by constructing 15 cm (6 in) wide concrete walls and excavating earth from each of the tanks. Agricultural grade bentonite clay was applied to the tank floor to prevent excess seepage. The algae tanks are approximately 6 x 15 x 0.8 m (20 x 50 x 2.6 ft). The fish culture tanks are approximately 3 x 6 x 0.9 m (10 x 20 x 3.0 ft). Internal plastic walls (Permalon Ply-X 210, catalog # 0390262, Reef Industries, Inc., Houston TX) were placed in each algae culture tank by attaching the plastic to plastic-coated wire strung between 10 cm (4 in) Schedule 40 PVC pipe endposts, creating a continuous channel 1.5 m wide and 61 m long (5 ft x 200 ft).

Each tank was fitted with a separate 5 cm (2 in) Schedule 40 water drain line and standpipe so that the water level could be adjusted independently for each tank. Also, an exterior standpipe was fitted for each tank at the point where the drain line was connected to the main drain pipe, so that the water level for each tank could be adjusted from outside of the culture tank. Water could be drawn from top of the water column by placing an interior standpipe in the tank.

Circulators

A six-blade paddlewheel circulator was mounted in each algae culture tank to move the culture water through the channel (Figure 2). Each paddlewheel blade was approximately 142 cm (56 in) wide and 91 cm (36 in) long (Figure 3). The total radial distance from center of shaft to edge of circulator blades was 95.9 cm. The blades were constructed by attaching fiberglass sheeting (0.2 cm Lasco sheet, Piedmont Plastics, Greenville SC) to a frame made of hot rolled 3.2 cm x 3.2 cm x 0.32 cm (1¼ in x 1¼ in x ⅛ in) angle iron. The circulators were mounted in each tank adjacent to the common wall between Tanks 1 and 2 and Tanks 3 and 4, so that one motor could be used to drive two circulators (Figure 4). Two adjustable speed, 373 W (½ Hp) electric gear drive motors were used (Dayton Electric Manufacturing Co., Chicago IL); Model # 4Z369 (minimum rpm of 64) and Model # 4Z370 (minimum rpm of 12). To reduce the rotational speed of the mixers, two 1:6 gear ratio arrangements were placed in series by installing an intermediate shaft, two 10 tooth sprockets and two 60 tooth sprockets in the drive between the motor and the circulator. As a safety feature, the key in the small sprocket on the intermediate shaft was replaced with a shear pin which would fail in case the chain or mixer blades became obstructed. Brass or steel rods 0.32 cm (⅛ in) in diameter were used as the shear pins.

Nutrient Supply

An inorganic nutrient feed solution was stored in two 760 l (200 gal) tanks and fed to each algae tank by means of a 10 channel peristaltic pump system (Masterflex 10 channel drive, catalog # 7568-00, pump heads (catalog # 7017-52) and 0.64 cm (¼ in) ID silicone tubing (catalog # CK 6411-17), Cole-Parmer Instrument Co., Chicago IL).
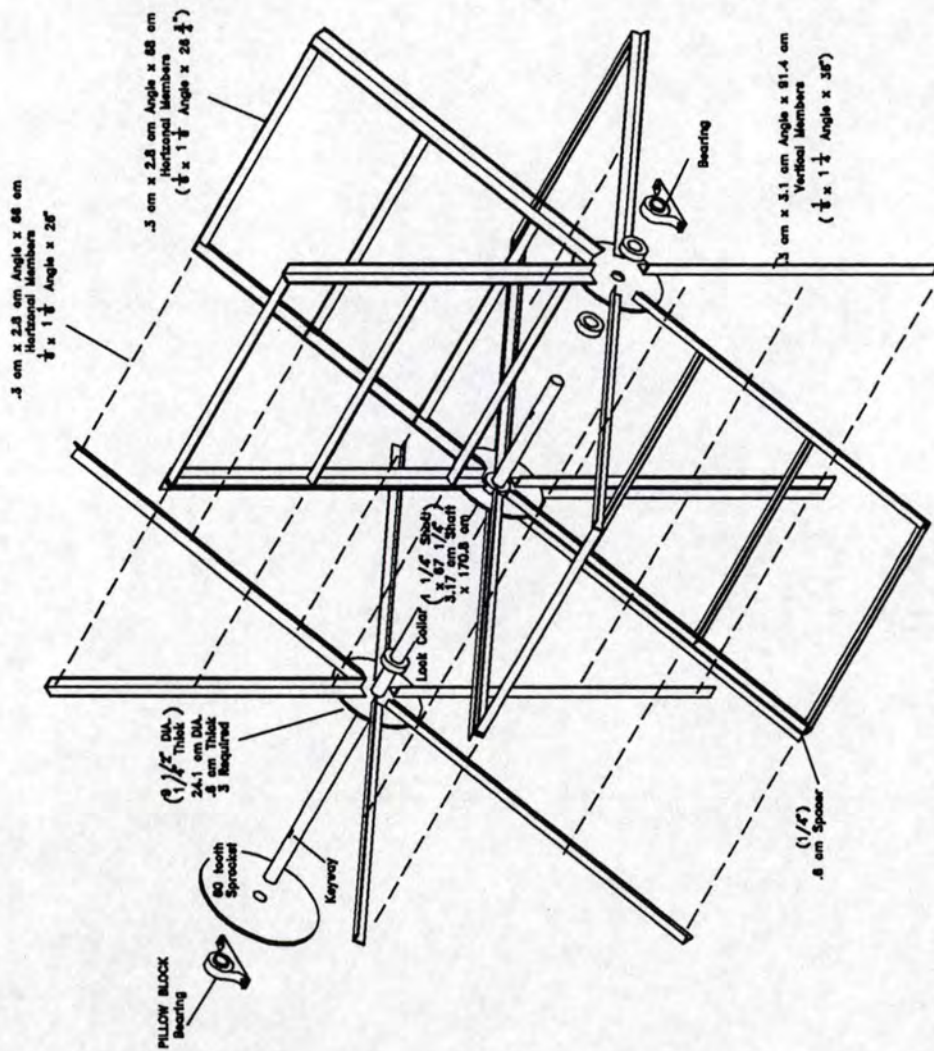
Figure 2. Six-blade paddlewheel circulator.
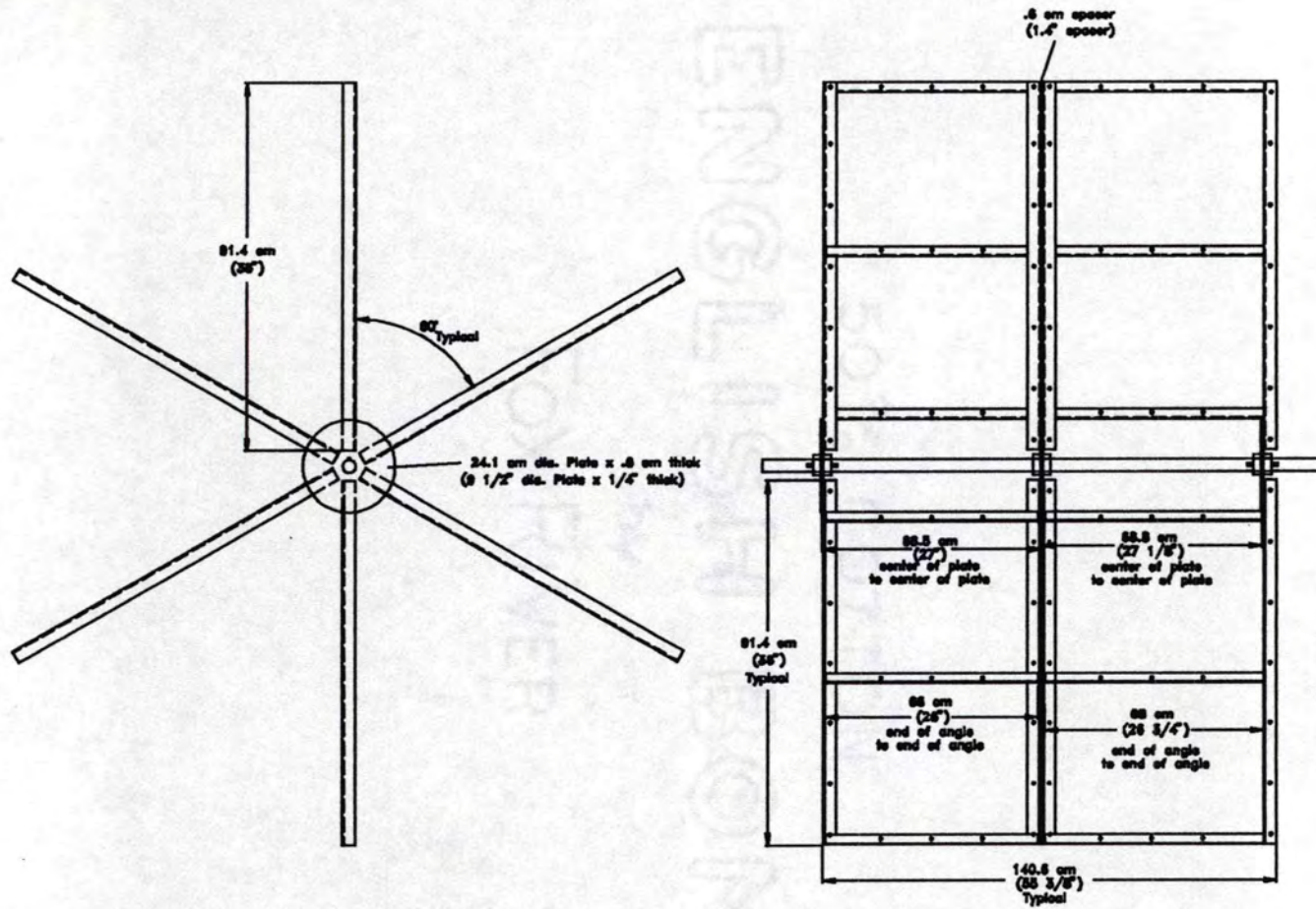
Figure 3. Paddlewheel circulator blade.
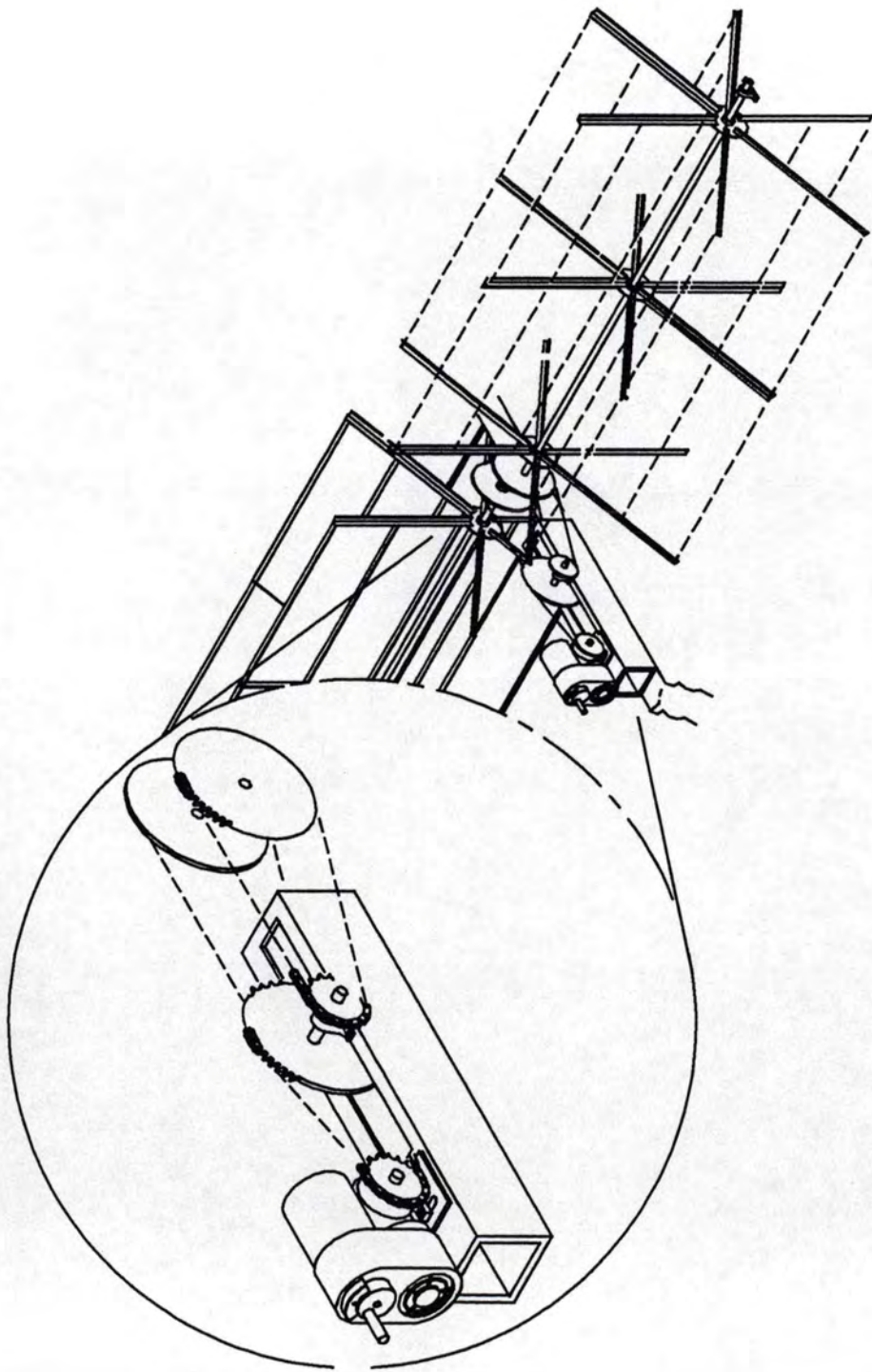
Figure 4. Circulator drive assembly.

Agricultural grade 20-20-20 N-P-K fertilizer (Nutri-Leaf soluble, Miller Chemical &

Fertilizer Corporation, Hanover PA) and ammonium-nitrate (34% N) (Nitram Inc., Tampa

FL) were mixed to supply nitrogen, phosphorus and trace nutrients to the algal cultures

(Table 1). The basic nutrient feed solution was prepared by mixing 5.0 g 20-20-20 and

6.4 g NH_4-NO_3 per liter, to provide a 16:1 total nitrogen to phosphorus ratio, or a 14:1

ratio of plant-available nitrogen (ammonium and nitrate nitrogen) to phosphorus on a

molar basis. For several experiments the nutrient solution was prepared at 0.5 to 2 times

the basic concentration. Agricultural feed-grade sodium bicarbonate (FMC Corporation,

Philadelphia PA) was added to the tanks once per day to supply varying amounts of

inorganic carbon for the algal cultures.

Table 1. Guaranteed analysis of the Nutri-Leaf 20-20-20 fertilizer[1]

Component	Percent
Total Nitrogen	20.0
Ammonia Nitrogen	6.2
Nitrate Nitrogen	6.2
Urea Nitrogen	7.6
Available Phosphoric Acid (P_2O_5)	20.0
Soluble Potash (K_2O)	20.0
Boron (B)	0.02
Copper (Cu) (chelated)	0.05
Iron (Fe) (chelated)	0.10
Manganese (Mn) (chelated)	0.05
Molybdenum (Mo)	0.0005
Zinc (Zn) (chelated)	0.05

[1] Nutri-Leaf soluble, Miller Chemical & Fertilizer Corporation, Hanover PA

Water Supply

Surface water was pumped from Hunnicutt Creek which flows near the aquaculture facility with a 1.5 kW (2 Hp) self-priming centrifugal pump (Model # 1P897, Teel Industrial Series, Dayton Electric Manufacturing Co., Chicago IL) through 5 cm (2 in) PVC line to the culture tanks. Water flow to each algae and fish culture tank was controlled with a 5 cm (2 in) brass gate valve and measured with a cumulative positive displacement water meter (Model C-700TP, Kent Meters, Inc., Ocala FL).

CHAPTER IV

PROCEDURES

Field Procedures

Characterization of Physical Parameters

Water depth. Direct measurement of the average tank depth could not be made due to the uneven bottom surface. Average depth was calculated by measuring the quantity of water required to fill the tank and dividing by the surface area of the tank.

Water velocity. Water velocity was measured by timing the passage of a float through the channel at circulator tip velocities of 0.1 - 0.4 m/s (corresponding to rotational speeds of 1 - 4 rpm) at water depths of 18, 28 and 64 cm. The circulator tip velocity was calculated as follows:

$$v_t = \frac{2\pi r f}{60} \tag{7}$$

where

v_t = tip velocity, m/s;

r = circulator radius, m;

f = frequency, rpm.

Average wind velocity. Average wind velocity at a 1 m height was measured by dividing the miles of wind passed recorded by an anemometer by the lapsed time. Wind velocity measurements at most weather stations are made at a height of 10 m and models for predicting oxygen transfer as a function of wind utilize wind velocity measurements

at a 10 m height. The wind velocity at any height can be calculated from the following equation (Sill, 1988):

$$V_{wind,z} = \frac{u_*}{k} \ln(\frac{z}{z_o}) \qquad (8)$$

where

$V_{wind,z}$ = wind velocity at elevation z;

u_* = shear velocity, equal to (shear stress/density of air)$^{1/2}$;

z = elevation; and

z_o = aerodynamic roughness factor.

Equation 9 can be used to predict wind velocity at one height from measured wind velocity at another height:

$$\frac{V_{wind,10m}}{V_{wind,1m}} = \frac{\frac{u_*}{k} \ln(\frac{10}{z_o})}{\frac{u_*}{k} \ln(\frac{1}{z_o})} \qquad (9)$$

After canceling the u_*/k term, Equation 9 simplifies to

$$V_{wind,10m} = V_{wind,1m} \frac{\ln(\frac{10}{z_o})}{\ln(\frac{1}{z_o})} \qquad (10)$$

The roughness parameter, z_o, ranges from 0.003 m, for large expanses of water, to 0.8 m, for cities with multiple-story buildings (Cook, 1985). A value of z_o equal to 0.1, corresponding to farmland with frequent boundary hedges, houses and trees, was chosen as most representative of the terrain surrounding the PAS system. Therefore, wind

speed at the PAS at a height of 10 m was calculated from the measured 1 m wind velocity as follows:

$$V_{wind, 10m} = V_{wind, 1m} \frac{\ln(\frac{10}{0.1})}{\ln(\frac{1}{0.1})} = 2.00 V_{wind, 1m} \quad .$$ (11)

Oxygen transfer coefficient. The oxygen transfer coefficient in the PAS as a function of water velocity due to the rotation of the circulators and ambient wind velocity was measured according to the EPA method for evaluating oxygen transfer devices (ASCE, 1984). This method is based on depleting the dissolved oxygen (DO) in the test tank by addition of a sodium sulfite solution and measuring the subsequent rise in oxygen with time due to the aerating device. The model that describes the rate of change of DO concentration is as follows (ASCE, 1984):

$$\frac{dC}{dt} = K_{1a}(C_s - C)$$ (12)

which upon integration becomes

$$C = (C_s - C_o) e^{(K_{1a} t)}$$ (13)

in which

C = oxygen concentration at time t, mg/l;

C_s = equilibrium oxygen concentration, mg/l;

C_o = oxygen concentration at time t=0, mg/l;

t = time, min; and

K_{1a} = reaeration coefficient, min⁻¹.

This method prescribes that the exponential form of the model be fit to the experimental data by non-linear least squares analysis. Parameter estimates for K_{1a}, C_s,

and C_o should be obtained from this analysis. To obtain an accurate estimate of C_s, the method states that the test be continued until the oxygen concentration approaches 98% of the saturation value. Due to the large water volume in the PAS, a test period of up to 20 hours would be required to achieve this condition. Since the goal was to determine the oxygen transfer rate as a function of both circulator rotational speed and wind velocity, the test durations were confined to periods with relatively stable wind velocities. An arbitrary limit was chosen so that if the wind speed differed by more than 25% of the average value, the test was concluded. Therefore, one modification needed for the current research was to calculate the value of C_s rather than estimate it from the data. The saturation value for fresh water at 1 atm pressure was calculated by use of Equation 14 (Standard Methods, 1989);

$$C_s = e^Q \tag{14}$$

where

$$Q = (-139.3441 + \frac{1.575701 \times 10^5}{TEMPK} - \frac{6.642308 \times 10^7}{TEMPK^2} + \frac{1.243800 \times 10^{10}}{TEMPK^3} - \frac{8.621949 \times 10^{11}}{TEMPK^4}) \tag{15}$$

and TEMPK = average water temperature, K.

Equation 16 can be used to calculate the effect of changing atmospheric pressure due to weather conditions and elevation changes on the saturation value;

$$C_{s,p} = (C_s P) \frac{(1-E)(1-XP)}{P(1-E)(1-X)} \tag{16}$$

where

$$X = 0.000975 - (1.426 \times 10^{-5} TEMPC) + (6.436 \times 10^{-8} TEMPC^2) \tag{17}$$

$$E = e^{(11.8571 - \frac{3480.70}{TEMPK} - \frac{216,961}{TEMPK^2})}$$ (18)

and

$C_{s,p}$ = saturation DO concentration at pressure P, mg/l;

TEMPC = average water temperature, °C; and

P = average air pressure, atm.

Average air pressure values were obtained from the National Weather Service station in Greenville, SC and corrected for air temperature and elevation differences between Clemson and Greenville by the following equation (Conrad and Pollack, 1950):

$$\log p_1 = \log p_2 + \frac{h_2 - h_1}{18,460 + 72 T_m}$$ (19)

where

p_1, p_2 = atmospheric pressure at points 1 and 2, atm;

h_1, h_2 = elevation of points 1 and 2, m;

T_m = mean temperature of air column between points 1 and 2.

Three experimental runs were conducted at each water velocity of 0.0313, 0.0625, 0.125 and 0.187 m/s, corresponding to rotational speeds of 0.5, 1.0, 2.0 and 3.0 rpm. The average wind velocity measured at 1 m height occurring over the test period was converted to velocity at 10 m height by use of Equation 11.

Daily System Monitoring

Daily measurements of the secchi disk visibility were made as per Standard Methods (1989) with a 20 cm secchi disk (Aquatic Eco-Systems, Inc., Apoka FL). The culture temperature at mid-depth was measured with a glass mercury thermometer. Average water flow was measured by dividing the cumulative water volume that passed

into each tank by the lapsed time between initial and final reading. The nutrient solution flow rate was determined and checked several times weekly by collecting the flow into a 100 ml graduated cylinder for one minute.

Dissolved Oxygen Measurements

Dissolved oxygen concentrations were measured by means of polarographic DO probes (Models 5720A and 5739) and DO meters (Model 54A) available from Yellow Springs Instrument Company (Yellow Springs OH). The maximum DO value that can be displayed with the meters used is 20 mg/l. To measure values greater than 20 mg/l, a titration technique was developed to lower the DO concentration to less than 20 mg/l in the sample to be measured by addition of a sodium sulfite solution. This technique was derived from the method for measurement of the oxygen transfer coefficient (ASCE, 1984). According to this method, 7.88/l mg of sodium sulfite are required to react with 1 mg/l of oxygen. The procedure developed for this work entails adding a small volume (1 - 3 ml) of sodium sulfite solution of known oxygen equivalence to two samples and measuring the final DO value. The original DO concentration of the sample is then calculated as the DO value measured plus the oxygen equivalent of the sulfite solution added. The procedure is detailed in Appendix A.

Dissolved oxygen levels in the algae culture tanks were made by one of three methods: 1) placing a field DO probe directly in culture tank and measuring DO if DO was less than 20 mg/l; 2) taking two samples and measuring DO with sodium sulfite technique if DO was greater than 20 mg/l; or 3) utilizing the field DO probe and meter with strip chart recorder to provide continuous monitoring of DO concentration.

Measurements of net photosynthesis were made by measuring the initial DO in two clear glass 300-ml BOD bottles, incubating the bottles horizontally at pre-set depths in the algae culture tanks for approximately two hours, and measuring final DO (Standard Methods Part 10200J.2). The gross photosynthetic rate was calculated by adding the respiration rate to the net photosynthetic rate. Respiration was measured by determining initial DO in two black plastic-coated BOD bottles, incubating in the algae tanks for approximately 12 or 24 hours, and measuring the final DO. Water temperature was measured at the beginning and end of the incubation period and the average was used as the incubation temperature. Photosynthetic and respiration rates were standardized to 20°C by use of the following equation (Goldman and Carpenter, 1974):

$$R_{20} = R_T e^{((20-T)K/10)} \tag{20}$$

where

R_{20}, R_T = rate at 20°C and at average culture temperature, mg DO/l/hr;

  T = average culture temperature, °C; and

  K = 0.7707 (Goldman and Carpenter, 1974).

Solar Radiation

Incoming solar radiation was measured with a pyranometer (Model 8-48, Eppley Lab, Inc., Newport RI) at the Clemson SPAR (Soil-Plant-Atmosphere Relationships) greenhouse system at McAdams Hall on the Clemson University campus (described in Dunlap, 1988). This system stores 15-minute averages of complete spectrum solar radiation values. However, solar radiation data were not available for September 1992, when many of the oxygen production measurements were made, so that a model was

needed to predict the solar radiation profiles for that period. The total daily solar radiation value was predicted first, then fitted to a curve to predict the hourly solar radiation profile.

Two existing models developed to predict evaporation from weather data, the Penman and Jenson-Haise equations, plus two regression model developed in this work were compared to determine their usefulness as predictors of solar radiation. The data set for this analysis consisted of weather data obtained from the Clemson University weather station (station # 38-1770) and the Greenville/Spartanburg weather station (station # 38-3747) for days with less than 0.05 cm (0.02 in) of precipitation for the period 6/1/92 - 9/30/92.

The first model investigated was the Penman equation, which was formulated to predict evaporation from weather data. The Penman equation can be written as (Penman, 1948 as given in Schwab et al., 1981):

$$ET = \frac{\Delta}{\Delta+\gamma}(R_n-G) + \frac{\gamma}{\Delta+\gamma}15.36(1+wind/160)(e_s-e_a) \tag{21}$$

where

ET = potential evapotranspiration, cal/cm^2/d;

Δ = slope of saturation vapor pressure curve at mean air temperature, mbar/°C;

γ = psychrometric constant, mbar/°C;

R_n = net radiant energy available at ground, cal/cm^2/d;

G = energy into the soil, cal/cm^2/d;

wind = wind velocity at 2 m height, km/d;

e_s = mean saturated vapor pressure, mbar; and

e_a = saturated vapor pressure at dew point temperature, mbar.

The variable G is generally ignored when applying the Penman equation (Rosenburg et al., 1983). When G is omitted, E_o, evaporation over a free water surface, can be substituted for ET. Evaporation and wind data were obtained from the Clemson University weather station. e_s and e_a were calculated from psychrometric relationships using the Clemson University weather station minimum air temperature as the dew point temperature. The ratios involving Δ and γ are functions of the mean air temperature and were obtained from Schwab et al., 1983 (Table 3.1, pg 62).

In general, the predicted net radiation values calculated using Equation 21 were lower than the measured radiation values (Figure 5). Net radiation, R_n, is defined as the difference between the total incoming and outgoing radiation fluxes. In contrast, the SPAR system measured the net incoming solar radiation, R_s, so R_s is greater than or equal to R_n. The Penman model does not adequately represent this data set.
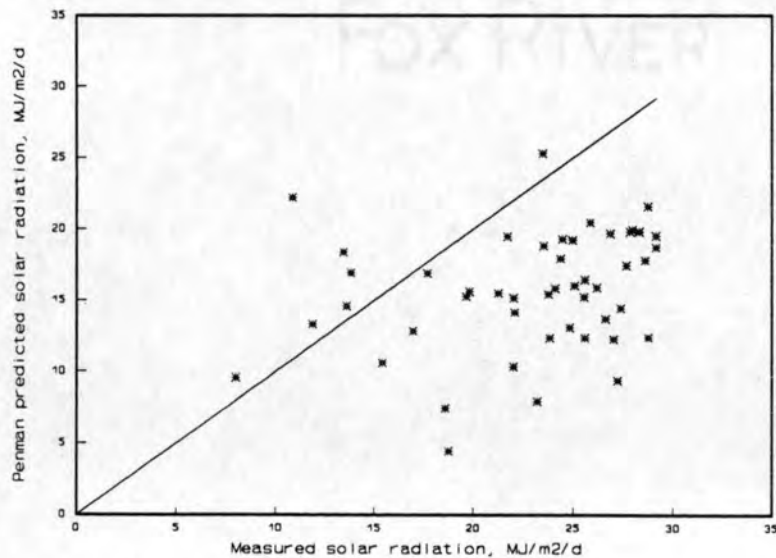
Figure 5. Measured vs predicted solar radiation for Pennman model (Equation 21).

The second model tested was the Jensen-Haise equation (Rosenburg et al., 1983)

$$ET = R_s(\alpha T_a + \beta)$$ (22)

where

ET = potential evapotranspiration;

R_s = daily total solar radiation; and

T_a=average air temperature.

After substitution of evaporation for ET, rearrangement of Equation 22 yields:

$$R_s = \frac{E}{\alpha T_a + \beta}$$ (23)

with units of R_s = MJ/m^2/d, E = cm/d and T_a =°C. The parameter estimates obtained from fitting this model to the data set are given in Table 2.

Table 2. Parameter estimates for Jensen-Haise model.

Parameters	Estimate	Standard Error	MSE
α	0.0001414	0.0003366	35.77
β	0.02208	0.008669	

Comparison of the actual solar radiation values and predicted values from the Jensen-Haise model (Figure 6) reveal that the predicted values differ greatly from the actual values in many cases. Analysis of the residuals for this model (Appendix B) also indicate that the model does not adequately describe solar radiation for the existing data.
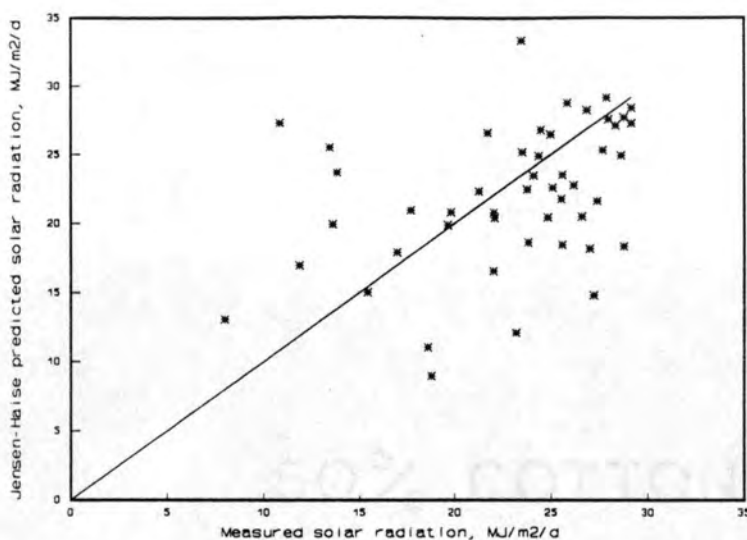
Figure 6. Measured vs predicted solar radiation for Jensen-Haise model (Equation 23).

Consequently, two regression models were developed to improve the predictive capability of the model. Data from the Clemson University weather station considered for these models were as follows: pan evaporation; average, maximum and minimum dry-bulb air temperature; daily rise in dry-bulb air temperature; daily wind; and maximum soil temperature and daily rise in soil temperature at 10 cm (4 in) depth. Relative humidity at the maximum and average air temperatures, maximum wet-bulb air temperature and daily rise in wet-bulb air temperature, calculated from psychrometric relationships, were also included. Variables considered from weather data obtained from the Greenville/Spartanburg weather station were sunshine duration and percent of possible sunshine.

Scatter plots (Appendix C) revealed a positive linear relationship between solar radiation and daily rise in dry-bulb air temperature,°C (DAIRT), sunshine duration in minutes (SUNMIN) and sunshine duration as percent of possible (PERCENT), and the

inverse of relative humidity at the maximum and average dry-bulb air temperatures (RHTMAX2 and RHTAVE2). A slight non-linear trend was evident in the plots of solar radiation vs the square of DAIRT (SQDAIRT).

A linear combination of the weather variables in their original form plus squared and inverse transformations of the variables were considered. A stepwise regression procedure was used to determine that the variables that contributed the most to the overall variation in solar radiation were SUNMIN, DAIRT and PERCENT. The intercept term did not add to the model. The linear model is given below;

$$R_s = \alpha SUNMIN + \beta DAIRT + \gamma PERCENT \tag{24}$$

with units of R_s = MJ/m^2/d, SUNMIN = min, DAIRT = °C, and PERCENT = %. The parameter estimates for this model are given in Table 3.

Table 3. Parameter estimates for linear solar radiation model.

Parameter	Estimate	t statistic	P	MSE
α	0.0761	5.50	0.0001	5.27
β	0.8880	5.39	0.0001	
γ	-0.4883	-4.22	0.001	

The linear model predictions closely matched the measured solar radiation data (Figure 7). Analysis of the residuals (Appendix B) indicated that the model appears to be correctly specified but that a variable or interaction between variables may be missing.
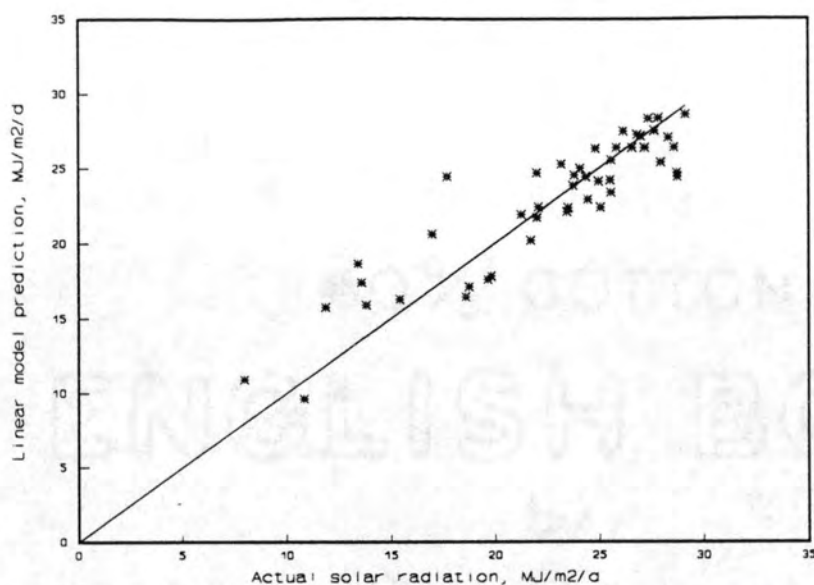
Figure 7. Actual vs predicted solar radiation for linear model (Equation 24).

A linear model with hyperbolic component, constructed to model the non-linear relationship between solar radiation and the square of the daily rise in air temperature (SQDAIRT), was also investigated (Equation 25):

$$R_s = \frac{\gamma SQDAIRT}{SQDAIRT + \lambda} + \beta SUNMIN + \alpha PERCENT \tag{25}$$

The parameter estimates are given in Table 4.

Table 4. Parameter estimates for hyperbolic model.

Parameter	Estimate	Standard error	MSE
γ	22.28	4.542	5.11
λ	162.2	74.71	
β	0.07647	0.01373	
α	-0.4865	0.1139	

The hyperbolic model also closely predicted the measured values (Figure 8). The MSE value for this model was slightly lower than for the linear model. The residuals analysis (Appendix B) indicated that similarly to the linear model, the hyperbolic model appears to be correctly specified but that some variable may be missing.
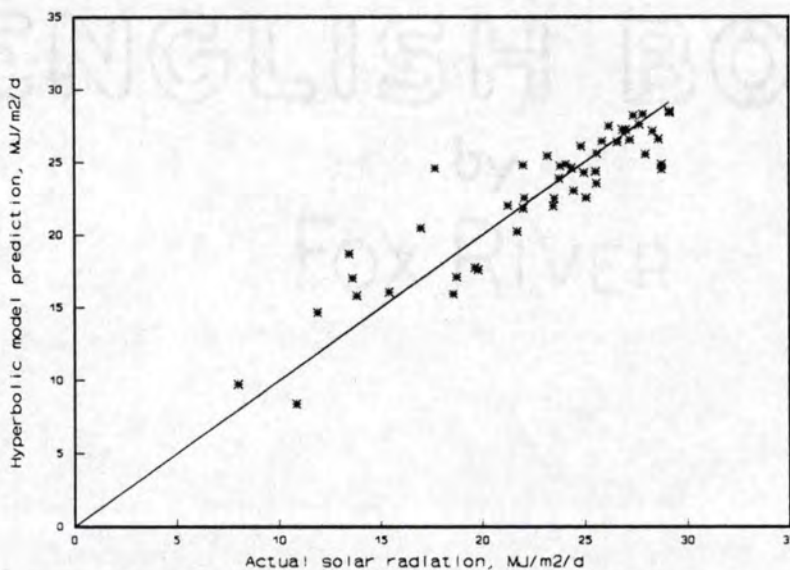
Figure 8. Actual vs predicted solar radiation for hyperbolic model (Equation 25).

Because the MSE was only slightly lower for the hyperbolic model than the linear model, the linear model (Equation 24) was chosen because of its simplicity as the best model to describe the solar radiation data and to predict the missing observations. Since both models developed showed some pattern in the plot of residuals vs solar radiation, future work investigating additional weather variables could improve the model's predictive capability further.

The predicted total daily solar radiation values for the missing days in September when field DO measurements were made are as follows:

Table 5. Predicted daily solar radiation.

Dates	Predicted solar radiation, MJ/m^2/d
9/2/92	15.56
9/3/92	13.54
9/4/92	16.49
9/9/92	18.58
9/10/92	16.85
9/11/92	17.82

The hourly solar radiation profile was obtained by comparing these predictions of total daily solar radiation to the actual daily profiles for the month of September, 1991 (Figure 9). The maximum or cloud-free profile can be modeled with the following equation:

$$SR = \gamma + \beta (x-\alpha)^2 \qquad (26)$$

where

SR = solar radiation, J/s·m^2 or W/m^2; and

x = time of day, hrs.

The parameter γ represents the maximum solar radiation value during the day, β is a shaping parameter, and α represents the time of day when the solar radiation is at the maximum. Based on the 1991 data, the characteristic maximum profile for September has parameter estimates of γ=870, β=-27.5 and α=13.625. The area under this curve,

which is the total daily solar radiation for clear day conditions, is 2.35×10^7 W•s/m²/d or 23.5 MJ/m²/d, which is obtained by integrating the profile equation. For each of the days in September for which a solar radiation profile was needed, the values of γ, β and α were adjusted until the area under the curve was equal to the predicted total daily value obtained from the linear regression. The profiles for the desired days in September are shown in Figures 10 through 15. This procedure, in effect, models cloud cover as a haze which acts to lower the maximum profile uniformly throughout the day, and cannot model the profile for an intermittently cloudy day.
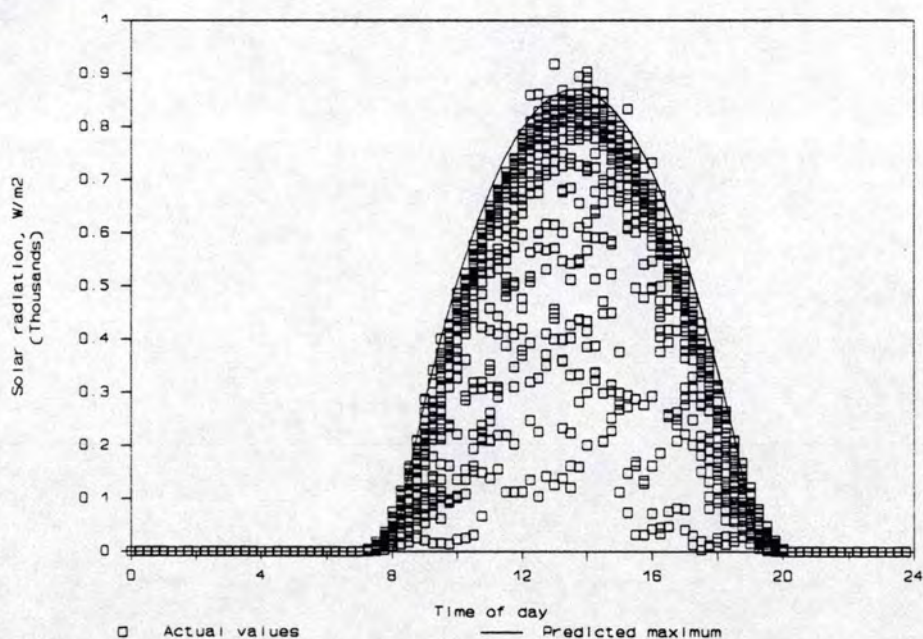
Figure 9. Observed and predicted maximum solar radiation for September 1991.
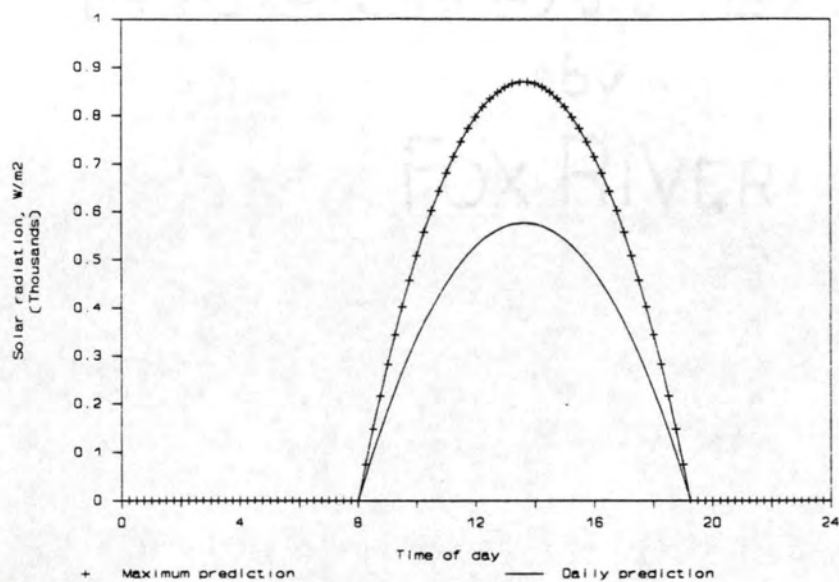
Figure 10. Predicted solar radiation profile for 9/2/92.
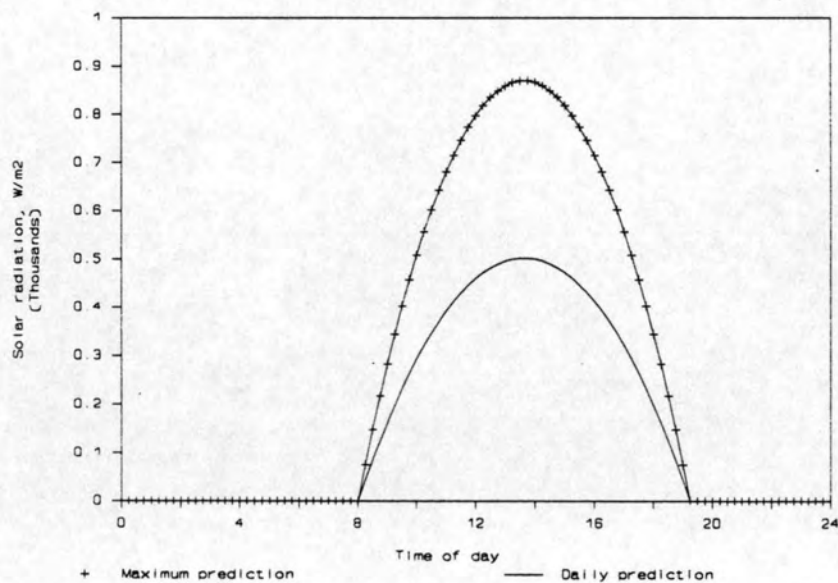
Figure 11. Predicted solar radiation profile for 9/3/92.
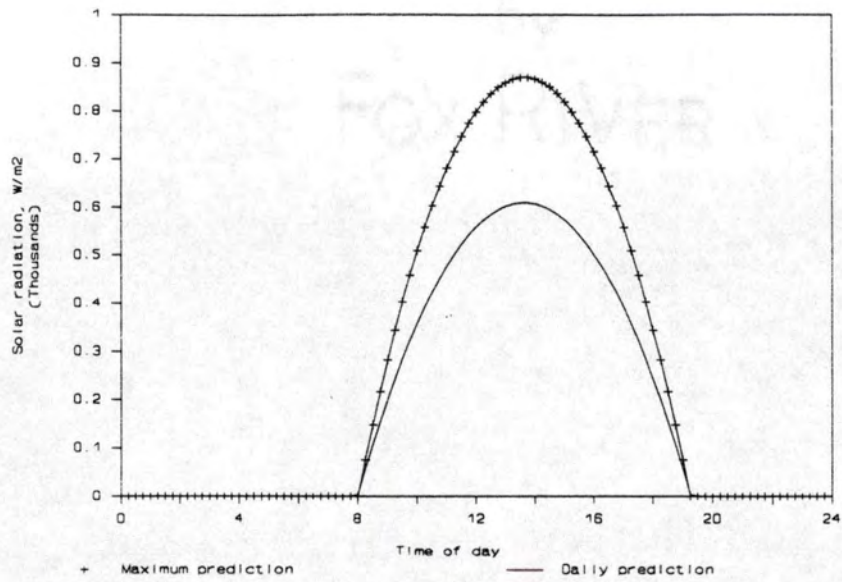
Figure 12. Predicted solar radiation profile for 9/4/92.
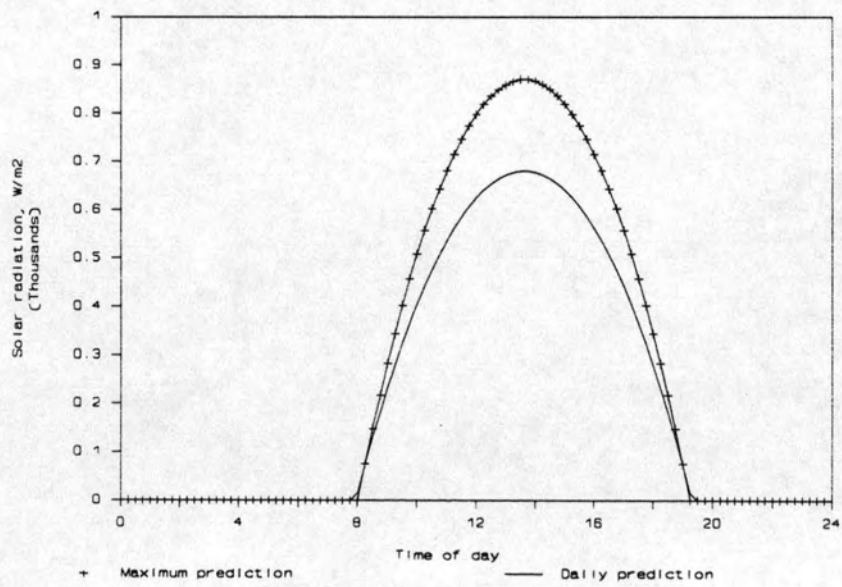
Figure 13. Predicted solar radiation profile for 9/9/92.
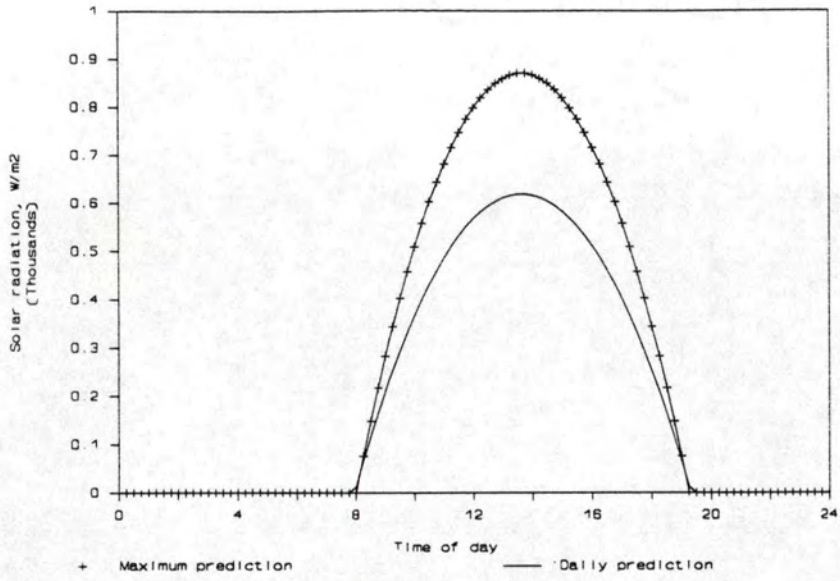
Figure 14. Predicted solar radiation profile for 9/10/92.
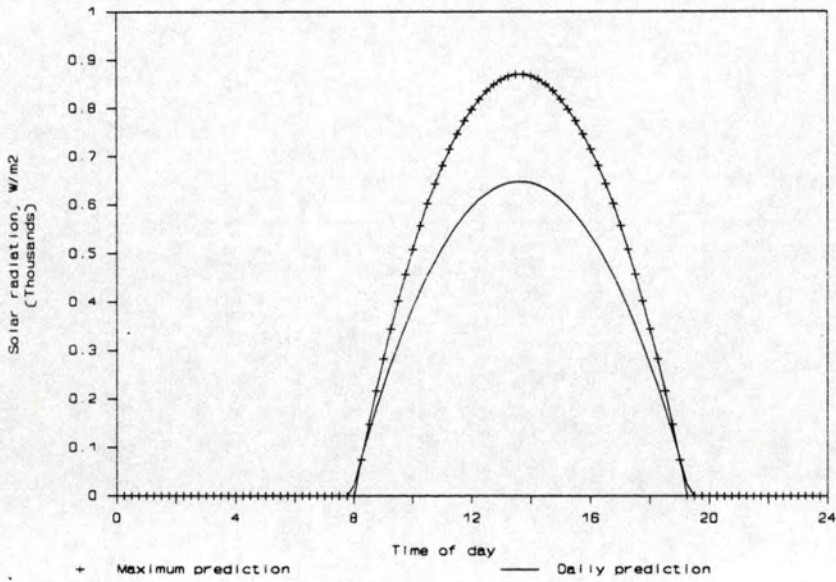
Figure 15. Predicted solar radiation profile for 9/11/92.

Laboratory Procedures

Algal Cell Identification

Grab samples of the algal culture were taken twice per month. A 10-ml sample was centrifuged and 9 ml of supernatant withdrawn to achieve a 10:1 concentration of the cells (Davis et al., submitted). Cell genus was determined by visual observation of the cells using Nikon Alpha-phot YS microscope (Nikon Instrument Co., Garden City NY). Cells were counted on a minimum of 5 grids using a Bright-line hemacytometer (American Optical, Buffalo NY) and the average value calculated.

Algal Biomass Determination

Algal biomass was determined by measuring the total suspended solids (TSS) of the algal culture. To account for variability in desiccator humidity or desiccation time, two blanks were run with each set of samples. Any weight change by the blanks was added to the sample weight to correct for the variability. Initially, algal TSS were measured using Gelman GF/C glass fiber filters (Part 2540D, Standard Methods, 1989). However, for samples containing predominantly blue-green algae, most of the algal solids were not retained on the filter. A comparison of the algal TSS measured with glass fiber and 0.45 μm filters indicated that TSS measured with glass fiber filters were up to 50% lower than TSS measured with 0.45 μm filters (Figure 16). Although 0.45μm filters would retain bacterial cells also, the 1 μm effective pore size of the Gelman glass fiber filters clearly did not capture the majority of the algal cells for the blue-green culture. Subsequently, TSS was measured by filtering 50 or 100 ml of sample through a desiccated, pre-weighed 0.45 μm filter and drying at 105°C (Part 10200I.5, Standard Methods, 1989).
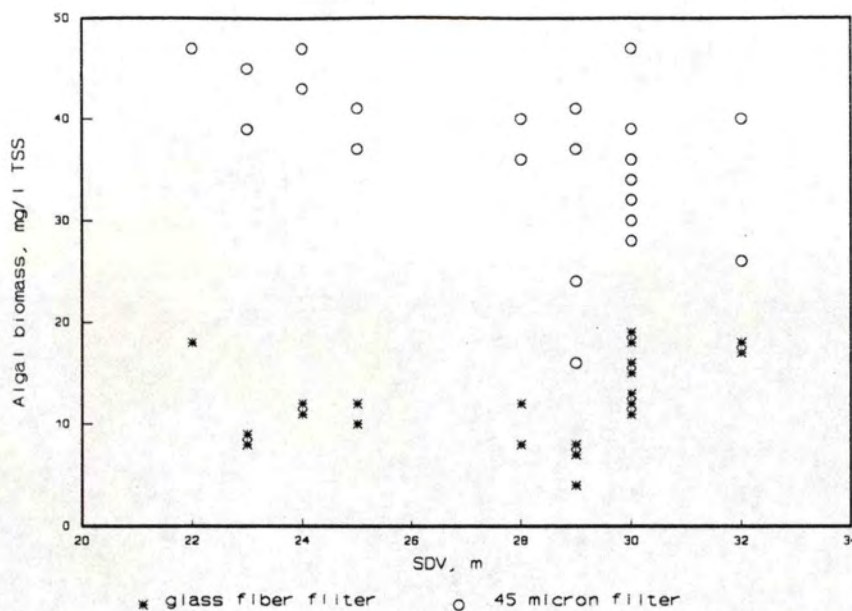
Figure 16. Comparison of algal TSS measured with glass fiber vs 0.45 μm filter.

Water Quality

pH was measured after calibration with pH 7.0 and 10.0 standards with a gel-filled combination pH electrode (Catalog No. 13-620-104, Fisher Scientific International, Springfield NJ) and pH meter. Alkalinity to pH 4.5 endpoint was measured (Part 2320B Standard Methods, 1989).

Statistical Procedure

A lack of fit analysis can be performed when replicate values of the response variable (y) are obtained for each concomitant (x) position to determine if a certain proposed model is appropriate to represent a given data set. The procedure used is as follows:

1. Fit the proposed model to the data set and obtain the total sum of squares error (SSE). The associated degrees of freedom (df_{SSE}) are the number of observations (n) minus the number of parameters in the model (p). Calculate the mean square error which is SSE/df_{SSE}.

2. Determine the within sum of squares (SSW) which provides an estimate of the observed variation among y_{ij}'s at each x_i position. This value is a measure of the variation in the observations and is not a function of the proposed model. The degrees of freedom (df_{SSW}) are the number of observations (n) minus the number of concomitant positions (m). The within mean square error (MSW) is calculated as SSW/df_{SSW}.

3. Determine the lack of fit sum of squares (SSL) which is a measure of the error associated with the lack of fit of the model to the data set. SSL is calculated as SSE-SSW. The degrees of freedom are $df_{SSE}-df_{SSW}=df_{SSL}$. The lack of fit mean square error (MSL) is calculated as SSL/df_{SSL}.

4. Calculate the f statistic as $f_{calc}=$ MSL/MSW.

5. Compare the calculated f statistic with the tabulated F value, with degrees of freedom of df_{SSL} and df_{SSW}, at the preferred level of significance.

CHAPTER V

RESULTS AND DISCUSSION

Characterization of Physical Parameters

Water Velocity

Water velocity was modeled as a linear function of the circulator tip velocity;

$$v_w = \alpha + \beta v_t \tag{27}$$

where

v_w = water velocity, m/s;

v_t = circulator tip velocity, m/s.

Least squares analysis indicated that the intercept did not contribute to the model. The calculated F statistic of 866.8 (P=.0001) indicates that the model given in Equation 28 (shown in Figure 17) is appropriate to model water velocity as a function of tip velocity;

$$v_w = 0.6224 v_t \quad . \tag{28}$$
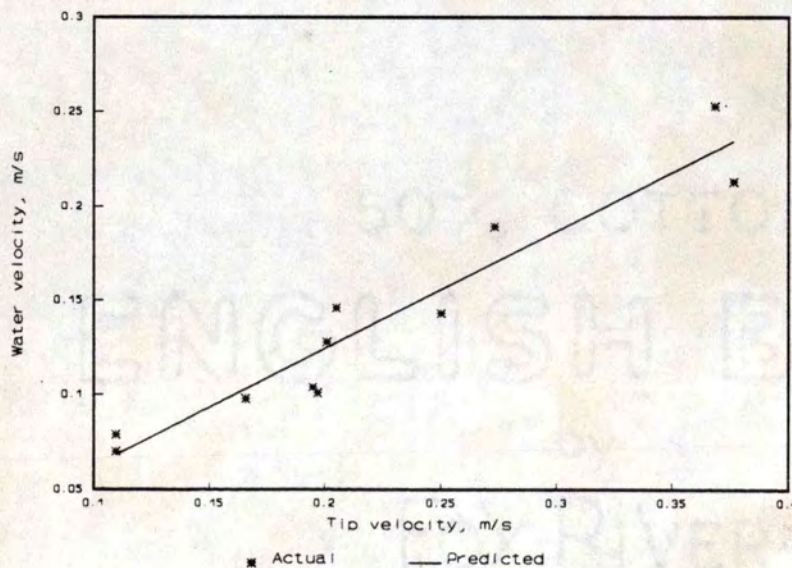
Figure 17. Water velocity vs circulator tip velocity.

Oxygen Transfer Coefficient

Twelve reaeration experiments were conducted at four water velocities. Three runs were discarded from the data set due to mechanical or weather interferences. The conditions for the nine remaining tests are given in Table 6.

Table 6. Conditions for determination of oxygen transfer coefficient.

Run	Average Air T, °C	Average Water T, °C	Water T Range, °C	Duration Test, min
2b	9.6	12.5	1	135
2c	13.5	14.0	0	120
2d	11.4	13.5	1	180
2e	12.9	12.5	1	120
2f	9.3	8.0	0	135
2h	12.2	12.0	0	240
2k	26.9	28.6	3	330
2l	26.9	27.4	2	270
2n	28.5	28.4	3	210

The exponential model (Equation 13) was fitted to the DO vs time data obtained for each run using non-linear least squares analysis to provide estimates of the reaeration coefficient, K_{la}. The predicted values closely matched the observations. A plot of the predicted and observed values for Run 2k are shown in Figure 18.
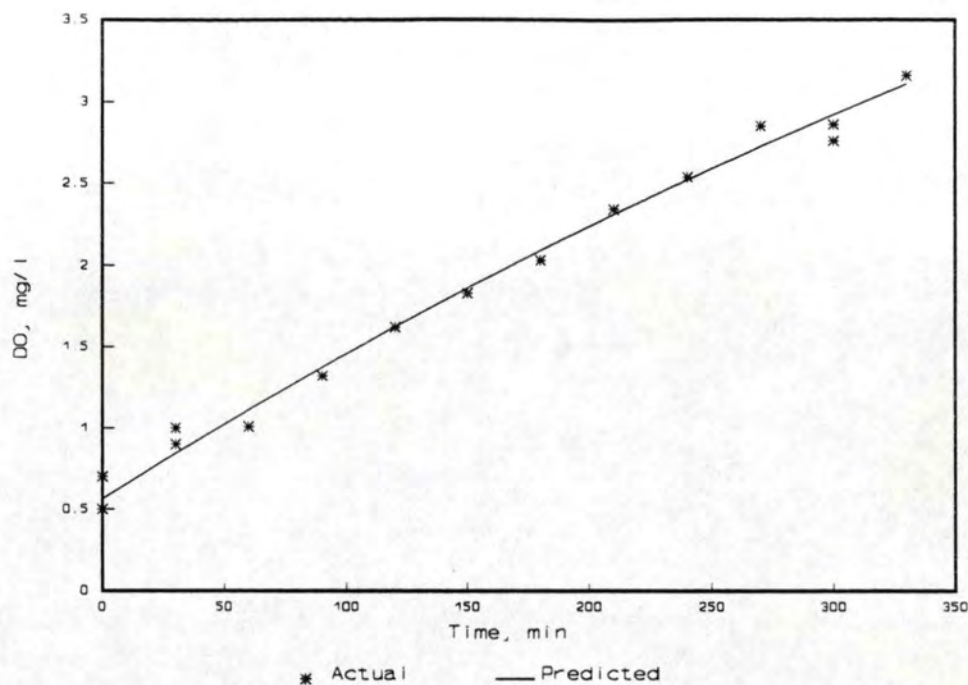
Figure 18. Actual and predicted DO values for reaeration run 2k.

The reaeration coefficient at test temperature, K_{laT}, was standardized to 20°C using Equation 29, with a value of 1.024 for θ (McCutcheon, 1989);

$$K_{laT} = K_{la20}\theta^{(T-20)} \quad .$$
(29)

The oxygen transfer coefficient K was calculated from K_{la} as follows:

$$K = K_{la} * \frac{V}{A}$$
(30)

where

    K = oxygen transfer coefficient, m/hr;

    K_{la} = reaeration coefficient, /hr;

    V = test volume, m³; and

    A = surface area available for gas transfer, m².

The K_{20} values were found to range from 0.033 - 0.170 m/hr (Table 7).

Table 7. Estimates of reaeration and oxygen transfer coefficient.

Run	v_w m/s	$v_{wind10m}$ m/s	K_{laT} hr^{-1}	Standard Error %	K_{la20} hr^{-1}	K_{20} m/hr
2k	0.0313	2.28	0.0822	2.0	0.0671	0.0369
2l	0.0313	2.36	0.0839	2.1	0.0705	0.0447
2n	0.0313	1.94	0.0665	2.9	0.0546	0.0330
2f	0.0813	2.50	0.0720	3.1	0.1028	0.0565
2h	0.0813	3.76	0.0884	1.5	0.1069	0.0545
2b	0.1250	2.56	0.1980	2.5	0.2366	0.1400
2e	0.1250	1.43	0.1572	1.2	0.1878	0.1030
2c	0.1875	1.81	0.2872	1.6	0.3312	0.1660
2d	0.1875	2.74	0.2652	0.7	0.3095	0.1700

v_w = water velocity; $v_{wind,10m}$ = wind velocity at 10 m height.

A nonlinear model was proposed to model the increase in K with increasing wind velocity at each level of water velocity (Equation 31);

$$K = \frac{\beta * v_{wind}}{v_w - \gamma} + \alpha v_w \qquad (31)$$

where

K = oxygen transfer coefficient, m/hr;

v_{wind} = wind velocity at 10 m height, m/s;

v_w = water velocity, m/s.

The calculated F statistic for this model is less than the tabulated $F_{.05,6,3}$ of 234, but greater than the $F_{.10,6,3}$ value of 58 (Table 8); therefore, the model does not adequately describe the data at the 95% level of significance but does at the 90% level. More data

are needed to determine if this model is appropriate to represent the oxygen transfer coefficient as a function of wind and water velocity.

Table 8.   Parameter estimates for nonlinear model (Equation 31).

Parameter	Estimate	Standard Error	F
α	0.8643	0.1757	103.8
β	-0.0004322	0.002330	
γ	0.2581	0.3418	

A multiple linear regression model (Equation 32) was investigated to model the transfer coefficient as a function of wind and water velocity, with parameters described above;

$$K = \alpha + \beta v_w + \gamma v_{wind} \quad . \tag{32}$$

Least squares analysis indicated that wind velocity did not significantly impact K under the narrow range of wind velocities encountered in the reaeration runs (P=.63). The intercept did not contribute to the model (P=.55). The F statistic of 411.7 (P=.0001) was calculated for the one parameter linear model. Therefore, the transfer coefficient was modeled as a function of water velocity (Equation 33) as shown in Figure 19.

$$K = 0.9003 * v_w \tag{33}$$

where

   K = transfer coefficient, m/hr;

   v_w = water velocity, m/s.
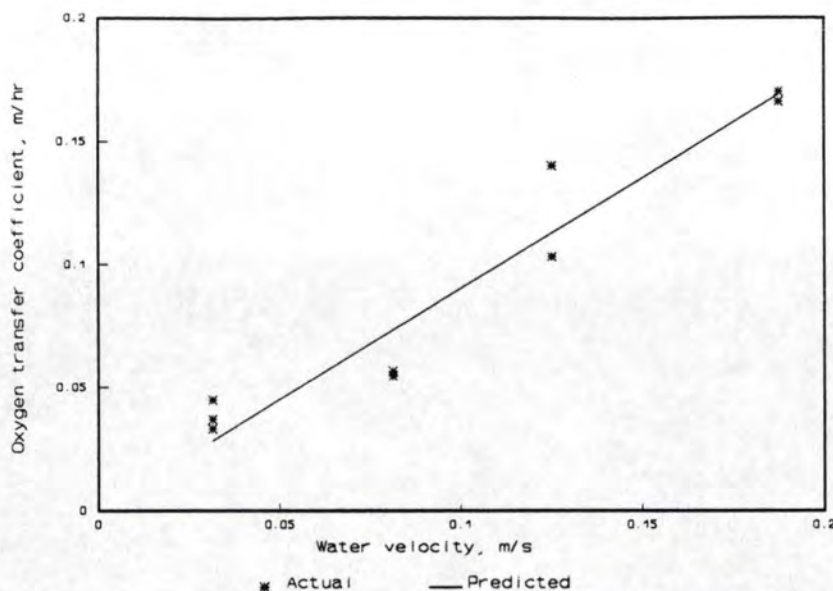
Figure 19. Oxygen transfer coefficient vs water velocity for PAS

The oxygen transfer coefficient as a function of wind velocity at 10 m height was formulated by Banks and Herrara (1977) as

$$K=10^{-6}(8.43v_{wind}^{\frac{1}{2}}-3.67v_{wind}+0.43v_{wind}^{2}) \tag{34}$$

where

K = transfer coefficient, m/s; and

v_{wind} = wind velocity, m/s.

For the north-western region of South Carolina, the average wind speed of 3.1 m/s results in a predicted oxygen transfer coefficient, K, of 0.027 m/hr. The K values measured at the lowest water velocity in the PAS were 0.033-0.045 m/hr. Boyd (1991) noted that wind velocity has a greater impact on surface reaeration in aquaculture ponds as pond size and fetch increases. Therefore, consideration of the impact of wind velocity on surface oxygen transfer may be necessary only for large aquaculture ponds or in areas of high average wind velocities.

Characterization of Algal Biomass

Relationship between SDV and Algal TSS

The relationship between the algal culture secchi disk visibility (SDV) and total suspended solids (TSS) measured with 0.45 μm filter was investigated to determine a predictive model of algal TSS from SDV data. Boyd (1979) suggested a hyperbolic model to express the relationship between algal solids measured with glass fiber filter and SDV (Equation 35);

$$y = \beta x^{-\tau}$$ (35)

where

y = algal solids, mg/l;

x = SDV;

β = 6.03; and

τ = 0.932.

When compared to the pooled data from the 1991 and 1992 seasons which included algae from the divisions Chlorophyta (green), Cyanophyta (blue-green) and Chrysophyta (diatoms), this relationship clearly underestimates the algal solids particularly at SDV values less than 0.3 m (Figure 20). The glass fiber filter technique used to develop Equation 35 may not have collected all of the algal cells that were present for the corresponding SDV value.
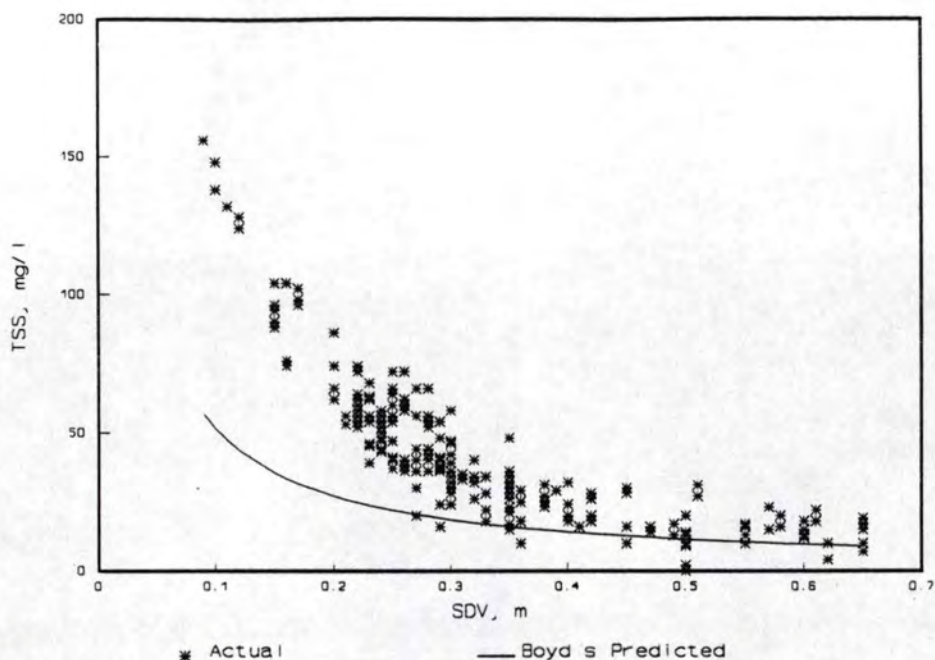
Figure 20. SDV vs algal TSS with hyperbolic model prediction.

When the hyperbolic model proposed by Boyd is fitted to the data using non-linear

least squares analysis, the following parameter estimates of β and τ are obtained:

β = 8.278; and

$\hat{\tau}$ = 1.272.

Since replicate TSS samples were taken at each SDV position, a lack of fit

analysis could be performed to test the hypothesis that the hyperbolic model was

appropriate to represent the data set. The calculated F statistic obtained from the lack of

fit analysis (Table 9) was greater than the tabulated $F_{.05,38,175}$ value of 1.407; therefore, the

hyperbolic model was not appropriate to represent this data set.

Table 9. ANOVA for hyperbolic model lack of fit analysis.

Source	df	Sum of Squares	Mean Square	F
SS Error	213	19,277.5		
SS Within	175	13,116.6	74.95	2.163
SS Lack of Fit	38	6,160.9	162.1	

As an alternative to the hyperbolic model, an exponential model was investigated;

$$y = \alpha + \beta e^{-\lambda x} \tag{36}$$

where

y = algal TSS, mg/l; and

x = SDV, m.

The parameter estimates obtained from non-linear least squares analysis are

$\hat{\alpha} = 11.659$;

$\hat{\beta} = 297.33$; and

$\hat{\lambda} = 8.2212$.

The calculated F value obtained from the lack of fit analysis for the exponential model was less than the tabulated $F_{.05,37,175}$ value of 1.414 (Table 10). In addition, the model predictions of algal TSS as a function of SDV closely match the observations (Figure 21). Therefore, algal TSS can be modeled as a function of SDV using the exponential model given below;

$$TSS = 11.659 + 297.33 e^{-8.2212 \cdot SDV} \tag{37}$$

Table 10. ANOVA for exponential model lack of fit analysis.

Source	df	Sum of Squares	Mean Square	F
SS Error	212	16,675.4		
SS Within	175	13,116.5	74.95	1.283
SS Lack of Fit	37	3,558.8	96.18	
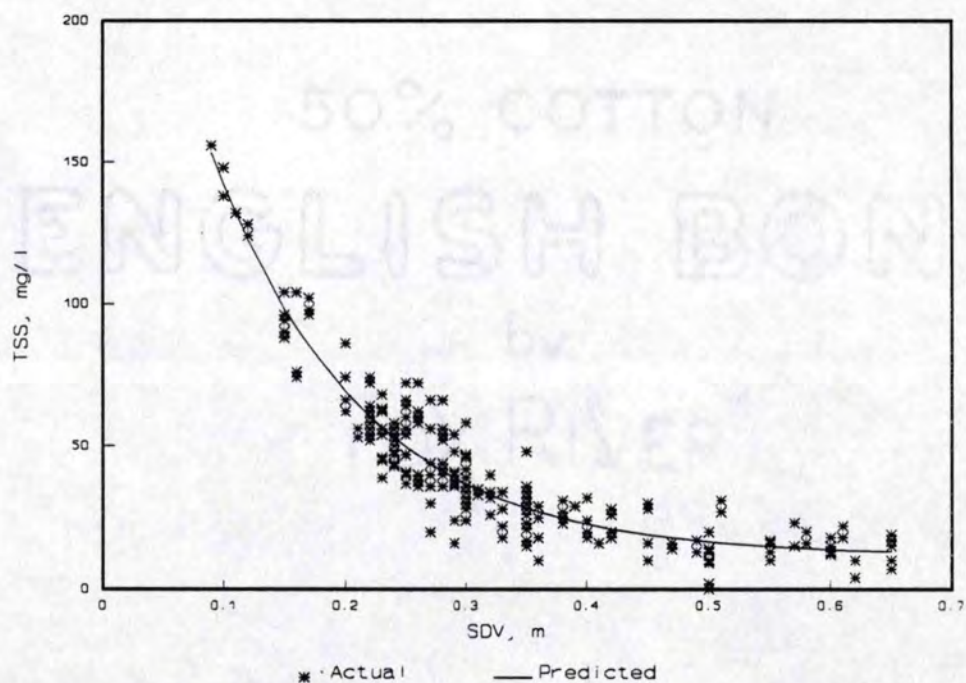
Figure 21. SDV vs algal TSS with exponential model prediction.

Algal Species Composition

Changes in the species composition and form of the algae due to inorganic carbon addition and water velocity were observed. The predominate genus present when no external inorganic carbon was added to the cultures during the 1991 runs was *Merismopedia*, a member of the division Cyanophyta or blue-green algae. *Merismopedia*

was commonly present at densities of 10^7 cells/ml. In tanks which were operated at 0.0313 m/s water velocity, sheets of $\geq$ 50 cells were commonly observed, whereas aggregates of < 5 cells were noted for water velocity of 0.0625 m/s. Species composition was not observed to change during the 1991 season as hydraulic detention time varied from 1.2 to 2.5 days. The color of the cultures cycled from bright green, to olive green to tan. In the 1992 runs when inorganic carbon was added at rates of 1.1 to 1.8 mmol/l/d, the predominate genera present in Tanks 1 and 2 were *Dictyospherium* and *Scenedesmus*, which are both members of the division Chlorophyta, or green algae. In Tanks 3 and 4 during the 1992 runs, where inorganic carbon was again added at rates of 1.1 to 1.8 mmol/l/d, the predominant genus present consistently was *Scenedesmus*. The color of the cultures did not vary as greatly during the carbon addition runs; the color ranged from bright green to olive green to milky green.

The addition of 1.1 to 1.8 mmol/l/d of inorganic carbon to the culture systems appeared to select for green algae species over blue-green algae. The role of inorganic carbon on the selection of algal type has been investigated (King, 1970). His studies indicate that algal growth responds to the free carbon dioxide concentration and that blue-green algae are able to photosynthesize at lower free carbon dioxide concentrations than most green algae. Therefore, blue-green algae have a competitive advantage at low free carbon dioxide concentrations while green algae will predominate at high free carbon dioxide levels (King, 1970). Since blue-green algae have been associated with off-flavor of catfish, culture techniques which discourage the predominance of blue-green algae are preferable for aquaculture systems.

Further, when inorganic carbon was added to the cultures in the 1992 runs, both the water depth and circulator rotational speed appeared to affect the species composition. In Tanks 1 and 2, which were operated at 0.34 m depth and 1 rpm for Run 9 and then at 0.66 m depth and at 2.0 rpm for Run 14 (Table 11), the predominant genera present were *Dictyospherium*, at densities of 10^5-10^6 cells/ml, and *Scenedesmus*, at densities of 10^4-10^5 cells/ml. In Tanks 3 and 4, which were operated at 0.66 m depth and 1 rpm for Run 10 and at 0.66 m depth and 0.5 rpm for 14, the predominant species was *Scenedesmus*, at densities of 10^5-10^6 cells/ml. Since depth and rotational speed affect the degree of light penetration, *Dictyospherium* may have a competitive advantage at high light levels.

Characterization of Algal Productivity

The culture conditions of inorganic carbon addition, water depth, water velocity and retention time were varied to determine the effect on algal productivity (Table 11). For each set of operating conditions, an acclimation period of up to five days was used to allow the cultures to come to a relatively constant biomass after the operational parameters were set. The run was terminated if a mechanical failure occurred that caused a disruption of the culture for an extended period or if unfavorable weather conditions persisted.

Table 11. Culture conditions for algal productivity runs.

Year	Run	Tanks	rpm	Tau, hr	Depth, m	Steady State dates	Inorg. C, mg/l	Inorg. N, mg/l
1991	3	3,4	1	60	0.66	6/11-7/8	10	6
1991	4	3,4	1	30	0.66	7/14-7/26	10	6
1991	5	1,2	0.5	56	0.64	7/17-7/26	10	12
1991	6	3,4	1	27	0.66	8/16-9/19	10	6
1991	7	1,2	0.5	53	0.64	8/19-9/2	10	12
1991	8	1,2	0.5	30	0.64	9/5-9/22	10	7
1992	9	1,2	1	40	0.34	7/6-7/20	29	5
1992	9a	1,2	1	40	0.34	7/9-7/15	28	5
1992	10	3,4	1	40	0.66	7/6-7/20	20	5
1992	10a	3,4	1	40	0.66	7/9-7/15	29	5
1992	10b	3,4	1	41	0.66	7/20-8/5	23	5
1992	10c	3,4	1	72	0.66	8/10-8/18	27	8
1992	14	1,2	2	38	0.66	8/29-9/25	19	5
1992	15	3,4	0.5	44	0.66	8/29-9/25	20	5

Runs which did not achieve steady state conditions due to mechanical or system failures were not included.

The algal culture density and color, an indicator of the relative health of the culture, cycled throughout the course of the runs. Occasions where the culture 'crashed' or suddenly changed color for no apparent reason were noted.

Algal biomass concentrations, expressed as total suspended solids (TSS), were predicted from SDV values (Equation 37). Algal productivity, expressed as daily average carbon fixation rate (ACFIX), was calculated from the biomass value and retention time using Equation 38 (Pipes and Koutsoyannis, 1961). The value of 2.79 is the ratio of g of algal TSS produced per g of carbon fixed through photosynthesis based on the algal cell composition discussed in Chapter II;

$$ACFIX = \frac{(TSS)(d)}{2.79\tau} \tag{38}$$

where

ACFIX = average algal carbon fixation rate, g $C/m^2/d$;

TSS = algal TSS, g/m^3;

d = water depth, m; and

τ = hydraulic retention time, d.

Effect of Inorganic Carbon Addition

The effect of inorganic carbon addition on the algal productivity in the PAS was investigated by comparing the algal TSS levels for the 1991 runs, when no carbon was added to the cultures, to the 1992 runs, when sodium bicarbonate was added to each tank once per day. The mean pH and alkalinity values for the influent water to the PAS used in the 1991 and 1992 experiments are shown in Table 12.

Table 12. PAS influent water chemistry.

Parameter	Mean	S.D.	Sample N
pH	7.2	0.15	27
Alkalinity, mg/l $CaCO_3$	36	3.7	27
Alkalinity, meq/l	0.71	0.074	27

The total inorganic carbon concentration in the influent water to the PAS was calculated from the influent pH and alkalinity (Appendix 4). The mean carbon concentration for the PAS influent water was 0.83 ± 0.11 mmol/l. With the average retention time of 1.2 days used in the zero carbon addition runs, the mass of carbon added to each tank by the influent water averaged 0.71 mmol C/l/day. For the carbon addition comparison, carbon was added at the rate of 0, 0.6 and 1.2 mmol/l/day. Therefore, the total inorganic carbon addition rate due to the influent water and the sodium bicarbonate was 0.71, 1.14 and 1.77 mmol/l/d (Table 13).

Table 13. Conditions for the carbon addition experiment.

Run	Average retention time, days	C added mmol/l/d
4, 6	1.2	0.71
10, 10a, 10b	1.7	1.14
10, 10a	1.6	1.77

Water velocity = 0.0625 m/s; water depth = 0.66 m; influent N = 5.5 mg/l.

The mean algal TSS concentration at the 1.14 and 1.77 mmol/l/d carbon addition rates did not differ from each other, but did differ from the mean TSS value at the 0.71

addition rate (Table 14). However, the ACFIX rates, which are calculated based on the depth and retention time, were not different for the three carbon addition levels (P>.05).

Table 14. Effect of carbon addition on algal productivity.

C added mmol/l/d	n	ACFIX[1] g C/m²/d	S.D.	TSS[1] mg/l	S.D.
0.71	52	5.386[a]	1.986	27.12[a]	10.68
1.14	36	6.269[a]	1.825	44.79[b]	13.18
1.77	12	6.380[a]	1.402	44.79[b]	9.94

[1] Means not sharing a common letter are significantly different using Tukey-Kramer method (P<.05).

When the data were grouped into two carbon addition levels (Table 15), the mean ACFIX and algal TSS were found to differ (P=.016 and P<.001, respectively). The mean ACFIX and TSS values at the combined higher carbon addition rate were 1.17 and 1.65 times the value at the lower addition level. Therefore, increasing the inorganic carbon addition rate from 0.71 to 1.14 mmol/l/d increased the TSS and ACFIX values, but increasing the rate to 1.77 mmol/l/d did not increase algal productivity further, indicating that the cultures were not carbon-limited at inorganic carbon addition rates greater than 1.14 mmol/l/d for the culture conditions and ambient solar radiation levels.

Table 15. Effect of two carbon addition rates on algal productivity.

C addition, mmol/l/d	n	ACFIX[1] g C/m²/d	S.D.[2]	TSS[1] mg/l	S.D.[2]
0.71	52	5.386[a]	1.986[a]	27.12[a]	10.68[a]
1.14, 1.77	48	6.297[b]	1.716[a]	44.79[b]	12.35[a]

[1] Means not sharing a common letter are significantly different using t-test (P<.05).
[2] Values not sharing common letter are significantly different using Folded F statistic for testing equality of variances (P<.05).

Effect of Water Depth

Algal biomass and average carbon fixation rates were compared at water depths of 0.34 and 0.66 m (Table 16). The data for the 0.45 m run were omitted due to the presence of a *Euglena*-like culture, which formed a layer on the water surface thereby preventing light penetration through the water column.

Table 16. Conditions for water depth comparison.

Run	Tanks	Water depth, m	Retention time, days
9	1,2	0.32-0.37	1.5-1.9
10	3,4	0.65-0.67	1.6-1.7

C addition = 1-2 mmol/l/d; water velocity = 0.062 m/s; influent N = 4.6 mg/l;

Algal carbon fixation rate was affected by culture depth (Table 17). The ACFIX and TSS values differed for the 0.34 and 0.66 m depths (P=.0008 and P<.0001). The mean ACFIX and TSS for the 0.34 m depth were 1.23 and 2.39 times, respectively, the mean values for the 0.66 m depth. If the total light absorbed was independent of culture depth, then it would be expected that the carbon fixation rate calculated on a surface area basis for a culture grown at a 1 meter depth would be the same as the rate for a culture grown at a 0.5 m depth, and the algal biomass per unit volume would double when the culture depth was halved. However, this result reveals that the carbon fixation rate was increased by decreasing culture depth, most likely due to increased exposure to solar radiation at the shallow depth.

Table 17. Effect of water depth on algal productivity.

Run	Water depth, m	n	ACFIX[1] g C/m²/d	S.D.[2]	TSS[1] mg/l	S.D.[2]
9	0.34	26	7.721[a]	1.264[a]	105.3[a]	16.75[a]
10	0.66	26	6.287[b]	1.598[a]	44.00[b]	11.36[a]

[1] Means not sharing a common letter are significantly different using t-test (P< .05).
[2] Values not sharing a common letter are significantly different using Folded F statistic for testing equality of variances (P<.05).

Effect of Mixing Level

Algal biomass was measured at water velocities of 0.0313, 0.0625 and 0.125 m/s, corresponding to circulator rotational speeds of 0.5, 1.0 and 2.0 rpm (Table 18).

Table 18. Conditions for mixing comparison.

Run	Water velocity, m/s	Water depth, m
15	0.0313	0.65-0.68
10	0.0625	0.65-0.67
14	0.125	0.64-0.68

Retention time = 1.7 days; C addition = 1-2 mmol/l/d; influent N = 5 mg/l.

The mean carbon fixation rate and algal TSS for cultures grown at 0.0313 and 0.0625 m/s water velocity did not differ from each other, but did differ from the rate for cultures grown at 0.125 m/s (Table 19).

Table 19. Effect of level of mixing on algal productivity.

Run	Water velocity, m/s	n	ACFIX[1] g C/m^2/d	S.D.	TSS[1] mg/l	S.D.
15	0.0313	44	6.695^a	2.499	52.10^a	19.54
10	0.0625	48	6.297^a	1.716	44.79^a	12.35
14	0.125	44	9.889^b	2.794	65.91^b	18.49

[1] Means not sharing a common letter are significantly different using Tukey-Kramer method (P<.05).

When the data were grouped into two levels based on level of mixing, LOW for 0.0313 and 0.0625 m/s water velocity and HIGH for 0.125 m/s, the mean ACFIX and TSS values for the two mixing levels were found to differ (P=.0001). The carbon fixation rate for the HIGH level was 1.52 times the fixation rate for the LOW level (Table 20).

Table 20. Effect of LOW and HIGH level of mixing on algal productivity.

Runs	Water velocity	N	ACFIX[1] g C/m^2/d	S.D.[2]	TSS[1] mg/l	S.D.[2]
15, 10	LOW	92	6.487^a	2.124^a	48.29^a	16.51^a
14	HIGH	44	9.889^b	2.794^b	65.91^b	18.49^a

[1] Means not sharing a common letter are significantly different using t-test (for equal variances) or Satterthwaite's t approximation (for unequal variances) (P<.05).
[2] Values not sharing a common letter are significantly different using Folded F statistic for testing equality of variances (P<.05).

Increasing the mixing velocity may increase algal productivity by increasing the exposure of the algal cultures to sunlight, by decreasing diffusional barriers around the algal cells by decreasing the liquid film layer, or by increasing the rate of oxygen transfer from the bulk fluid to the atmosphere. Bosca et al. (1991) found that algal cultures mixed at approximately 0.25 m/s were more productive than non-mixed cultures. Carbon

fixation rates were more than two times greater for the mixed cultures at low light levels occurring near dawn and dusk. The culture depth for the study was 50 cm. Persoone et al. (1980) reported an increase in algal density due to mixing of culture with an air lift mixer. The algal densities at the two highest mixing regimes (14 and 10.5 l/min) were nearly identical and approximately 1.2 times greater than the density at the lower mixing level (7.1 l/min) after 17 days and approximately 1.3 times greater than the density for the static (no mixing) condition after 9 days (Persoone et al., 1980). Increased algal productivity with increased circulator mixing speed was also noted by Richmond et al. (1980). Algal growth rates were greater at a mixer speed of 30 rpm than at 15 rpm. The corresponding water velocities were not given for Persoone et al. (1980) or Richmond et al. (1980).

However, Weissman et al. (1988) reported no difference in algal productivity for *Chlorella* cultures at water velocities of 1, 3, 10, 13 and 30 cm/s. The ponds were operated at nearly constant pO_2 and pH of 7.3, and water depth of 20 cm. Shelef et al. (1968) summarized research conducted on the effect of mixing on the light intensity gradient as a function of depth in algal cultures. They concluded that since the response of algal cells to light is practically instantaneous, (reaction times on the order of 10^{-9} to 10^{-3} seconds for photochemical reactions), then the effect of conventional mixing on the light intensity gradient would be negligible. However, the models that they constructed incorporating this conclusion were used to predict algal productivity in extremely shallow cultures (<2 cm). Therefore, algal productivity may be affected by the level of mixing due to the impact of mixing on the light intensity gradient in 30 - 60 cm deep cultures.

Effect of Cell Retention Time

Algal productivity was measured for hydraulic retention times of approximately 5, 2.5, and 1.2 days. The data for the 5 day retention time were obtained in 1990, when the glass fiber filters were used to measure algal TSS, and were therefore not comparable to the results obtained at the 2.5 and 1.2 day retention times, when the 0.45 μm filters were used. In addition, more frequent system failures occurred in the 1990 run which caused less consistent algal growth. Consequently, the data obtained from the 5 day retention time were not included in this analysis. The 1.2 and 2.5 day retention time runs were operated at constant influent nitrogen concentration (Table 21).

Table 21. Conditions for the retention time comparison.

Run	Retention time, days	Influent N, mg/l	Water depth, m
4, 6	1.2	6.1	0.66
3	2.5	6.5	0.66

Water velocity = 0.062 m/s; C addition= 0.7 mmol/l/d.

The results of these runs indicate that algal productivity and biomass differed at the 1.2 and 2.5 day retention times (Table 22). Pipes and Koutsoyannis (1961) determined that in laboratory cultures grown at very low light levels, algal productivity was constant while algal biomass was a linear function of retention time (Figures 22 and 23). However, Shelef et al. (1968) found that for shallow culture depths, productivity reached a maximum at 24 - 30 hour retention time. Since the data from the 5 day retention time run could not be included in the analysis, carbon fixation rate as a function

of retention time cannot be fully modeled. Further data is needed to conclusively model

the productivity of deep cultures as a function of retention time.

Table 22. Effect of retention time on algal productivity.

Runs	Retention time, days	n	ACFIX[1] g C/m²/d	S.D.[2]	TSS[1] mg/l	S.D.[2]
4, 6	1.2	52	5.386[a]	1.986[a]	27.12[a]	10.68[a]
3	2.5	50	4.124[b]	0.8422[b]	43.93[b]	9.009[a]

[1] Means not sharing common letter are significantly different using t-test (for equal variances) or Satterthwaite's t approximation (for unequal variances) ($P < .05$).
[2] Values not sharing common letter are significantly different using Folded F statistic testing equality of variances ($P < .05$).

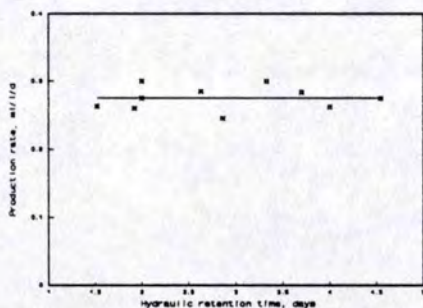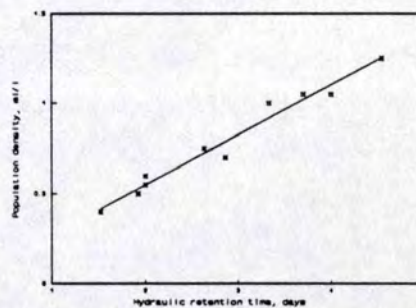Figure 22. Algal productivity vs retention time for light-limited cultures (Pipes and Koutsoyannis, 1961).

Figure 23. Algal biomass vs retention time for light-limited culture (Pipes and Koutsoyannis, 1961).

Characterization of Algal Oxygen Production

Photosynthetic oxygen production rates as a function of solar radiation throughout

the day were measured periodically as the operational parameters were varied. The model

chosen to represent oxygen production as a function of light intensity is given as (Steele 1962, Lehman 1975, Welch 1980):

$$P_{20} = (P_{max20}) \frac{I}{I_{opt}} e^{(1 - \frac{I}{I_{opt}})} \tag{39}$$

where

P_{20} = photosynthetic oxygen production, 20°C, mg O_2/mg TSS/hr;

P_{max20} = maximum photosynthetic oxygen production, 20°C, mg O_2/mg TSS/hr;

I = effective light intensity, W/m^2; and

I_{opt} = optimal or saturating effective light intensity, W/m^2.

This equation models increased oxygen production with increased light intensity up to the optimum or saturating light intensity, beyond which oxygen production decreases due to inhibitory light levels.

The value of the effective light intensity can be calculated from the complete solar spectrum surface intensity according to Beer's Law;

$$I = I_o e^{(-Kd)} \tag{40}$$

where

I_O = complete spectrum surface intensity, W/m^2;

K = extinction coefficient (/m); and

d = depth, m.

The extinction coefficient is a function of the wavelength of light, suspended solids and algae species in the water column. Parsons (1984) gives the following expression for estimating the average extinction coefficient, K;

$$K = 1.7/SDV \tag{41}$$

where SDV = secchi disk visibility, m.

The model can be fitted to the data obtained from individual days using non-linear least squares analysis. For example, the maximum oxygen production rate for Tanks 1 and 2 on 9/14/91 was approximately 0.1 mg O_2/mg TSS/hr (Figure 24). The parameter estimate for P_{max20} was determined to be 0.096 mg O_2/mg TSS/hr (Table 23).
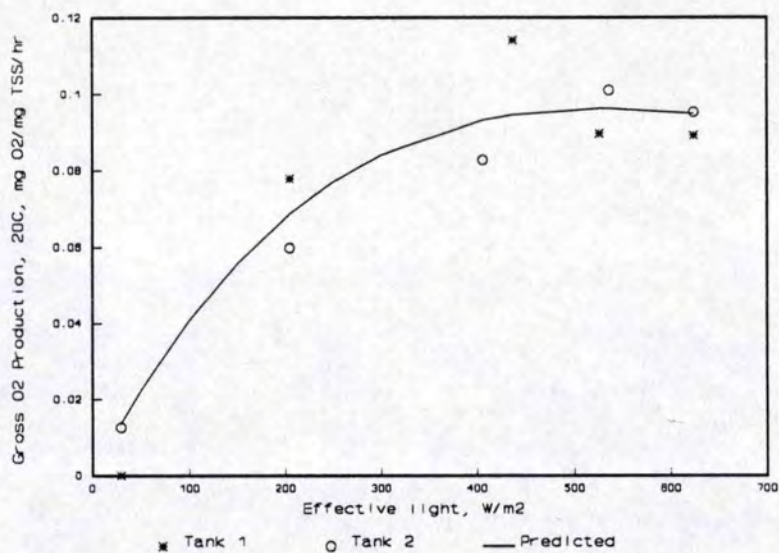
Figure 24. Oxygen production for Tanks 1 and 2, 9/14/91.

Table 23. Parameter estimates for Tanks 1 and 2, 9/14/91.

Parameter	Estimate	Approximate standard error
P_{max20}, mg O_2/mg TSS/hr	0.09633	0.004444
I_{opt}, W/m^2	530.6	85.83

The oxygen production profiles for Tank 3 and 4 for 9/14/91 (Figures 25 and 26) differed greatly even though the culture conditions were the same. The production profile for Tank 3 did not exhibit the same trend as Tanks 1, 2 and 4, and the iterative procedure

used to determine the parameter estimates for the light model did not converge. The maximum oxygen production for Tank 4 is half the value obtained for Tanks 1 and 2.
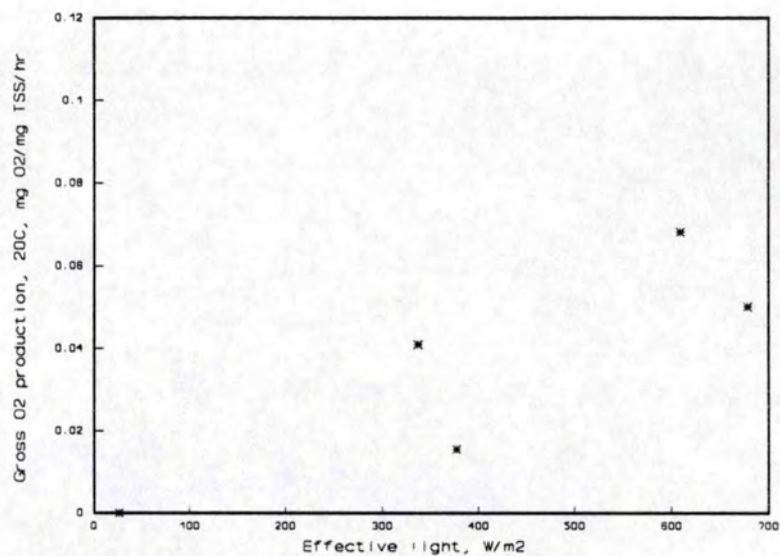
Figure 25. Oxygen production for Tank 3, 9/14/91.
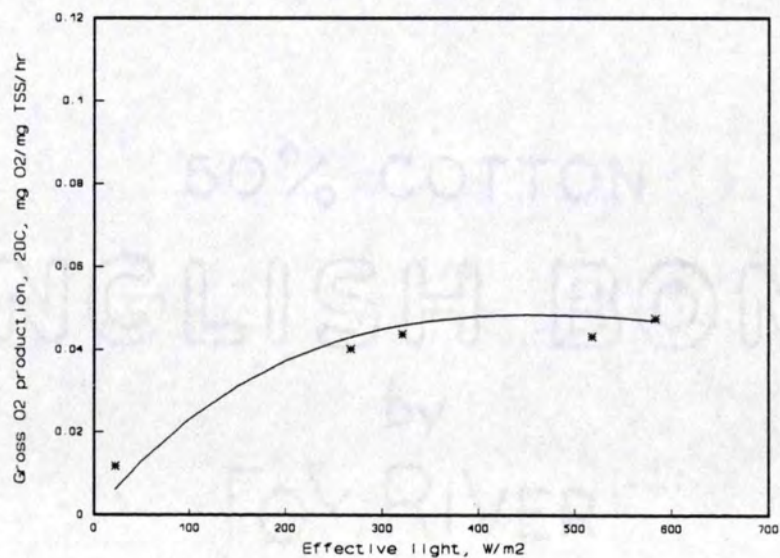
Figure 26. Oxygen production for Tank 4, 9/14/91.

Since the algal cultures' response to light in the 1991 and 1992 seasons varied greatly, the method chosen to characterize all of the data was to model the average and maximum oxygen production response (Figures 27 and 28). The solar radiation values predicted for the missing 1992 data were not included in this analysis; therefore, no data are shown for low light levels (Figure 28). Fitting the inhibitory light model to the data using least squares analysis was used to represent the average response. The maximum response curve was based on a visual 'best fit' of the maximum production values.
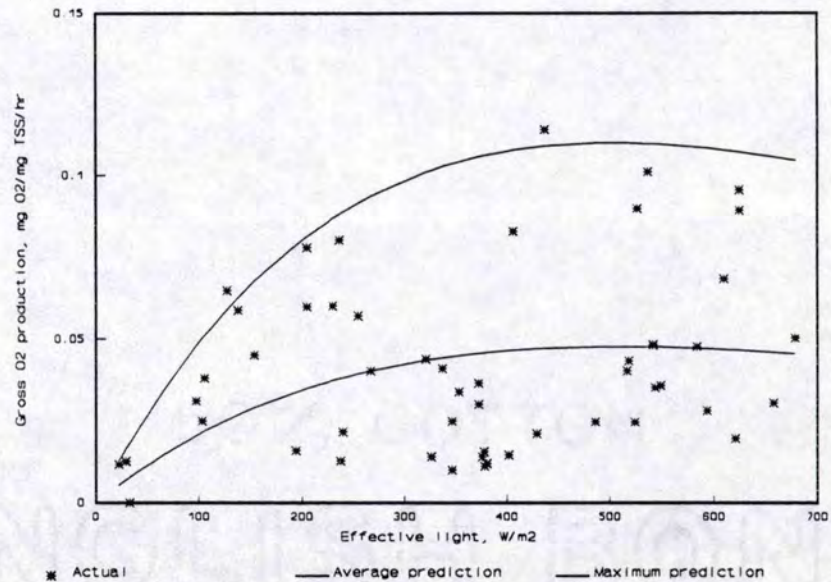
Figure 27. Oxygen production for pooled 1991 data.

The average and maximum oxygen production values were greater for the 1992 data than for the 1991 data (Tables 24 and 25). This result is consistent with the finding that average carbon fixation rates were 1.2 times greater in the PAS for inorganic carbon addition rates of 1.1 - 1.7 mmol/l/d than for 0.7 mmol/l/d (see Table 15).
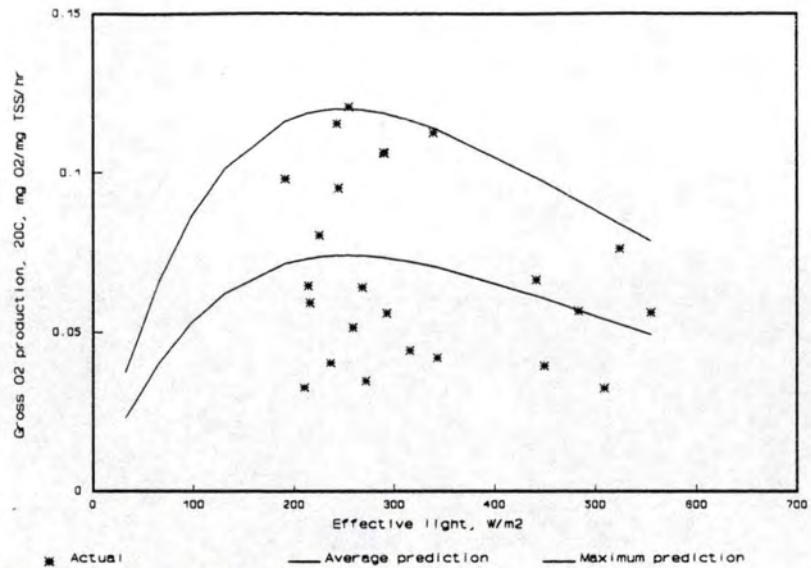
Figure 28. Oxygen production for pooled 1992 data.

Table 24. Parameter estimates for 1991 oxygen production data.

Parameter	Average response estimate	Approximate standard error	Maximum response value
P_{max20}, mg O_2/mg TSS/hr	0.04755	0.004650	0.11
I_{opt}, W/m^2	500	150	500

Retention time=1-3 days; water velocity=0.0313-0.0625 m/s; depth=0.64 m; C addition=0.7 mmol/l/d.

Table 25. Parameter estimates for 1992 oxygen production data.

Parameter	Average response estimate	Approximate standard error	Maximum response value
P_{max20}, mg O_2/mg TSS/hr	0.07413	0.006842	0.12
I_{opt}, W/m^2	253.0	56.87	250

Retention time=1.5-2 d; water velocity=0.0313-0.125 m/s; depth=0.31-0.68 m; C addition=0.7-1.8 mmol/l/d.

Utilizing the algal cell composition proposed by Redfield et al. (1963) and the P_{max20} estimates for 1991 and 1992, a maximum specific growth rate, μ_{max20}, of 0.0887/hr or 2.13/day and 0.0968/hr or 2.32/day was predicted for 1991 and 1992 respectively (Table 26). These values lie within the range of values reported of 1.32/day (Goldman, 1974) to 2.08/day (Lehman, 1975) to 2.4/day (Larsen et al, 1978).

Table 26. Parameter estimates for 1991 and 1992 algal cultures.

Parameter	1991 estimate	1992 estimate
P_{max20}, mg O_2/mg TSS/hr	0.11	0.12
μ_{max20}, /hr	0.0887	0.0968

Characterization of Algal Respiration Rates

Measurements of the 24-hour algal respiration rate corrected to 20°C (AR_{20C}) were made as a function of water velocity, water depth, hydraulic retention time and carbon addition. The mean respiration rate for cultures grown at water velocities of 0.0313, 0.0625 and 0.125 m/s did not differ (Table 27). The lack of a significant result may be due to the small sample size for each of the treatments. In the comparison of algal productivity as a function of water velocity, the values at 0.0313 and 0.0625 m/s did not differ from each other, but did differ from the 0.125 m/s values. The mean respiration rates and standard deviations for the two lowest water velocities were similar and nearly twice as great as the rate and standard deviation for the highest water velocity. More data are needed to characterize the respiration rate as a function of water velocity.

Table 27. Respiration rates for water velocity comparison[1].

Run	Water velocity, m/s	n	AR_{20C},[2] mg O_2/mg TSS/hr	S.D.
15	0.0313	10	0.002198[a]	0.001544
10	0.0625	6	0.002140[a]	0.001298
14	0.125	10	0.001303[a]	0.000624

[1] Water depth=0.66 m; Carbon addition=1.1-1.8 mmol/l/d; retention time=1.5-1.8 d.
[2] Means not sharing a common letter are significantly different using Tukey-Kramer method (P<.05).

The mean algal respiration rates at the 0.34 and 0.66 m water depth were not found to differ (Table 28).

Table 28. Algal respiration rates for water depth comparison[1].

Run	Water depth, m	n	Mean AR_{20C}[2] mg O_2/mg TSS/hr	S.D.[3]
9	0.34	6	0.001596[a]	0.001042[a]
10	0.66	6	0.002140[a]	0.001298[a]

[1] Water velocity=0.0625 m/s; C addition=1.1 - 1.8 mmol/l/d; retention time=1.5-1.9 d.
[2] Means not sharing common letter are significantly different using t-test (P<.05).
[3] Values not sharing common letter are significantly different using Folded F statistic testing equality of variances (P<.05).

Comparison of the respiration rate as a function of retention time revealed that the mean rate did not vary at hydraulic retention times of 1.2 and 2.4 days (Table 29).

Table 29. Algal respiration rates for retention time comparison[1].

Run	Retention time, days	n	Mean AR_{20C}[2] mg O_2/mg TSS/hr	S.D.[3]
4,6,8	1.2	30	0.003504[a]	0.004468[a]
3,7	2.4	18	0.002318[a]	0.001202[b]

[1] C addition=0.7 mmol/l/d; water velocity=0.0625 m/s; water depth=0.61-0.68 m.
[2] Means not sharing common letter are significantly different using Satterthwaite's t approximation (for unequal variances) ($P<.05$).
[3] Values not sharing common letter are significantly different using Folded F statistic testing equality of variances ($P<.05$).

The difference in algal respiration during the day and night was also compared for 15 paired samples (Table 30).

Table 30. Algal respiration rates for day/night comparison.

Period	n	Mean AR_{20C} mg O_2/ mg TSS/hr	S.D.
Day	15	0.002578	0.003282
Night	15	0.004685	0.003244

The difference between the mean day and night respiration values was determined to be significant (Table 31).

Table 31. Difference in day/night respiration rate.

Mean Difference in AR_{20C} mg O_2/mg TSS/hr	Standard Error	P
0.002107	0.0004138	0.002

The mean 24-hour respiration rate for the entire pooled 1991 and 1992 data set was determined to be 0.00299 mg O_2/mg TSS/hr (N=82). Jewell (1977) reported an algal respiration rate of 0.0071 mg O_2/mg algal biomass/hr. Cohen (1990) reported an average algal respiration rate of 0.88 mg O_2/mg chlorophyll a/hr, which corresponds to an respiration rate of 0.0132 mg O_2/mg algal biomass/hr assuming chlorophyll a constitutes 1.5% of algal dry weight (Standard Methods, 1989, pg 10-40). The average 24-hour respiration value of 0.0030 mg O_2/mg TSS/hr determined for the PAS is well below these respiration values.

CHAPTER VI

DEVELOPMENT OF DYNAMIC MODEL OF ALGAL PRODUCTIVITY

AND DISSOLVED OXYGEN PROFILE IN THE PAS

Model Basis

The basis for the PAS model is a mass balance of algal biomass. The PAS configuration for the current research was to waste algal biomass from the system through the effluent flow. No other biomass separation or biomass removal techniques were used. Therefore, the hydraulic retention time (volume/flow rate) and the cell retention time (volume/wastage flow rate) were equal. The mass balance of algal cells in the PAS can be represented by the following equation:

$$V\frac{dX}{dt} = QX_o - QX \pm \Sigma rV \tag{42}$$

where

V = algal culture tank volume, l;

t = time, h;

X, X_o = algal TSS concentration in tank and influent flow, mg/l;

Q = flow rate through tank, l/hr; and

Σr = all reaction rates involving algal biomass occurring within tank, mg/l/hr.

The rates of algal biomass formation and cell loss included in the model for the current configuration of the PAS are as follows:

Algal growth rate. The rate of algal growth, r_{AR}, is represented as

$$r_{AR} = \mu X \tag{43}$$

where μ = algal specific growth rate, /hr.

Algal cell decay rate. The algal cell decay rate is assumed to be neglible due to the relatively short retention times used in the PAS.

Algal settling rate. The settling rate is assumed to be neglible in the water velocity range used of 0.0325 - 0.125 m/s. Settling rates would need to be considered in static water conditions.

Grazing rate. The predation or grazing rate due to filter feeding organisms is not included in current model since filter feeding fish were not used. Effect of grazing by zooplankton was assumed to be negligible.

At steady-state, the diel-averaged algal biomass concentration is constant and $dX/dt \equiv 0$. Assuming that the concentration of algal cells in the influent flow is zero, Equation 42 simplifies to

$$\mu = \frac{1}{\tau} \tag{44}$$

where

μ = algal specific growth rate, /hr; and

τ = hydraulic retention time, h.

Therefore, at steady state, the algal growth rate is determined by the hydraulic retention time. During the start-up of a continuous algal culture, the algal biomass will

be less than the steady state biomass concentration and the actual growth rate will be greater than the steady state growth rate, resulting in an increase in the biomass concentration with time. As steady state conditions are reached, the diel-averaged growth rate will approach the required growth rate and the average biomass level will become constant. Therefore, the PAS model can be used to simulate both non steady state and steady state conditions. For non steady state conditions, the value chosen for the initial biomass can be set to any value and the response of the system will be simulated. To simulate steady state conditions, the initial biomass value entered in the model must be raised or lowered until the calculated growth rate is equal to the growth rate required for steady state, based on $1/\tau$.

In addition, in outdoor cultures the absence of solar radiation will limit algal growth to roughly 12 hours per day; therefore, the average day time algal growth rate will equal two times the diel-averaged growth rate. The algal growth rate throughout the day will be determined as the minimum of the light-limited, carbon-limited, and nitrogen-limited growth rates.

Dynamic Responses

The dynamic responses are predicted by calculating the mass balance equations for each simulated 15-minute time interval.

Algal Biomass

Although the diel-averaged algal biomass concentration will reach a steady-state level, during the course of the day the biomass concentration will change as solar

radiation and nutrient levels change. The dynamic response of algal biomass can be represented as

$$\frac{dX}{dt} = \mu X - \frac{X}{\tau} \quad .$$
(45)

The solution to the dynamic response can be approximated by using small time increments as shown below;

$$\frac{\Delta X}{\Delta t} = \mu X - \frac{X}{\tau}$$
(46)

or

$$\Delta X = (\mu X - \frac{X}{\tau}) \Delta t \quad .$$
(47)

The change in biomass concentration, ΔX, equals the biomass concentration at time 2 minus the biomass at time 1 ($X_2 - X_1$). Equation 47 can be rearranged to predict the biomass at time 2;

$$X_2 = X_1 + (\mu - \frac{1}{\tau}) X_1 \Delta t \quad .$$
(48)

Dissolved Oxygen

The mass balance of dissolved oxygen is given as

$$V\frac{dDO}{dt} = QDO_o - QDO \pm \Sigma rV$$
(49)

where

DO$_o$ = dissolved oxygen concentration in influent flow, mg/l; and

DO = dissolved oxygen concentration, mg/l; and

Σr = all reactions rates involving oxygen occurring within tank, mg/l/hr.

Rearrangement of Equation 49 yields

$$DO_2 = DO_1 + (\frac{DO_o - DO_1}{\tau} \pm r) \Delta t \quad . \tag{50}$$

The reactions which affect the oxygen concentration are given below.

Surface oxygen transfer. The rate of oxygen transfer, r_{OT}, across an air-water interface can be calculated as

$$r_{OT} = \frac{KA}{V} (DO_{sat} - DO) \tag{51}$$

where

r_{OT} = rate of surface oxygen transfer, mg/l/hr or (g/m^3/hr).

K = oxygen transfer coefficient, m/hr;

A = surface area of gas transfer, m^2;

V = culture volume, m^3;

DO_{sat} = saturation dissolved oxygen concentration, mg/l; and

DO = dissolved oxygen concentration, mg/l.

The saturation DO concentration, DO_{sat}, is calculated using Equation 52 (modified from Standard Methods, 1989);

$$DO_{sat} = e^Q \tag{52}$$

where

$$Q = (-139.34 + \frac{1.5757 * 10^5}{TEMPK} - \frac{6.6423 * 10^7}{TEMPK^2} + \frac{1.2438 * 10^{10}}{TEMPK^3} - \frac{8.6219 * 10^{11}}{TEMPK^4}) * EF \tag{53}$$

and

DO_{sat} = saturation DO concentration at elevation, mg/l;

TEMPK = temperature, K; and

EF = elevation correction factor.

The elevation correction factor, EF, is included to correct the saturation DO concentration for atmospheric pressure changes due to elevation. DO_{sat} been found to decrease approximately 7% per 610 m (2000 ft) (McCutcheon, 1989), or roughly 1.15% per 100 m. Therefore, EF can be calculated as

$$EF = \frac{100 - (0.0115 \times EL)}{100} \qquad (54)$$

where EL = elevation, m.

The oxygen transfer coefficient, K, can be determined as a function of water velocity and wind. Measurements made in the PAS revealed that wind did not significantly affect K in the water velocity range used of 0.0325-0.125 m/s. Therefore, K is modeled as a function of wind only if water velocity is zero.

The transfer coefficient as a function of wind velocity was modeled by Banks and Herrara (1977) as given below:

$$K = 0.0036 (8.43 v_{wind}^{0.5} - 3.67 v_{wind} + 0.43 v_{wind}^2) \qquad (55)$$

where

K = transfer coefficient, m/hr; and

v_{wind} = wind velocity at 10 m height, m/s.

The transfer coefficient as a function of water velocity for the PAS is given as

$$K = 0.9003 * v_w \qquad (56)$$

where v_w = water velocity, m/s.

Photosynthetic oxygen production. According to the Redfield et al. (1963) equation for algal cell composition, 1.24 g of oxygen are produced per g of algal biomass fixed during photosynthesis. Therefore, the rate of oxygen production, r_{OP}, is

$$r_{OP} = \mu * 1.24 * TSS \quad . \tag{57}$$

Algal respiration. Algal respiration, AR, measured in the PAS averaged 0.002 and 0.004 mg DO/mg TSS/hr during the day and night, respectively. The rate of oxygen consumed due to algal respiration, r_{AR}, is

$$r_{AR} = AR * TSS \quad . \tag{58}$$

Fish respiration. Catfish respiration rates were measured by Andrews and Matsuda (1975) as a function of fish weight, feeding conditions and temperature. Assuming that fasted conditions occur during the night and fed conditions occur during the day, Equations 59 and 60 were formulated using Andrews and Matsuda's data to predict catfish respiration as a function of fish weight and feeding conditions, at 26 °C. Changes in respiration due to temperature were not included in the current model.

$$FRD = 1.761 * FISHWT^{-0.2108} \tag{59}$$

$$FRN = 1.263 * FISHWT^{-0.2294} \tag{60}$$

where

FRD, FRN = fish respiration during day or night, g DO/kg fish/hr; and

FISHWT = fish weight, g.

The rate of oxygen consumed by fish respiration, r_{FR}, is therefore

$$r_{FR} = \frac{FR*FISHLOAD}{DEPTH} * \frac{ha}{10,000m^2} \tag{61}$$

where FISHLOAD = fish loading, kg/ha.

Fish waste oxygen demand. Oxygen consumed by fish wastes was quantified by Boyd (1985) as 0.83 g of chemical oxygen demand (COD) produced per g of fish feed. The oxygen demand of the fish waste in the pond be calculated as follows:

$$FWOD = 0.83 \times FEEDRATE \tag{62}$$

where

FWOD = fish waste oxygen demand, g DO/g fish/d;

FEEDRATE = feeding rate, g feed/g fish/d; and

0.83 = factor of g COD produced/g feed.

The feed rate used is based on Lovell (1977) (Table 32).

Table 32. Catfish feeding rates used in model.

FISHWT, g	FEEDRATE, g feed/g fish/d
< 27	0.035
27<=FISHWT<=450	$0.035-(3.889\times10^{-5}\times FISHWT)$
> 450	.0175

The rate of oxygen consumed by fish waste, r_{WOD}, is therefore

$$r_{WOD} = \frac{FWOD*FISHLOAD}{DEPTH} * \frac{1000g}{kg} * \frac{ha}{10,000m^2} * \frac{day}{24hr} \tag{63}$$

Therefore, the total oxygen balance can be written as

$$DO_2 = DO_1 + \frac{DO_o - DO_1}{\tau} + r_{OT} + r_{OP} - r_{AR} - r_{FR} - r_{WOD})\Delta t \quad . \tag{64}$$

Nitrogen

The mass balance of nitrogen in the PAS can be written as follows:

$$\frac{dN}{dt} = \frac{N_o - N}{\tau} \pm \Sigma r \tag{65}$$

where

N_o, N = inorganic nitrogen concentration in influent flow and tank, mg/l; and

Σr = all reactions involving nitrogen occurring in tank, mg/l/hr.

The rates of nitrogen formation and loss from the culture system included in the model

are as follows:

Nitrogen excretion by fish. Boyd (1985) measured the amount of nitrogen

excreted by catfish as 0.035 g N/kg fish/hr. The rate of nitrogen excreted by fish, r_{NE}, is

given as

$$r_{NE} = \frac{0.035 * FISHLOAD}{DEPTH} * \frac{ha}{10,000m^2} \quad . \tag{66}$$

Nitrogen uptake by algae. Nitrogen uptake by algae is based on the algal cell

composition (Redfield et al., 1963) of 0.0631 mg N/mg algal biomass. The rate of n

nitrogen uptake by algal growth, r_{NU}, is given as

$$r_{NU} = 0.0631 * TSS * \mu \quad . \tag{67}$$

The concentration of nitrogen can be calculated as

$$N_2 = N_1 + \frac{N_o - N_1}{\tau} + r_{NE} - r_{NU} \quad .$$

(68)

Inorganic Carbon

The mass balance of total inorganic carbon in the PAS can be written as follows:

$$\frac{dC}{dt} = \frac{C_o - C}{\tau} \pm \sum r$$

(69)

where

C_o, C=inorganic carbon concentration in influent flow and tank, mg/l; and

$\sum r$ = all reactions involving inorganic carbon occurring in the tank, mg/l/hr.

The reactions rates involving inorganic carbon included in the model are as follows:

Carbon uptake by algae. Carbon uptake by algae is based on the Redfield et al. (1963) ratio of 0.358 g C/g algal biomass. The rate of carbon uptake, r_{CU}, is given as

$$r_{CU} = 0.358 * TSS \quad .$$

(70)

Other gains and losses of inorganic carbon such as surface transfer of CO_2 between the air/water interface and the production of CO_2 due to fish and algal respiration were not included in the current PAS model. These rates were assumed to have minor impact in the culture system since inorganic carbon was added through influent water flow and/or external carbon addition.

The concentration of carbon can be calculated as

$$C_2 = C_1 + \frac{C_o - C_1}{\tau} - r_{CU} \quad .$$

(71)

Dynamic Response of Algal Growth Rates

Algal growth rates for each time increment are calculated based on light, nitrogen and inorganic carbon levels. The growth rate for that time increment is chosen as the minimum of the light, nitrogen and carbon limited growth rates.

Light-limited Growth Rate

Light-limited growth of algae based on algal photosynthetic oxygen production was modeled as a function of light intensity (Steele 1962, Lehman 1975, Welch 1980);

$$P_{20} = P_{max20}(I/I_{opt}) e^{(1-(I/I_{opt}))} \tag{72}$$

where

P_{20} = photosynthetic oxygen production at 20 C, (mg O_2/mg TSS/hr);

P_{max20} = maximum photosynthetic production at 20 C, (mg O_2/mg TSS/hr);

I = effective light intensity, W/m²; and

I_{opt} = optimal or saturating effective light intensity, W/m².

The value of the effective light intensity can be calculated as follows:

$$I = I_o e^{(-Kd)} \tag{73}$$

where

I_O = complete spectrum surface intensity, W/m²;

K = extinction coefficient (/m); and

d = effective water depth, m.

The average extinction coefficient can be calculated as follows (Parsons, 1984):

$$K = 1.7/SDV \tag{74}$$

where SDV = secchi disk visibility, m.

Equation 72 is used to predict the oxygen production assuming no nutrient limitation. The production at the culture temperature is calculated using Equation 75;

$$P_T = P_{20} e^{\left((T-20)\frac{k}{10}\right)}$$ (75)

where

P_T, P_{20} = oxygen production at culture temperature and 20°C, mg O_2/mg TSS/hr; and

  k = 0.7707.

The ratio of 1.24 mg O_2 per mg of algal TSS produced during photosynthesis can be used to calculate the light limited growth rate at the culture temperature as

$$\mu_L = \frac{P_T}{1.24} \quad .$$ (76)

Nitrogen-limited Growth Rate

The Monod model was chosen to predict the nitrogen-limited algal growth as

$$\mu_N = \frac{\mu_{maxT} N}{K_{sN} + N}$$ (77)

where

  μ_N = nitrogen limited growth rate, day^{-1};

μ_{maxT} = maximum specific growth rate at culture temperature °C, day^{-1};

  N = inorganic nitrogen concentration, mg/l; and

K_{sN} = half-saturation constant, mg/l.

A K_{sN} value of 0.070 mg/l N (Lehman et al., 1975) was used to calculate the nitrogen-limited growth rate, μ_{N20}. The μ_{max20} value of 0.0887 /hr determined for the PAS was

used. Maximum growth rate at culture temperature, μ_{maxT}, is calculated from the equation

of Goldman and Carpenter (1974)

$$\mu_{maxT} = \mu_{max20} e^{\left((T-20)\frac{k}{10}\right)} \tag{78}$$

where

T = temperature, °C; and

k = 0.7707.

Carbon-limited Growth Rate

Carbon-limited algal growth rates may best be described as a function of carbon

dioxide concentration (King 1970, Brune 1983). In a dynamic model of algal growth,

however, this would require the calculation of free carbon dioxide concentration present

as a function of alkalinity and pH which would be beyond the scope of the current model.

Therefore, the carbon-limited algal growth rate was calculated based on total inorganic

carbon concentration (Goldman 1974). The Monod model was chosen to predict the

inorganic carbon limited growth rate as shown below

$$\mu_c = \frac{u_{maxT}C}{K_{sC}+C} \tag{79}$$

where

μ_C= carbon-limited growth rate, day^{-1};

$\mu_{max,T}$= total inorganic carbon concentration, mg/l;

K_{sC} = half-saturation constant, equal to carbon concentration when = 1/2 u max.

A K_{sC} value of 0.12 mg/l C was used in the growth rate equation (Brune, 1978).

Model Summary

The PAS model is written in a Lotus 123 spreadsheet to calculate the dynamic response equations using a 15-min time interval for a 2 day period. Hardware and software requirements needed to use the program are given in Appendix E. Cells in the program are identified in this discussion by column and row number, as in [A5] for column A, row 5. Ranges are identified by column and the included rows; for example, [A5..A232] represents column A, rows 5 through 232. A flowchart of the major components of the model is given in Figure 29. The format of the PAS spreadsheet model is given in Table 33.
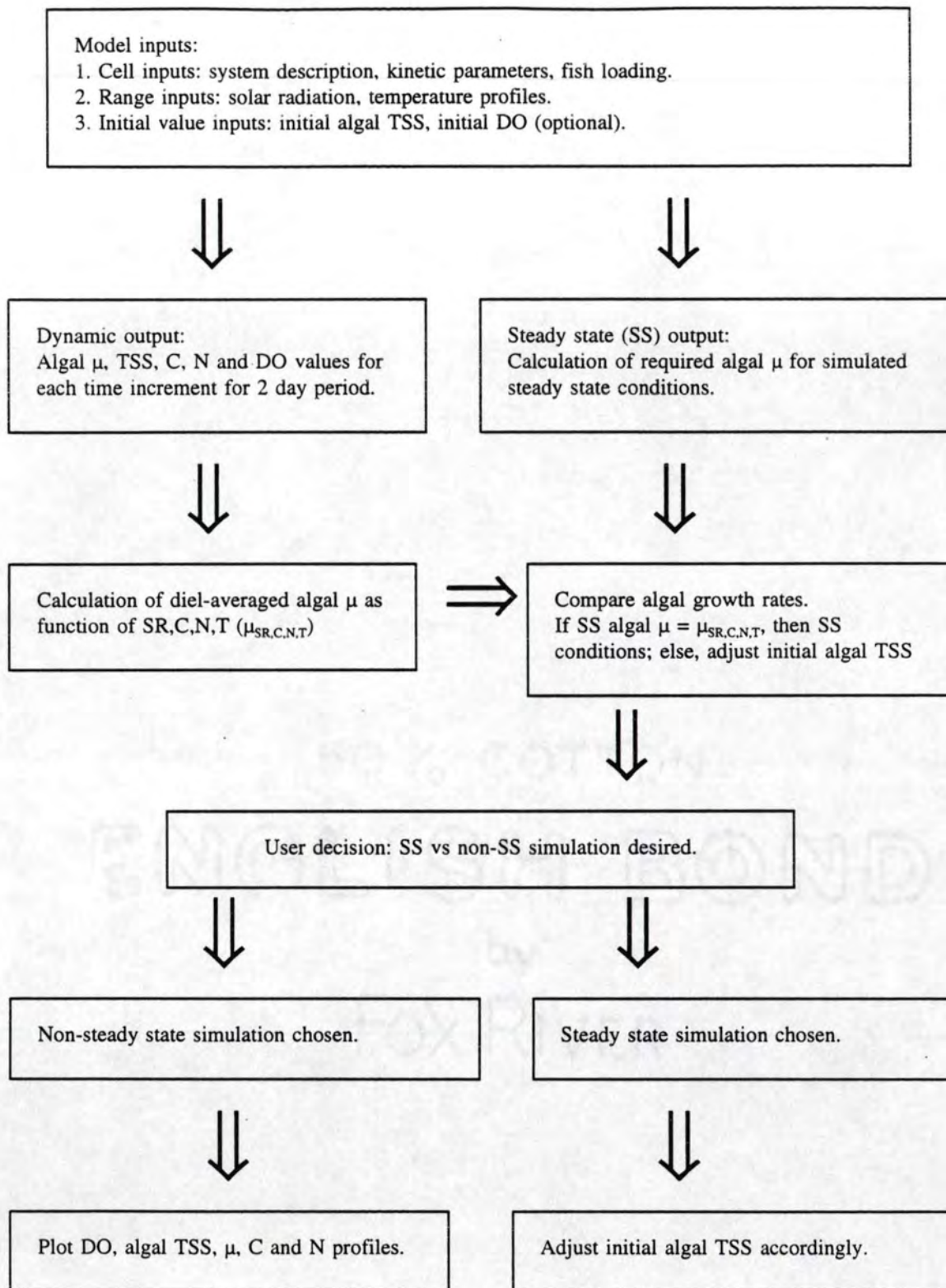
Model inputs:
1. Cell inputs: system description, kinetic parameters, fish loading.
2. Range inputs: solar radiation, temperature profiles.
3. Initial value inputs: initial algal TSS, initial DO (optional).

Dynamic output:
Algal μ, TSS, C, N and DO values for each time increment for 2 day period.

Steady state (SS) output:
Calculation of required algal μ for simulated steady state conditions.

Calculation of diel-averaged algal μ as function of SR,C,N,T ($\mu_{SR,C,N,T}$)

Compare algal growth rates.
If SS algal μ = $\mu_{SR,C,N,T}$, then SS conditions; else, adjust initial algal TSS

User decision: SS vs non-SS simulation desired.

Non-steady state simulation chosen.

Steady state simulation chosen.

Plot DO, algal TSS, μ, C and N profiles.

Adjust initial algal TSS accordingly.

Figure 29. Major components of PAS algal productivity and DO profile model.

Table 33. Format of the PAS spreadsheet model.

	A	B	C	D	E	F	G	H	I	J	K	L
1	PAS program							< Description of Algal Culture System >				
2								'TAU' Detention time, hrs =				36
3	< Oxygen Transfer Information >							'DEPTH' Water depth, m =				0.6
4	'ELEV' Elevation, m =					186		'AREA' Tank area, m2 =				100
5	'EF' Elevation factor =					0.98		'FLOW' Water flow, lpm =				27.78
6	'WINDD' Wind (day), m/s=					0		'VOL' Tank volume, l =				60000
7	'WINDN' Wind (night), m/s=					0		'DOI' Influent DO, mg/l=				7.3
8	'RADIUS' Mixer blade radius, m =					0.959						
9	'RPMD' Mixer rpm (day),0.5-2 rpm					0.5		< Algal Respiration Rates >				
10	'RPMN' Mixer rpm (night),0.5-2 rpm					0.5		'ARD' Resp (day), mgO2/mgTSS/hr =				0.002
11	'WVD' Water velocity (day), m/s=					0.0313		'ARN' Resp (night), mgO2/mgTSS/hr=				0.004
12	'WVN' Water velocity (night),m/s=					0.0313						
13								< Algal Growth Parameters >				
14	<Calculated Oxygen Transfer Coefficient >							'UMAX' Max growth rate, /hr, 20C =				0.0887
15	< due to wind or mixer @20C >							'KSN' Ks value for N, mg/l=				0.05
16	'K20WD' K20 (wind, day), m/hr =					0		'KSC' Ks value for C, mg/l =				0.12
17	'K20WN' K20 (wind, night),m/hr =					0		'PMAX' Max photo rate mgDO/mgTSS/hr=				0.12
18	'K20D' K20 (mixer, day), m/hr =					0.0281		'IOPT' Optimum light level, W/m2 =				250
19	'K20N' K20 (mixer, night), m/hr=					0.0281		'ALGAE' Species:1=green 0=blue-green				1
20								'EFFDEPTH' Effective depth =				0.56

Table 33. Format of the PAS spreadsheet model (continued).

	N	O	P	Q	R	S	T	U	V	W	X	Y
1	< Fish Loading >							< Daily Oxygen Balance >				
2	'FISHLOAD' Fish, kg/ha =				*0*			Algal respiration, gO2/d=			248	
3	'FISHWT' Fish weight, g =				*450*			Fish oxygen demand, gO2/d=			0	
4	'FEEDRATE' Feed rate,g feed/g fish/d=				0.0175			Surface reaeration, gO2/d=			-1760	
5								Algal DO production, gO2/d=			2820	
6	< Oxygen Demand due to Fish >							DO in effluent, gO2/d=			1222	
7	'rFRD' Rate fish respiration (day), mg/l/hr @26C =					0.00		DO in influent, gO2/d=			292	
8	'rFRN' Rate fish respiration (night), mg/l/hr @26C =					0.00		Net DO production, gO2/d=			3402	
9	'rWOD' Rate fish waste oxygen demand, mg/l/hr=					0.00						
10								< Daily Summary >				
11	< Nutrient Load from Fish and Fertilizer >							'DOMIN' DO minimum, mg/l=			19.11	
12	'NFISH' N excreted by fish gN/kgfish/hr =					*0.035*		'DOMAX' DO maximum, mg/l=			40.78	
13	'rNE' Rate N excretion by fish, mg/l/hr =					0.000		'DOAVE' DO average, mg/l=			30.55	
14	'NADDED' N addition rate, mg/min =					*140.0*		'TSSMIN' TSS minimum, mg/l=			47.65	
15	'NIN' Total influent N, mg/l =					5.04		'TSSMAX' TSS maximum, mg/l=			65.79	
16	'ALGALN' N content, mgN/mgTSS=					0.0631		'TSSAVE' TSS average, mg/l=			57.69	
17	'CADDED' NaHCO3 added, kg/day=					*3.3*		'CFIX' C fix rate, gC/m2/d=			8.27	
18	'CWATER' C in supply water, mg/l =					*10.01*						
19	'CIN' Total influent C, mg/l =					21.8		'SSGR' Steady state algal growth rate, /hr=				0.0278
20	'ALGALC' C content, mgC/mgTSS =					0.358		'DGR' Diel-averaged algal growth rate, /hr =				0.0278
21								Adjust initial algal TSS? =			NO. AT STEADY STATE	

Table 33. Format of PAS spreadsheet model (continued).

	A	B	C	D	E	F	G	H	I	J	K	L	M
24						< Oxygen Transfer >			<Solar Radiation>		< Light Limited Growth >		
25													
26											DO prod	DO prod	Light
27		Day/	Actual	Water	Water	K		Reaer	Surface	Effective	@ 20C	@ T	Limited
28		Night	DO	Temp	Temp	@ T	Cs	@ T	Light	Light	mgDO/m	mgDO/m	u @T
29	Hour	Code	mg/l	C	K	m/hr	mg/l	mg/l/hr	W/m2	W/m2	TSS/hr	TSS/hr	/hr
30													
31	6.00	0		26.0	299.2	0.032	7.95	-0.62	0.7	0.1	0.000	0.000	0.000
32	6.25	0		26.0	299.2	0.032	7.95	-0.60	0.9	0.1	0.000	0.000	0.000
33	6.50	0		26.0	299.2	0.032	7.95	-0.59	4.2	0.5	0.000	0.000	0.000
34	6.75	0		26.0	299.2	0.032	7.95	-0.57	16.2	1.9	0.001	0.001	0.001
35	7.00	0		26.0	299.2	0.032	7.95	-0.56	37.4	4.4	0.002	0.004	0.003
36	7.25	0		26.0	299.2	0.032	7.95	-0.55	69.8	8.3	0.006	0.009	0.007
37	7.50	0		26.0	299.2	0.032	7.95	-0.54	104.4	12.5	0.010	0.017	0.013
38	7.75	0		26.0	299.2	0.032	7.95	-0.53	141.5	17.0	0.015	0.025	0.020
39	8.00	1		26.0	299.2	0.032	7.95	-0.54	201.3	24.3	0.021	0.033	0.027
40	8.25	1		26.0	299.2	0.032	7.95	-0.54	247.7	29.9	0.029	0.046	0.037
41	8.50	1		26.0	299.2	0.032	7.95	-0.56	304.2	36.6	0.035	0.055	0.044
42	8.75	1		26.0	299.2	0.032	7.95	-0.58	357.5	42.7	0.041	0.065	0.053
43	9.00	1		26.0	299.2	0.032	7.95	-0.60	414.2	49.1	0.047	0.075	0.060

Table 33. Format of PAS model spreadsheet format (continued).

		N	O	P	Q	R	S	T	U	V	W	X	Y	Z
24		<Carbon Limited Growth>				<Nitrogen Limited Growth>			<Minimum Growth Rate and DO Profile>					
25														
26		Total	Carbon	Rate of			Nitrogen	Rate of						
27		Inorganic	Limited	Carbon	u max		Limited	Nitrogen	Minimum	Predicted	Algal	Predicted	C fix	DO
28		Carbon	u @ T	Uptake	@ T	Nitrogen	u @ T	Uptake	u	DO	TSS	SDV	rate	prod
29		mg/l	/hr	mg/l/hr	/hr	mg/l	/hr	mg/l/hr	/hr	mg/l	mg/l	m	g C/m2/d	mg/l/hr
30														
31		7.27	0.139	0.000	0.141	1.68	0.137	0.000	0.000	*19.11*	*46.00*	0.263	0	0.000
32		7.37	0.139	0.002	0.141	1.70	0.137	0.000	0.000	18.83	45.68	0.264	0.031	0.008
33		7.47	0.139	0.003	0.141	1.73	0.137	0.000	0.000	18.56	45.36	0.265	0.040	0.010
34		7.56	0.139	0.013	0.141	1.75	0.137	0.002	0.001	18.29	45.05	0.266	0.188	0.045
35		7.66	0.139	0.050	0.141	1.77	0.137	0.009	0.003	18.04	44.75	0.267	0.725	0.174
36		7.75	0.139	0.115	0.141	1.79	0.137	0.020	0.007	17.83	44.47	0.268	1.660	0.399
37		7.81	0.139	0.212	0.141	1.81	0.137	0.037	0.013	17.68	44.24	0.269	3.060	0.735
38		7.86	0.139	0.313	0.141	1.82	0.137	0.055	0.020	17.61	44.08	0.270	4.515	1.085
39		7.88	0.139	0.418	0.141	1.83	0.137	0.074	0.027	17.64	44.00	0.270	6.027	1.448
40		7.87	0.139	0.579	0.141	1.84	0.137	0.102	0.037	17.78	43.98	0.270	8.348	2.006
41		7.82	0.139	0.699	0.141	1.83	0.137	0.123	0.044	18.05	44.08	0.270	10.07	2.420
42		7.74	0.139	0.836	0.141	1.82	0.137	0.147	0.053	18.42	44.26	0.269	12.05	2.897
43		7.63	0.139	0.960	0.141	1.81	0.137	0.169	0.060	18.90	44.54	0.268	13.83	3.324

The procedure for using the model is summarized below. A complete listing of the program statements is given in Appendix 6.

Input Values

Appropriate values must be entered in the unprotected cells or ranges listed below. All other cells in the program are protected so that values cannot be inadvertently entered into an incorrect cell, thus potentially erasing an equation.

Cell inputs. Enter the values for the physical system parameters, kinetic parameters and fish loading into the input cells. The cell values, which are highlighted on the computer screen if a color monitor is used, are shown in italics in Table 31.

Range inputs. Input values of surface solar radiation [I31..I232] must be entered for each 15-min time increment. Input values of water temperature may be entered in range [D31..D232] if available or an initial value can be entered into the first cell and copied to fill the range. The program originally is set with constant water temperature of 26°C and the solar radiation profile measured for 7/2/91 (see Figure 66). Actual dissolved oxygen concentrations, if available, can be entered in cells in range [C31..C232], corresponding to the time the measurement was made.

Initial values. An initial value of algal TSS [W31] must be given. For the initial predicted DO concentration [V31], an actual value can entered if comparison to data is desired. The value of the minimum predicted dissolved oxygen concentration may also be used by entering $DOMIN. Press the F9 key to recalculate the worksheet. This results in a symmetrical DO profile for the simulated 2 day period.

Algal Growth Rate Comparison

The algal growth rate required for steady state conditions is calculated in cell [Y19]. The predicted diel-averaged algal growth rate is shown in [Y20]. These two values, which must be equal for steady state conditions to be simulated, are compared in cell [Y21]. If the diel-averaged rate is greater than the steady state rate, then the initial TSS value should be increased. Conversely, if the actual rate is less than the steady state rate, the initial TSS value should be decreased. If the two rates are equal, no adjustment of the initial algal TSS value is needed to simulate steady state algal growth. The comparison of the rates in [Y21] will output a note to the user to instruct whether an adjustment of the initial algal TSS value is needed.

If a non-steady state simulation is desired, the initial algal TSS value can be set to any value desired and the response of the system will be predicted.

Model Results

The results of the model calculations are shown in corresponding cells. Any range can be plotted vs time to illustrate the calculated profile. The program was originally set to graph DO concentration with time.

Iterative calculations. The model calculations for each time interval include:

1. algal growth rate at culture temperature as function of solar radiation, inorganic carbon and nitrogen concentrations;

2. minimum of light-, carbon- and nitrogen-limited algal growth rates;

3. DO, algal biomass, inorganic carbon and nitrogen concentrations; and

4. algal respiration, surface reaeration, and oxygen production rates.

Daily calculations. The model calculates the daily summaries for the following parameters based on the calculated daily profiles:

1. minimum, maximum and average DO concentration;

2. minimum, maximum and average algal TSS concentration;

3. total oxygen produced or lost through algal respiration, fish oxygen demand (respiration plus waste oxygen demand), surface reaeration, algal oxygen production, and the influent and effluent flow; and

4. average carbon fixation rate.

CHAPTER VII

MODEL CALIBRATION

The main factor not accounted for in the PAS model was the effect of the degree of mixing on light penetration. In the operation of the PAS, algal productivity was found to be 1.5 times greater at the highest water velocity (0.125 m/s) than at the lower water velocities (0.0313 and 0.0625 m/s). The effective light level for a static water column is modeled to decrease exponentially with depth (see Equation 40). Welch (1980) stated that for well-mixed ponds an effective depth equal to one half the actual water depth could be used to calculate the average light gradient. However, increased mixing may decrease the effective depth. An effective depth factor could be used to adjust the degree of light penetration. Therefore, the model calibration phase involved adjusting the effective depth factor until the predicted DO profile and algal biomass value approached the actual values.

Twenty randomly-selected days from the 1991 runs, when external inorganic carbon was not added to the system and blue-green algae were predominant, and the 1992 runs, when external carbon was added and green algae were predominant were used for the calibration. The actual values for the physical system parameters, nutrient addition rates, solar radiation, and water temperature were used as input values for the model simulations. The first measured DO value was used for the initial DO concentration in the simulation. Actual algal respiration values were used if available, or the average values for the year. Table 34 gives the values for the kinetic parameters used.

Table 34. Kinetic parameters used in model calibration simulations.

Parameter[*]	1991	1992
P_{max}, mg DO/mg TSS/hr	0.11	0.12
I_{opt}, W/m^2	500	250
K_{sC}, mg/l C	0.12	0.12
K_{sN}, mg/l N	0.05	0.05
μ_{max}, hr^{-1}	0.0887	0.0887
Algal N, mg N/mg TSS	0.0631	0.0631
Algal C, mg C/mg TSS	0.358	0.358
ARD, mg DO/mg TSS/hr	0.002	0.002
ARN, mg DO/mg TSS/hr	0.004	0.004

[*] Parameters described in Chapter VI.

The conditions for the calibration runs included the range of water velocities, carbon addition rates, and retention times tested for the PAS (Table 35). Because sufficient DO profiles were not available for the 0.34 m water depth, all calibration simulations used were for the 0.66 m depth.

Table 35. Conditions for calibration runs.

Year	Algal type	Water velocity, m/s	# runs	Water depth, m	Influent C, mg/l	Retention time, hr
1991	blue-green	0.0313	4	0.66	10	30-60
1991	blue-green	0.0625	4	0.66	10	30-60
1992	green	0.0313	4	0.66	20	45
1992	green	0.0625	4	0.66	20-30	40
1992	green	0.1250	4	0.66	20	40

The results of these calibration runs (Figures 30 through 49) indicate that the model DO predictions closely match the actual values, in particular those shown in Figures 33 through 36. The appearance of a "jagged" edge in the predicted DO profile (for example, Figure 34) occurs in those simulations where nutrient-limited conditions were predicted. The predicted algal growth rate remains near the maximum rate until the nutrient concentration falls to near the half-saturation constant value in these simulations. The algal growth rate then cycles between zero and near maximum growth for every 15 min interval until the light level decreases at the end of the day and becomes the growth limiting factor. Although the on and off cycling is an artifact in the model due to the discreet time interval used, the resulting plateaus in the DO profile closely predict the actual DO profiles (Figures 34 and 36). The predicted limiting nutrient in these simulations was inorganic carbon. Inorganic carbon for these cultures was supplied solely through the influent water.

The smooth profile predicted in Figure 33 indicates light-limited growth conditions. The solar radiation value at each time increment is an input value in the program; therefore the solar radiation level cannot be predicted to drop to zero due to a mass balance within the model. The simulations for which light limited conditions are predicted are those in September, when maximum total daily solar radiation ranges 18-20 MJ/m^2, and nutrient limitation is predicted for the July runs, when the maximum total radiation ranges 26-28 MJ/m^2.
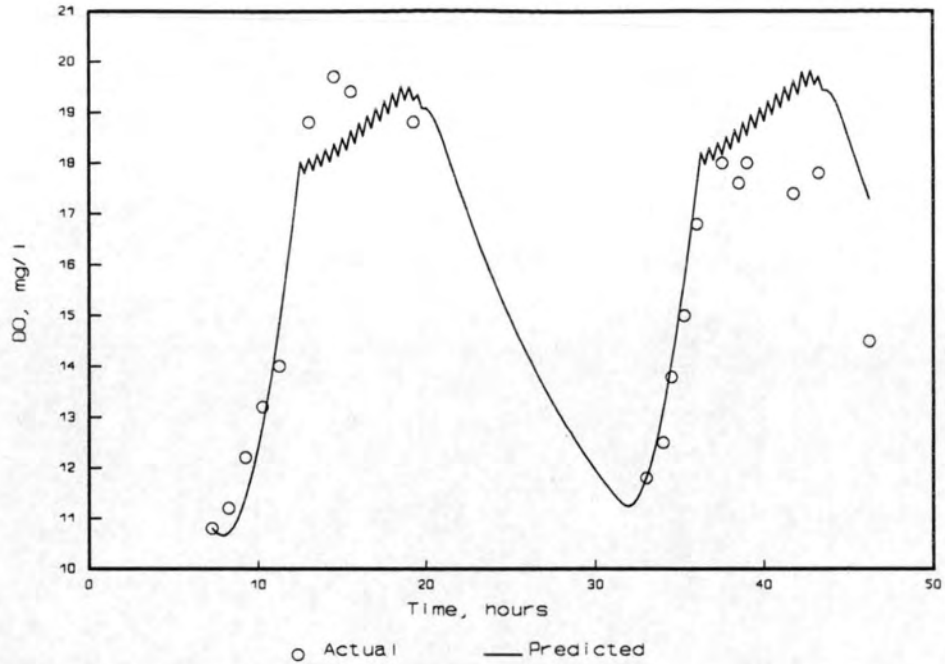
Figure 30. DO profile for Tank 1, 7/22/91. Water velocity=0.0313 m/s, retention time= 54 hr, effective depth factor=0.60.
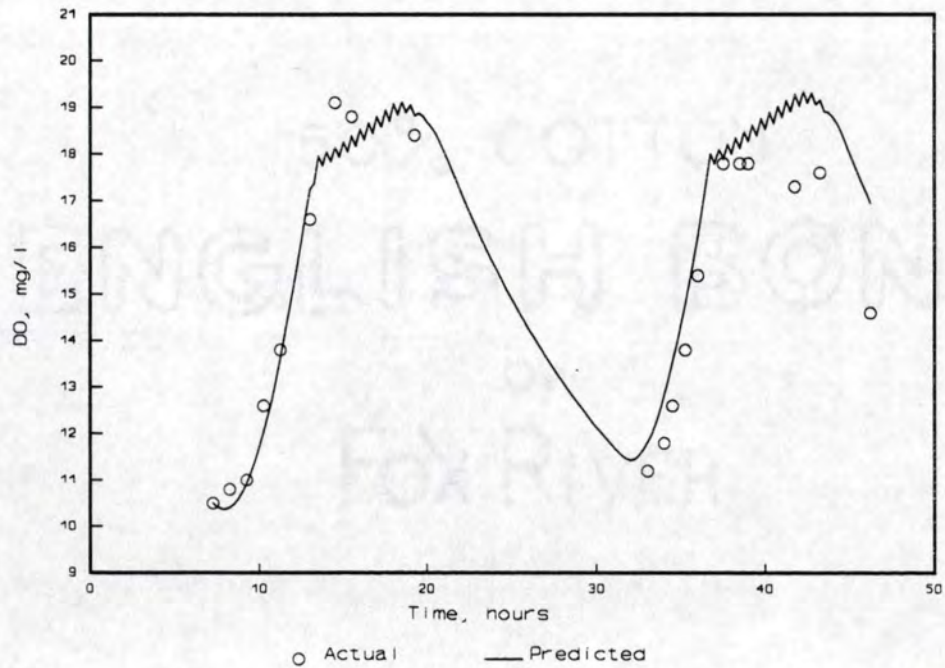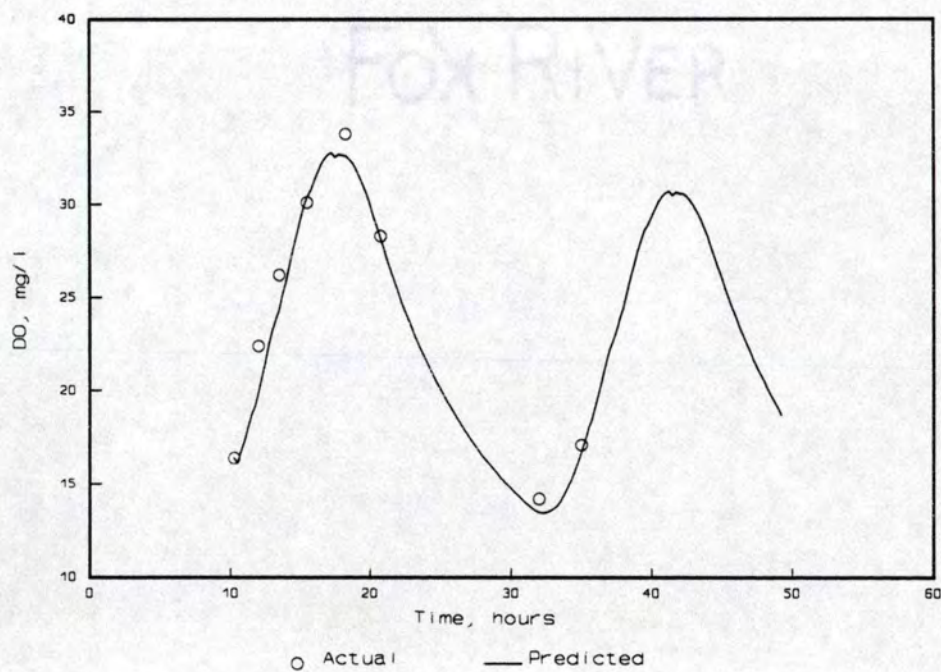

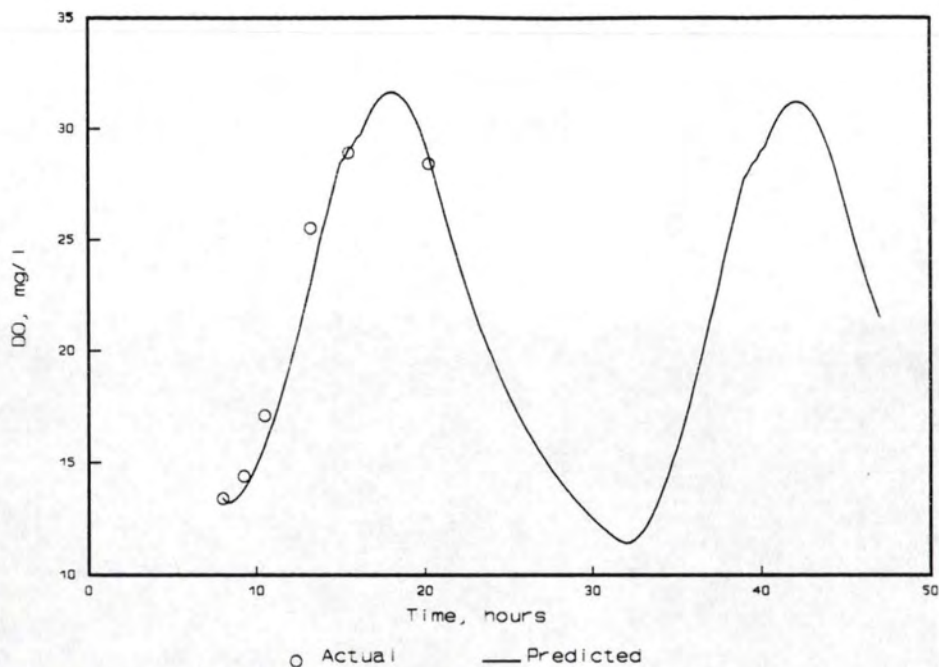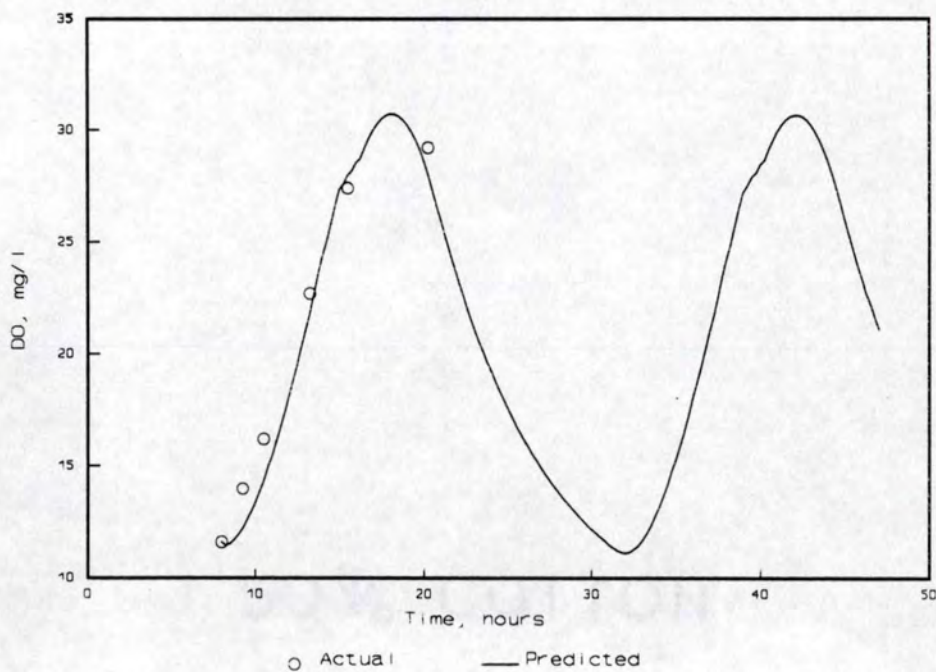Figure 31. DO profile for Tank 2, 7/22/91. Water velocity=0.0313 m/s, retention time=57 hr, effective depth factor=0.62.
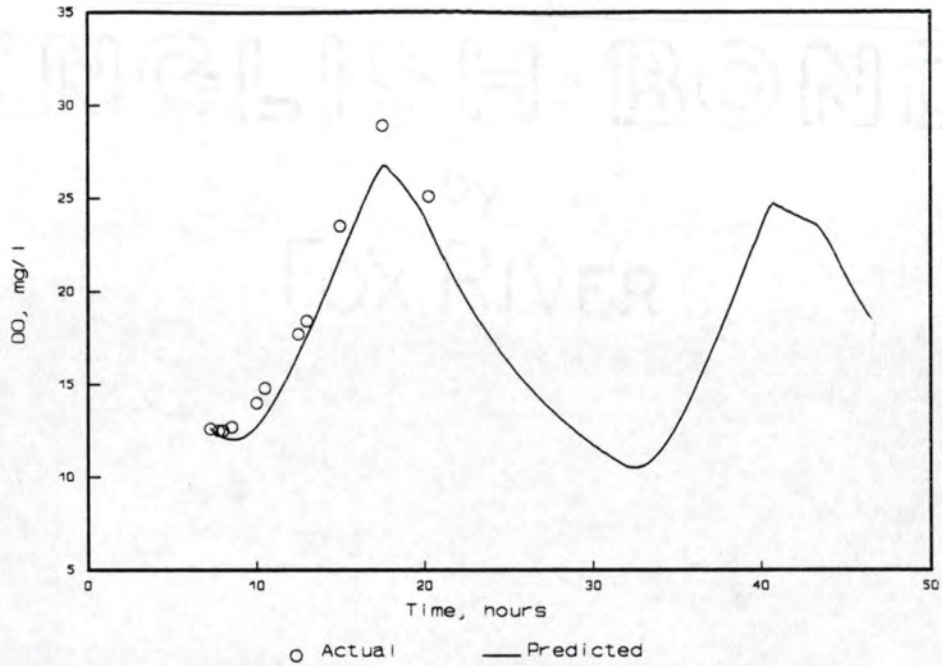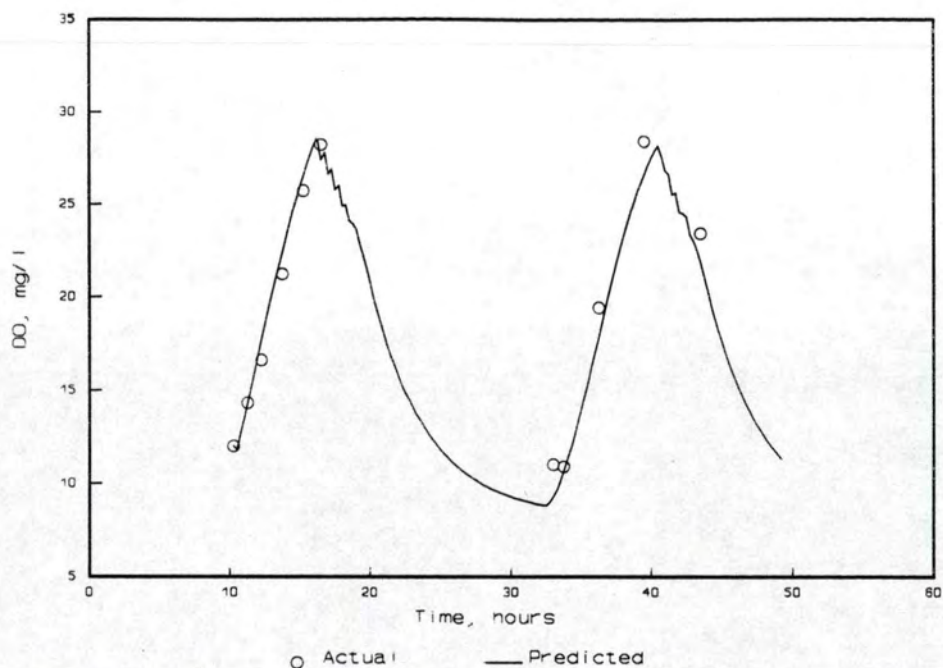
Figure 32. DO profile for Tank 1, 9/14/91. Water velocity=0.0313 m/s, retention time= 28 hr, effective depth factor=0.34.
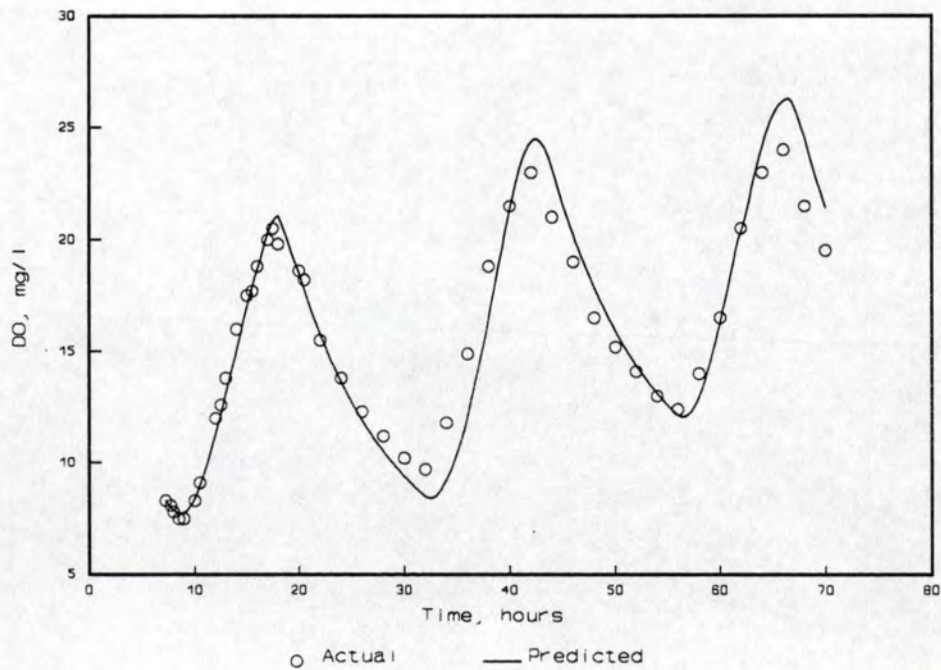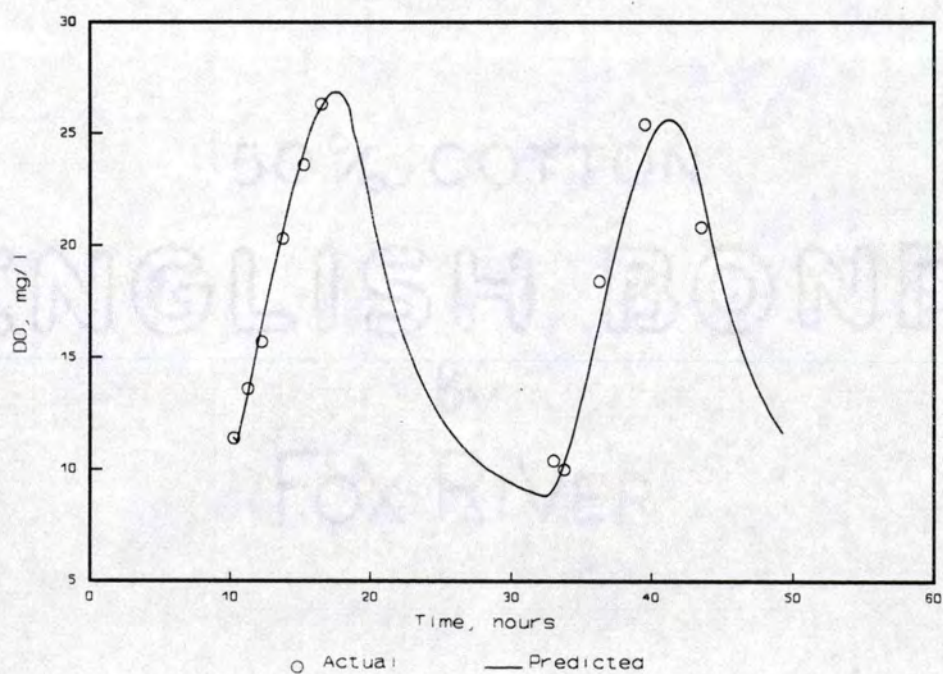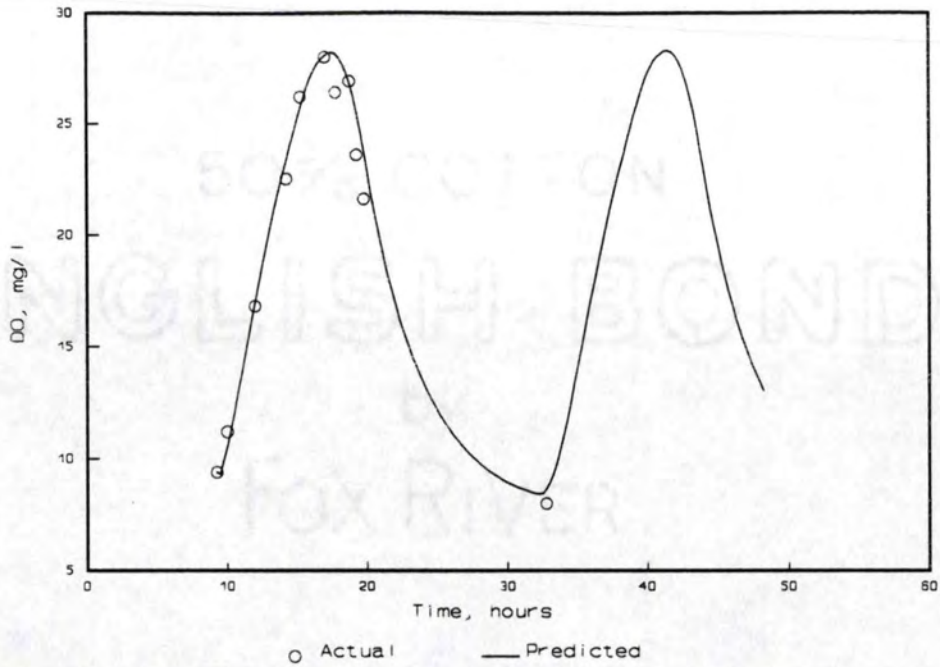

Figure 33. DO profile for Tank 2, 9/14/91. Water velocity=0.0313 m/s, retention time=24 hr, effective depth factor=0.5.
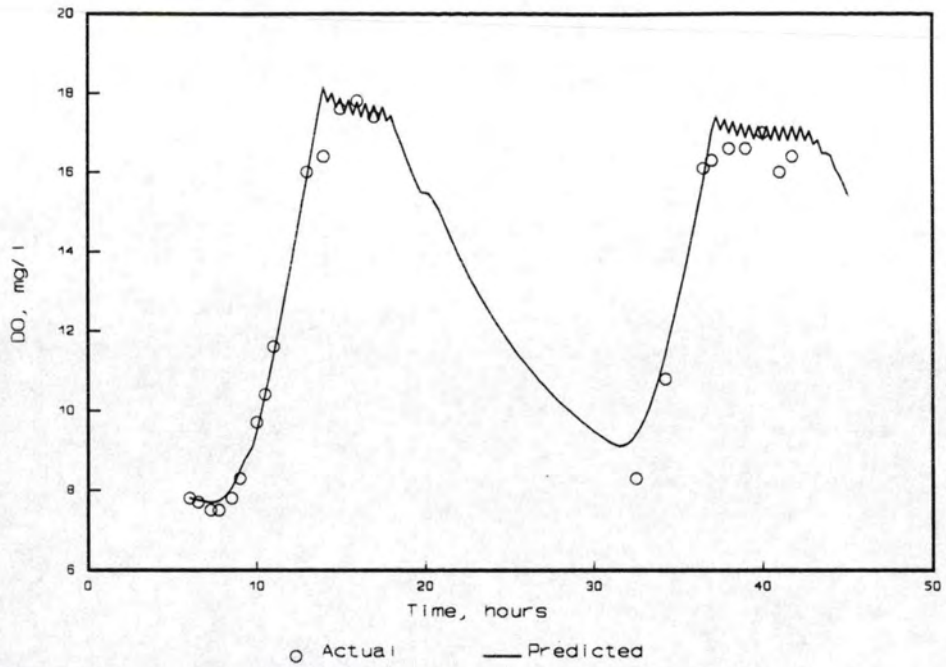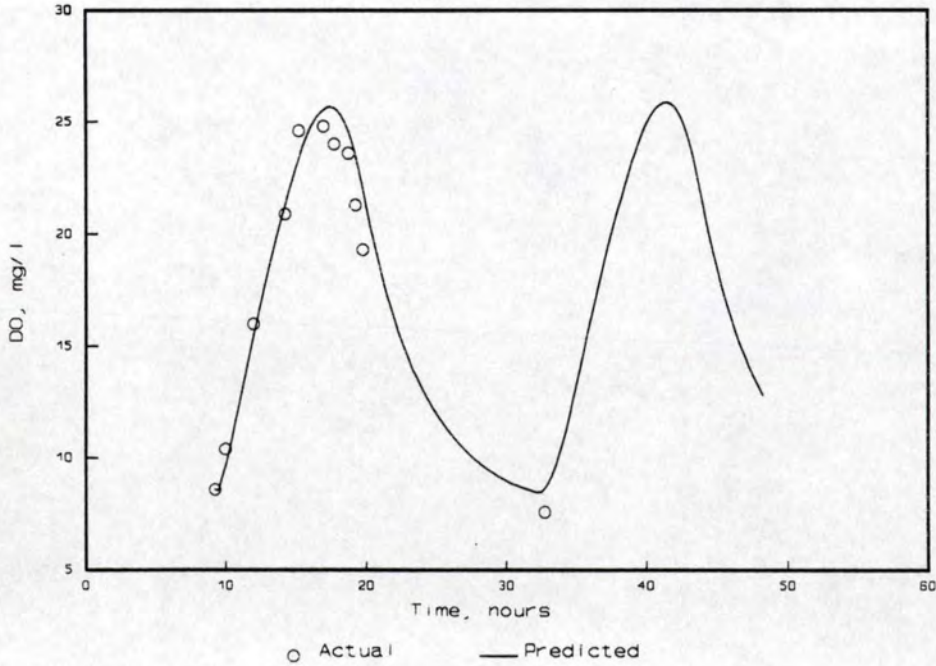
Figure 34. DO profile for Tank 4, 7/2/91. Water velocity=0.0625 m/s, retention time=47 hr, effective depth factor=0.60.
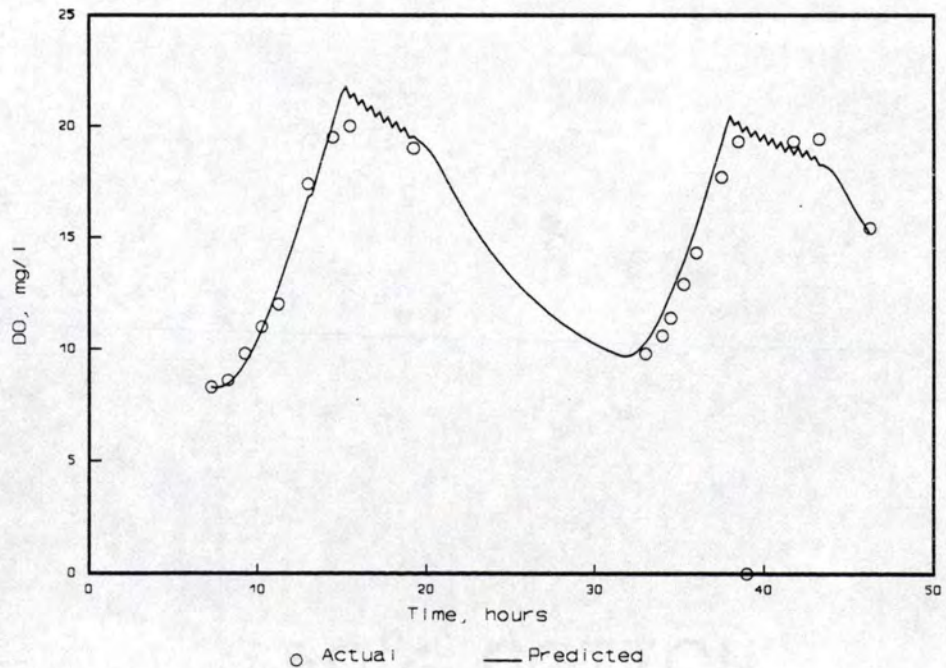
Figure 35. DO profile for Tank 3, 7/22/91. Water velocity=0.0625 m/s, retention time=31 hr, effective depth factor=0.50.
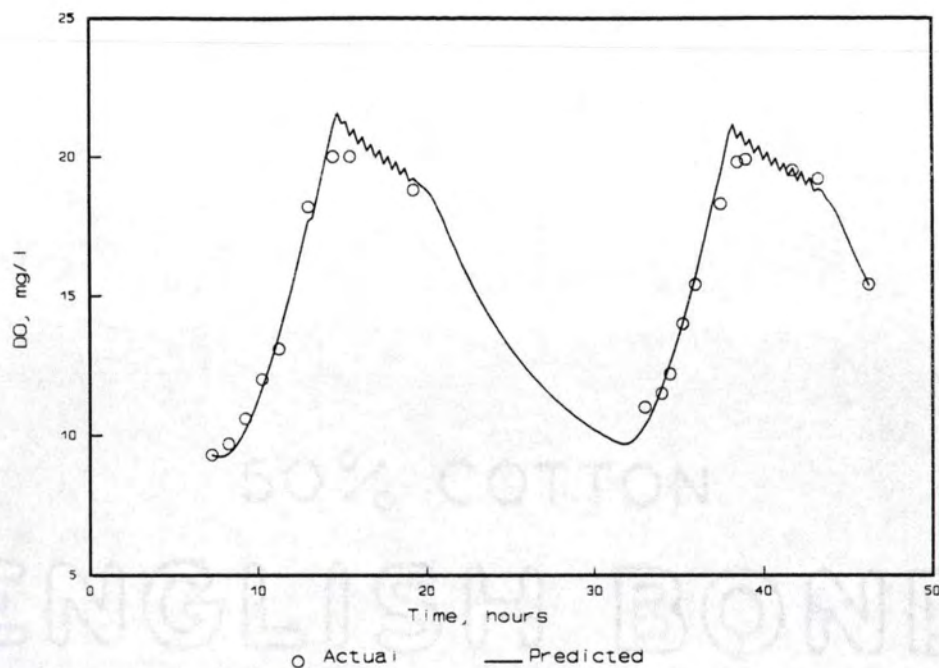
Figure 36. DO profile for Tank 4, 7/22/91. Water velocity=0.0625 m/s, retention time=29 hr, effective depth factor=0.48.
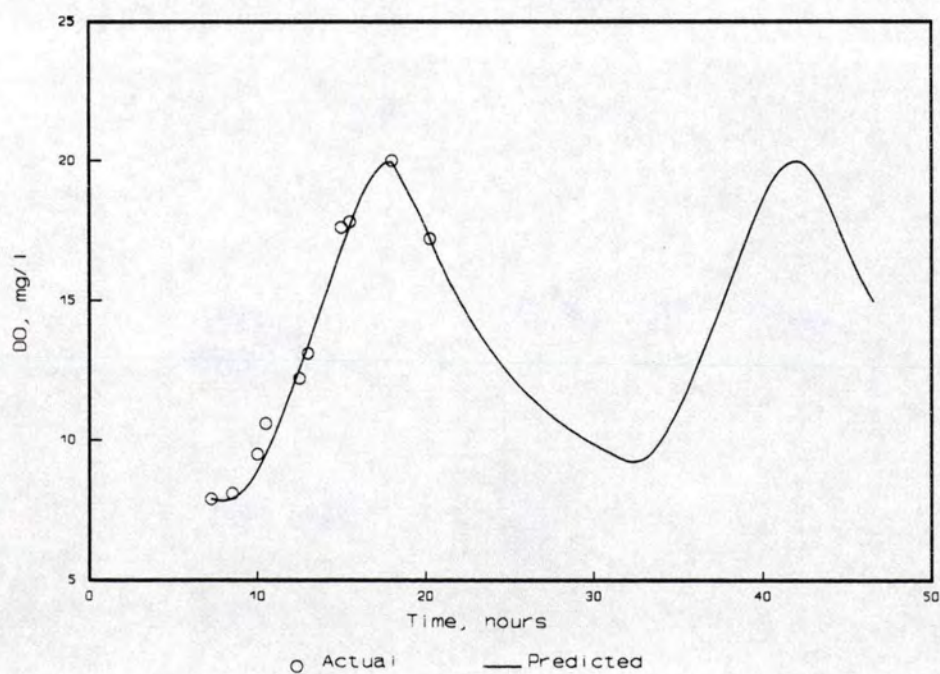
Figure 37. DO profile for Tank 4, 9/14/91. Water velocity=0.0625 m/s, retention time=32 hr, effective depth factor=0.49.
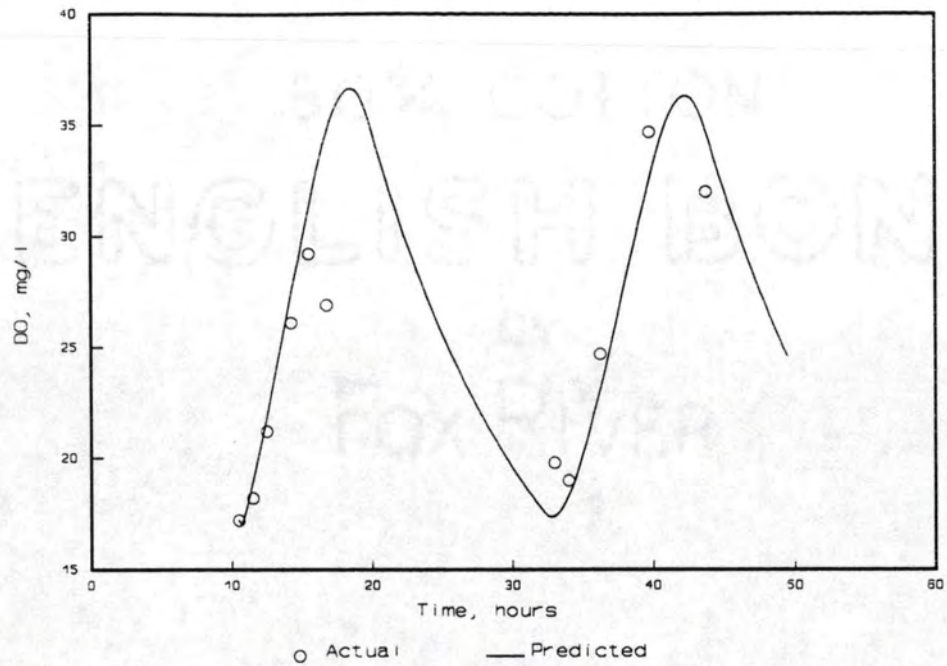
Figure 38. DO profile for Tank 3, 9/9/92. Water velocity=0.0313 m/s, retention time=38 hr, effective depth=0.55.
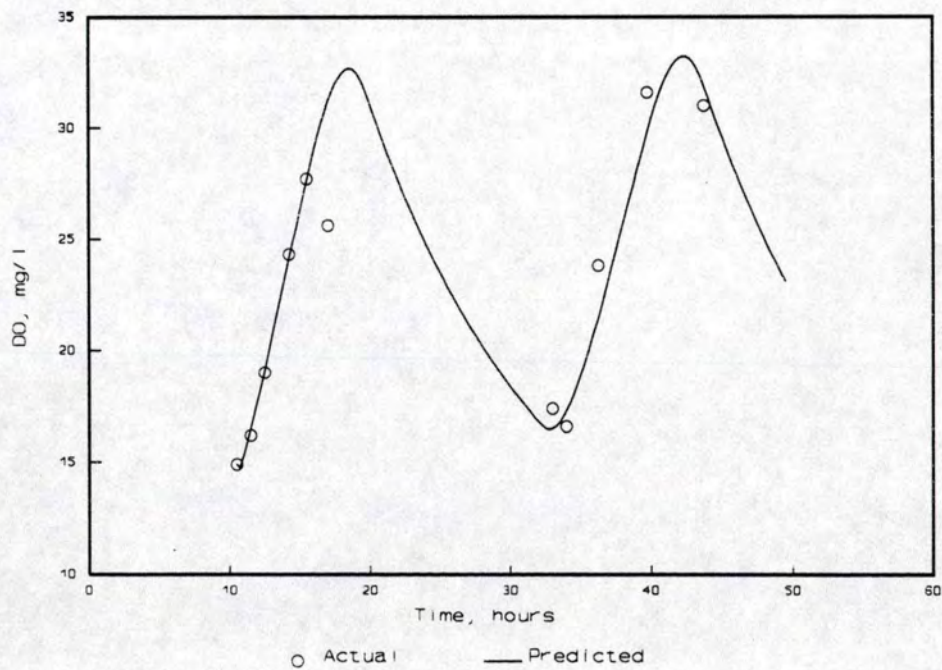
Figure 39. DO profile for Tank 4, 9/9/92. Water velocity=0.0313 m/s, retention time=36 hr, effective depth factor=0.57.
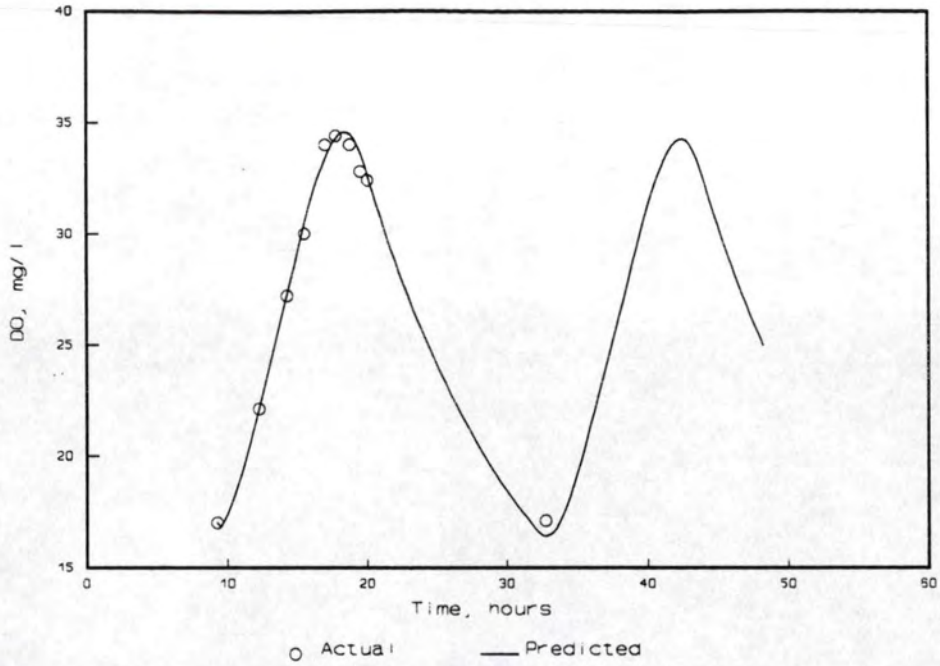
Figure 40. DO profile for Tank 3, 9/11/92. Water velocity=0.0313 m/s, retention time=36 hr, effective depth factor=0.58.
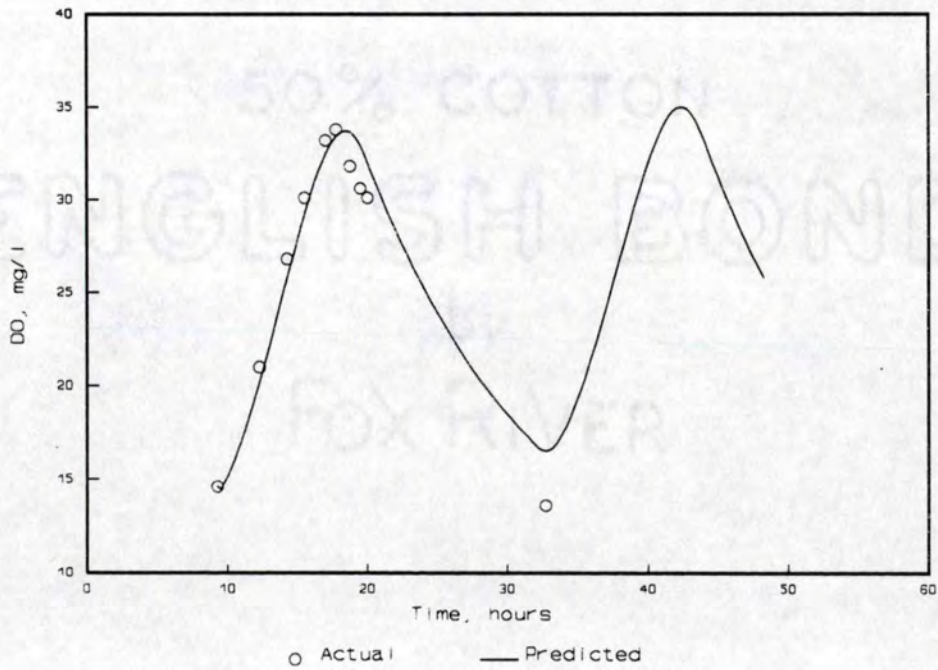
Figure 41. DO profile for Tank 4, 9/11/92. Water velocity=0.0313 m/s, retention time=39 hr, effective depth factor=0.54.
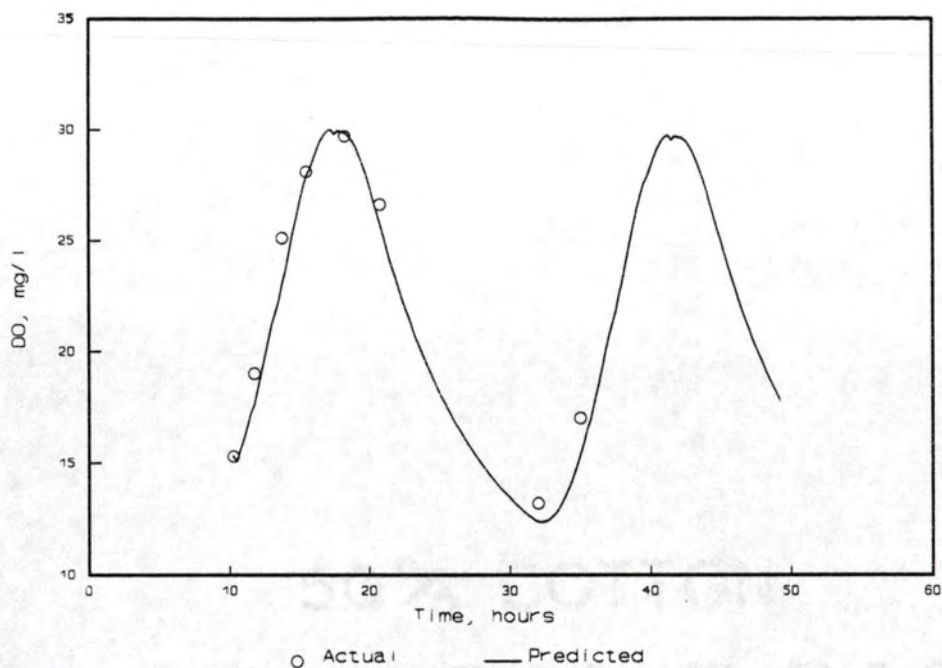
Figure 42. DO profile for Tank 3, 8/11/92. Water velocity=0.0625 m/s, retention time=40 hr, effective depth factor=0.65.

Figure 43. DO profile for Tank 4, 8/11/92. Water velocity=0.0625 m/s, retention time=50 hr, effective depth factor=0.58.

Figure 44. DO profile for Tank 3, 7/29/92. Water velocity=0.0625 m/s, retention time=26 hr, effective depth factor=0.61.

Figure 45. DO profile for Tank 4, 7/29/92. Water velocity=0.0625 m/s, retention time=27 hr, effective depth factor=0.61.

Figure 46. DO profile for Tank 1, 9/9/92. Water velocity=0.125 m/s, retention time=33 hr, effective depth factor=0.44.

Figure 47. DO profile for Tank 2, 9/9/92. Water velocity=0.125 m/s, retention time=38 hr, effective depth factor=0.47.

Figure 48. DO profile for Tank 1, 9/11/92. Water velocity=0.125 m/s, retention time=36 hr, effective depth factor=0.41.

Figure 49. DO profile for Tank 2, 9/11/92. Water velocity=0.125 m/s, retention time=38 hr, effective depth factor=0.46.

The predicted vs observed algal biomass values are shown in Figure 50.
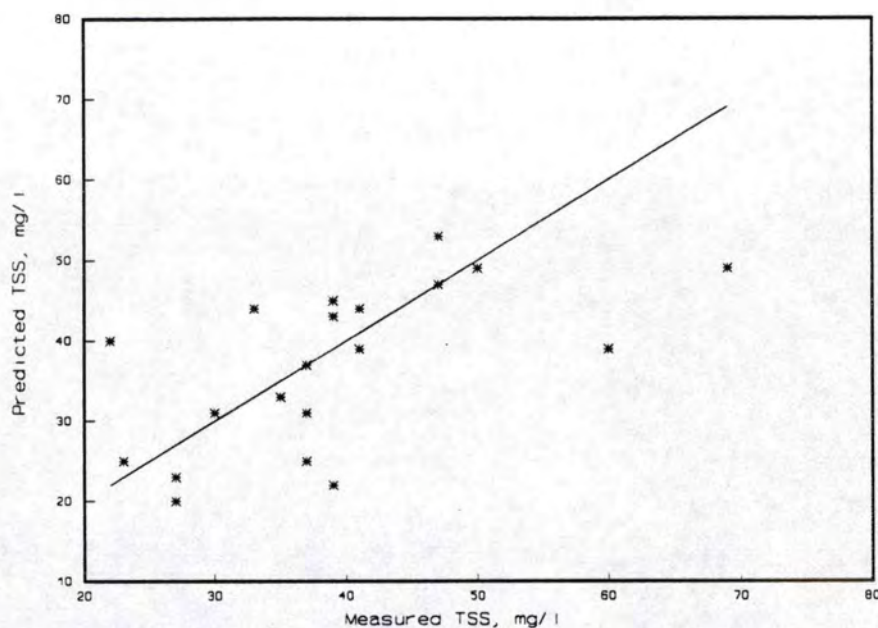
Figure 50. Measured algal TSS values vs PAS model predictions for runs examined in calibration phase.

The average effective depth values obtained from the calibration simulations ranged from 0.46 - 0.61 (Table 34).

Table 36. Average effective depth values for calibration runs.

Year	Water Velocity, m/s	Average effective depth	Range
1991	0.0313	0.52	0.34-0.62
1991	0.0625	0.52	0.48-0.60
1992	0.0313	0.56	0.54-0.58
1992	0.0625	0.61	0.58-0.65
1992	0.125	0.46	0.44-0.47

Plots of the effective depth factors determined from the calibration simulations are given in Figures 51 and 52. If the predominant species is blue-green algae, the effective depth factor was predicted to be 0.52 for water velocity range of 0.0313 - 0.0625 m/s. No data was taken at water velocities greater than 0.0625 m/s with predominantly blue-green algae cultures. If the predominant species is green algae, the effective depth factor was modeled as (1.60 WATVEL+0.51) for water velocity range of 0.0313-0.0625 m/s, or (-2.56 WATVEL + 0.77) for water velocity range of 0.0625-0.125 m/s.
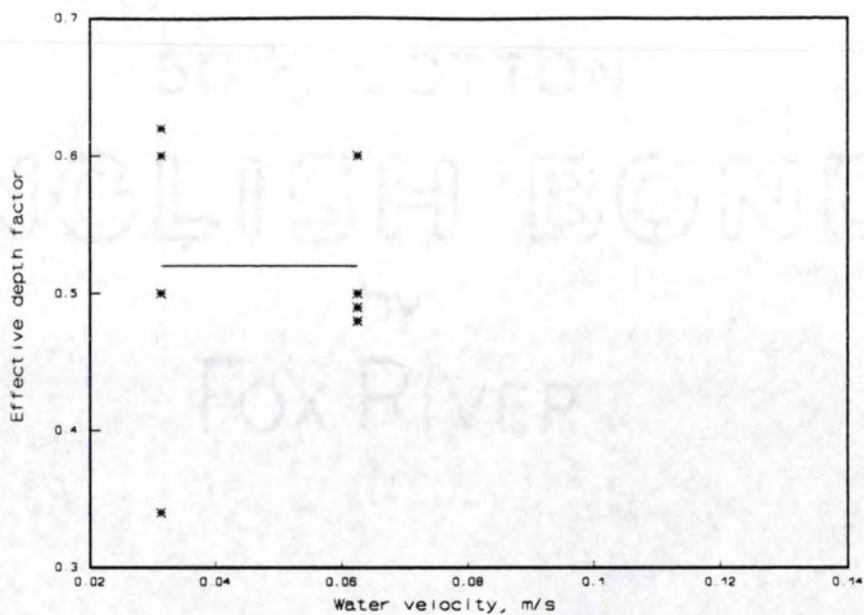
Figure 51. Effective depth values and prediction for 1991 calibration simulations.
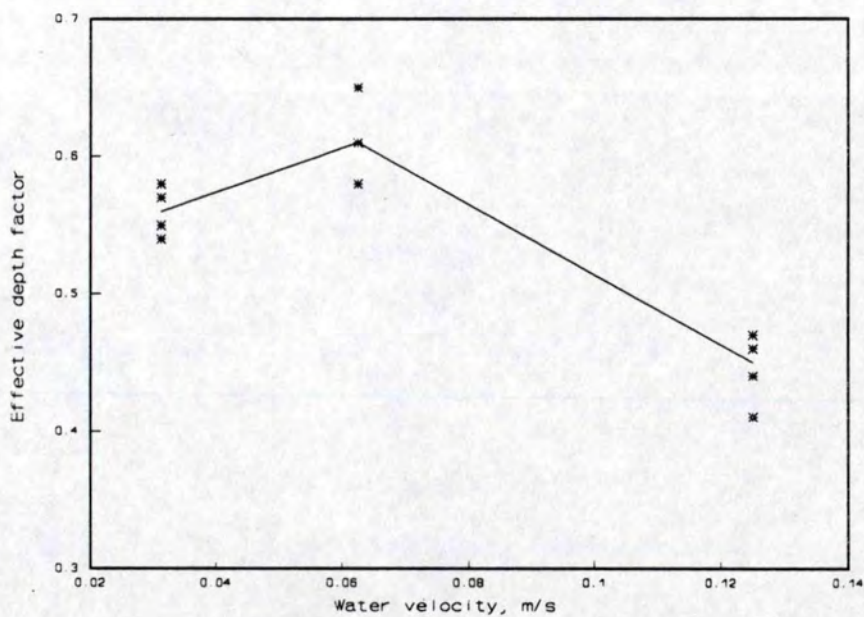
Figure 52. Effective depth values and prediction for 1992 calibration simulations.

CHAPTER VIII

MODEL VERIFICATION

The model verification phase involved simulating the DO profiles from 11 runs which were not used in the calibration phase. As with the calibration runs, the actual values for the physical system parameters, solar radiation and water temperature were used as well as the initial DO concentration. The values of the kinetic parameters used for the calibration simulations (Table 34) were used. The effective depth values used were calculated using the relationship developed in the calibration phase.

The actual and predicted DO profiles are given in Figures 53 through 65. The predictions for Tanks 3 and 4, 7/5/91 (Figures 53 and 54) approximate the actual DO values. The maximum DO value was underestimated for Tank 3 and the minimum DO is overestimated for Tank 4.

The profiles for Tanks 3 and 4, 6/27/91 (Figures 55 and 56) indicate that the model is able to predict the algal response under varying solar radiation levels. The total daily solar radiation nearly doubled from 11 MJ/m^2 on 6/27 to 21 MJ/m^2 on 6/28. The predicted DO profile for Tank 3 (Figure 55) closely matched the actual values. The algal biomass in Tank 4 decreased from 47 to 27 mg/l TSS between 6/25 and 6/26. The culture in Tank 4 may not have reached steady state by 6/28, which may be the cause of the difference between the actual and predicted profiles for the second day.

For culture depth of 0.3 m, the model substantially underestimates the maximum DO achieved, and in general the predicted profile does not fit the shape of the actual

profile well (Figures 57 and 58). The model predicts that nitrogen limited growth occurs during daylight hours, thus limiting the oxygen production. One attempt to improve the prediction was to lower the algal nitrogen ratio from 0.0631 to 0.040 mg N/mg TSS. These plots (Figures 59 and 60) indicate that lowering the nitrogen ratio improves both the maximum DO prediction and the general shape of the DO profile. This evidence indicates that either the actual nitrogen ratio of the freshwater algae present is less than 0.0631 mg N/mg TSS or that the algae were able to adjust their nitrogen use in response to decreased nitrogen availability without substantially inhibiting photosynthesis.

Although the DO profiles for Tanks 1,2,3 and 4 on 9/4/92 (Figures 61 - 64) were not complete, the model predictions seem to closely match the actual values. Figure 65 shows a full DO profile at the 0.125 m/s water velocity that is closely predicted by the model.

These simulations indicate that by modeling the change in effective depth factor resulting from water velocity, the PAS model adequately predicts the increased algal productivity associated with increased water velocity. The model closely simulates the actual DO profile and algal biomass level for both light and carbon limited cultures at 0.6 m deep cultures. However, the model underestimates the algal productivity and DO profile for the shallow water depth (0.32 m). Although greater algal productivity was achieved at the shallower depth, most catfish ponds are designed at depths greater than 0.32 m in order to minimize large water temperature variations. Further data needs to be taken on a wide range of water depths to determine the relationship between water depth and the effective depth factor.
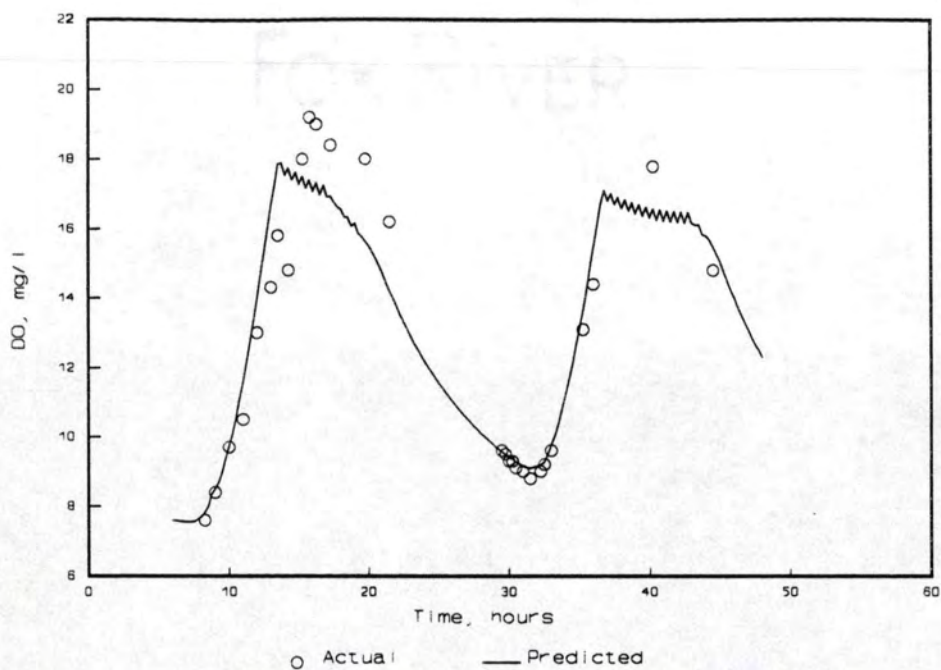
Figure 53. DO profile for Tank 3, 7/5/91. Water velocity=0.0625 m/s, retention time=47 hr, water depth=0.66 m.
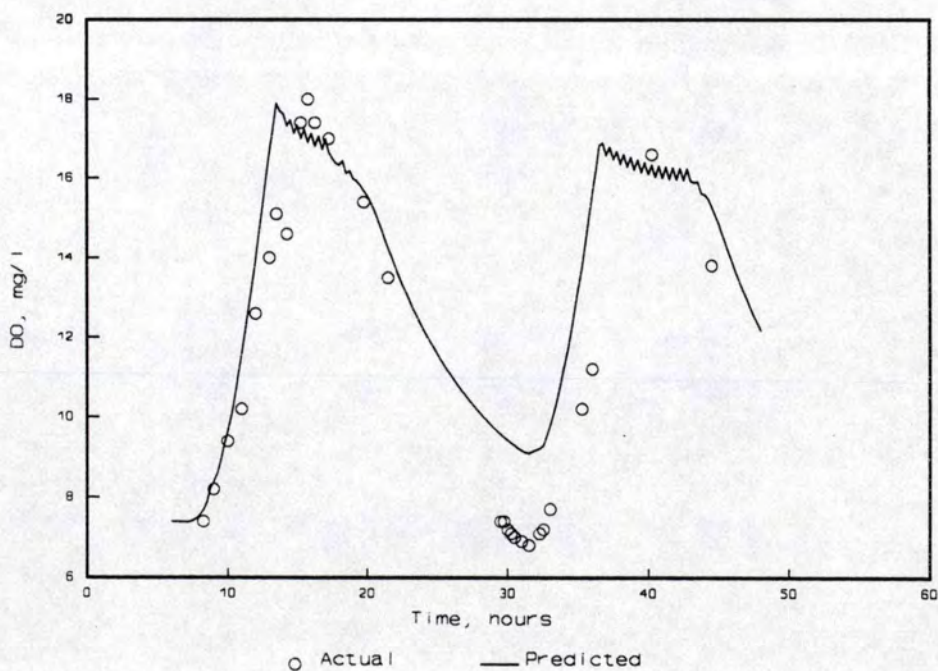
Figure 54. DO profile for Tank 4, 7/5/91. Water velocity=0.0625 m/s, retention time=47 hr, water depth=0.65 m.
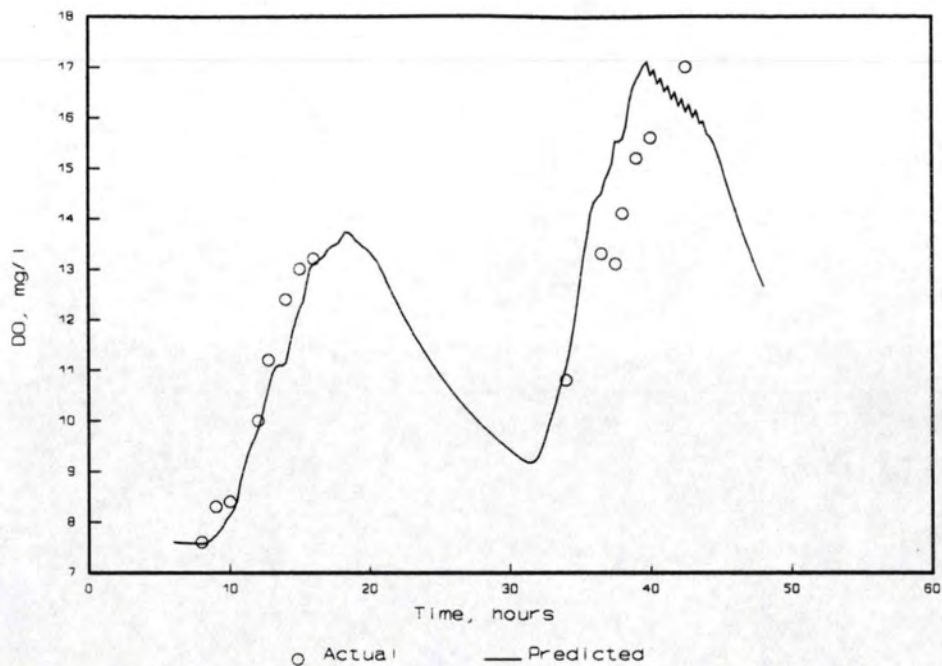
Figure 55. DO profile for Tank 3, 6/27/91. Water velocity=0.0625 m/s, retention time=61 hr, water depth=0.66 m.
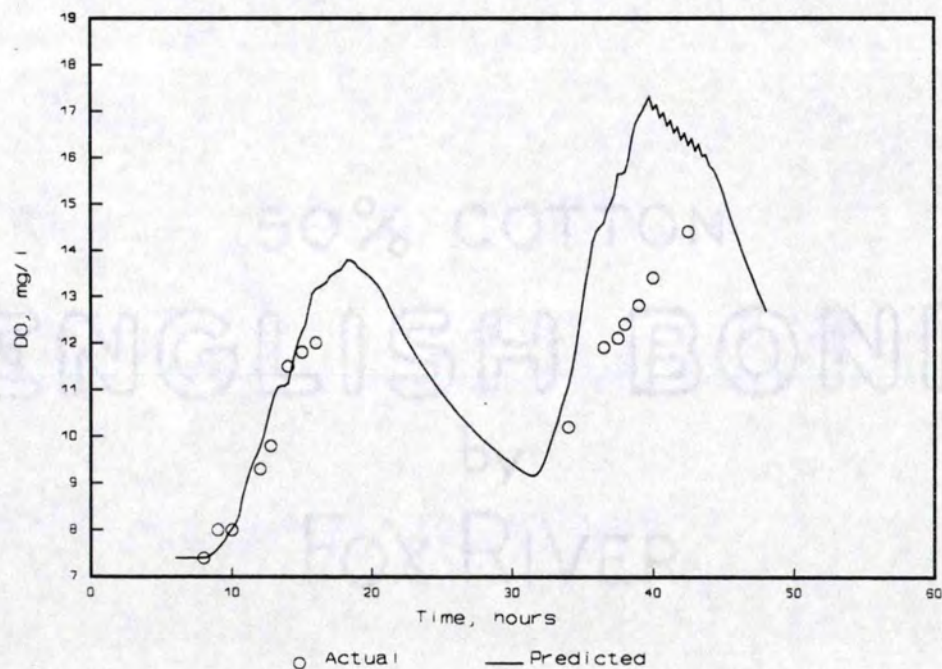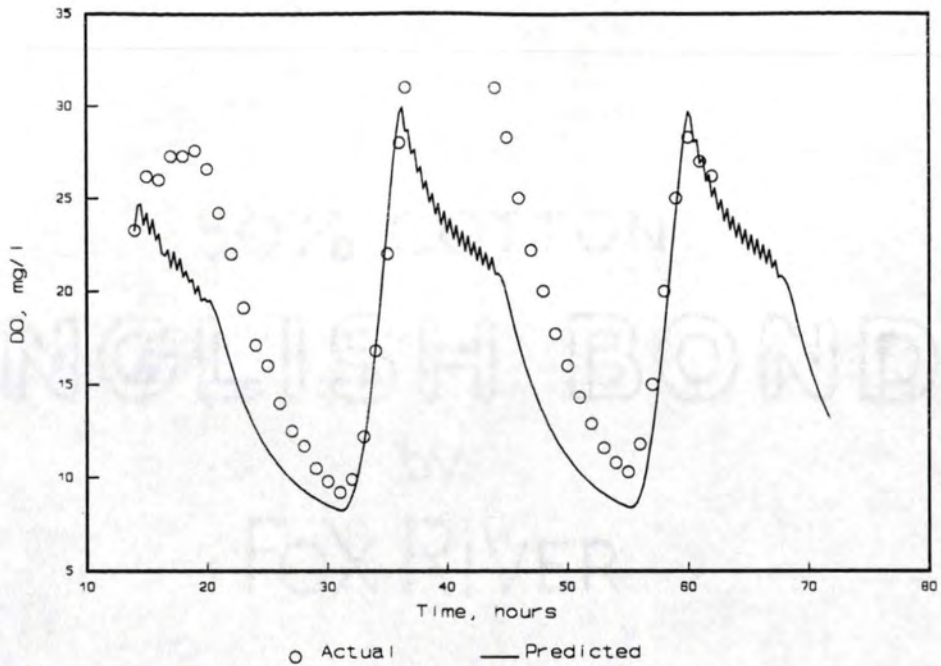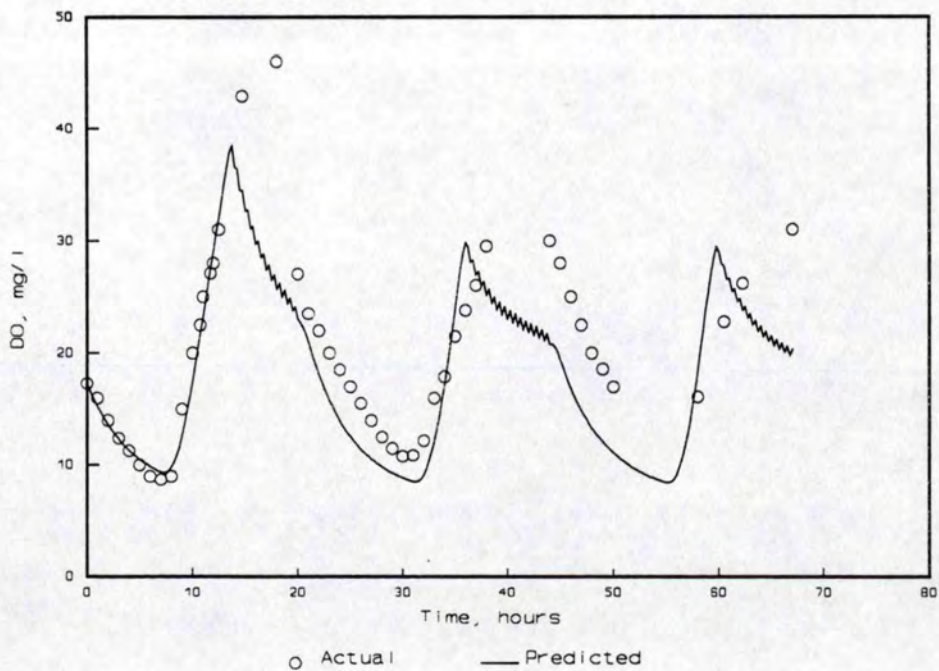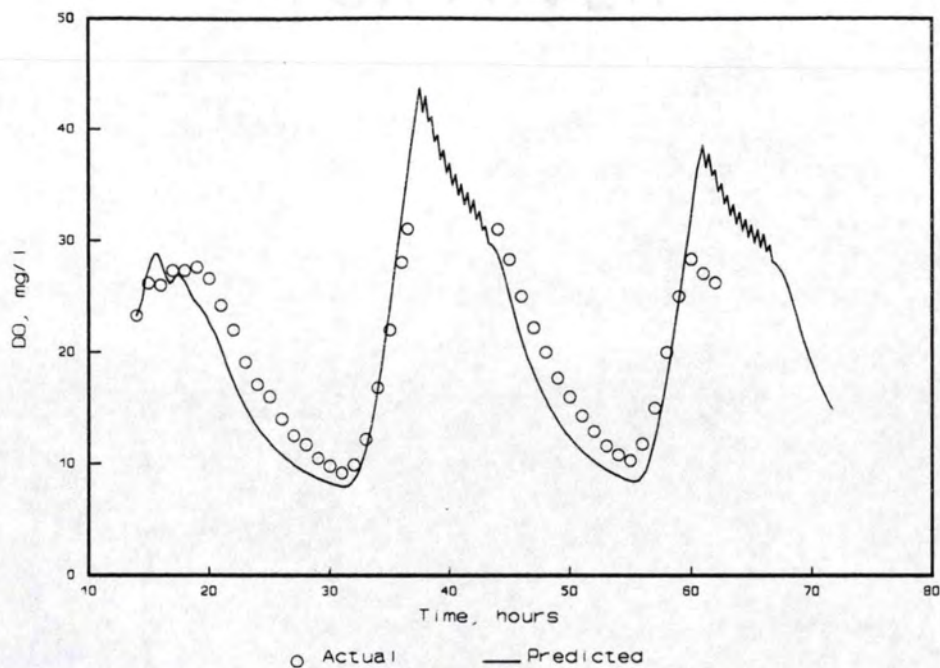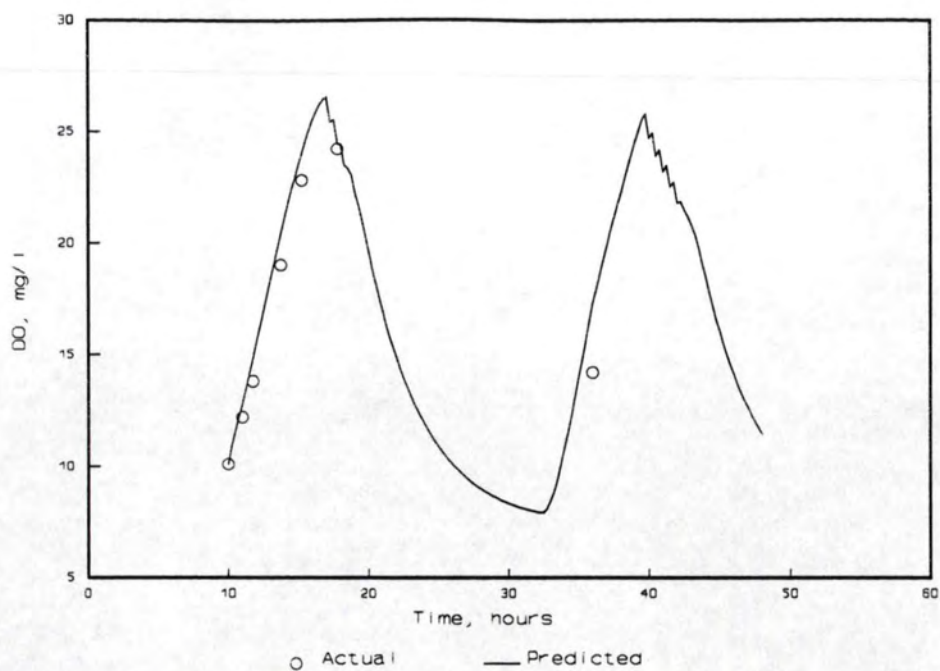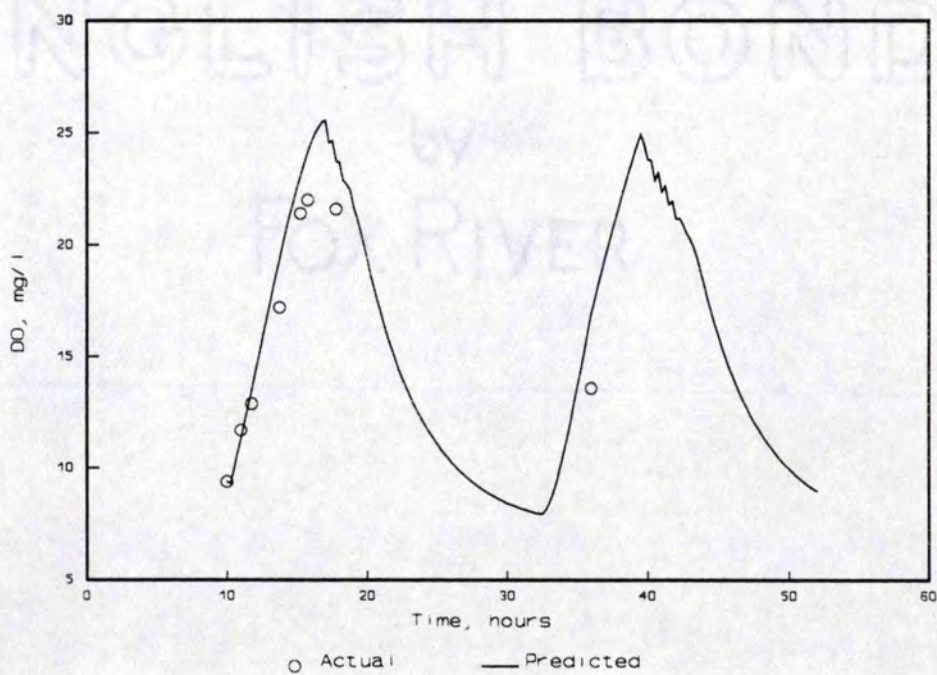

Figure 56. DO profile for Tank 4, 6/27/91. Water velocity=0.0625 m/s, retention time=59 hr, water depth=0.65 m.

Figure 57. DO profile for Tank 1, 7/4/92. Water velocity=0.0625 m/s, retention time=35 hr, water depth=0.32 m.
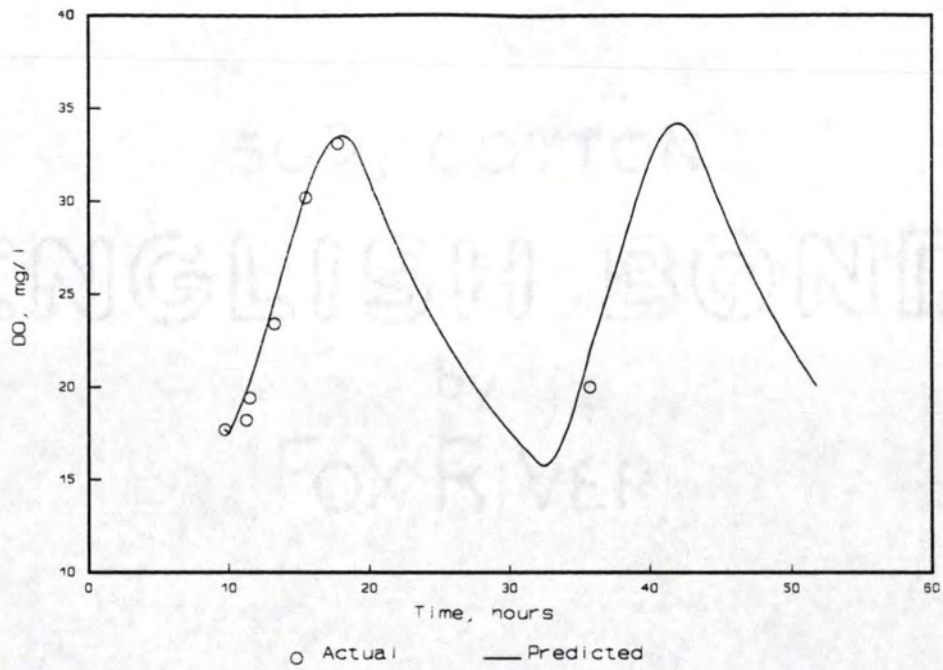

Figure 58. DO profile for Tank 1, 7/7/92. Water velocity=0.0625 m/s, retention time=34 hr, water depth=0.32 m.

Figure 59. DO profile for Tank 1, 7/4/92. N ratio=0.04 mg N/mg TSS.
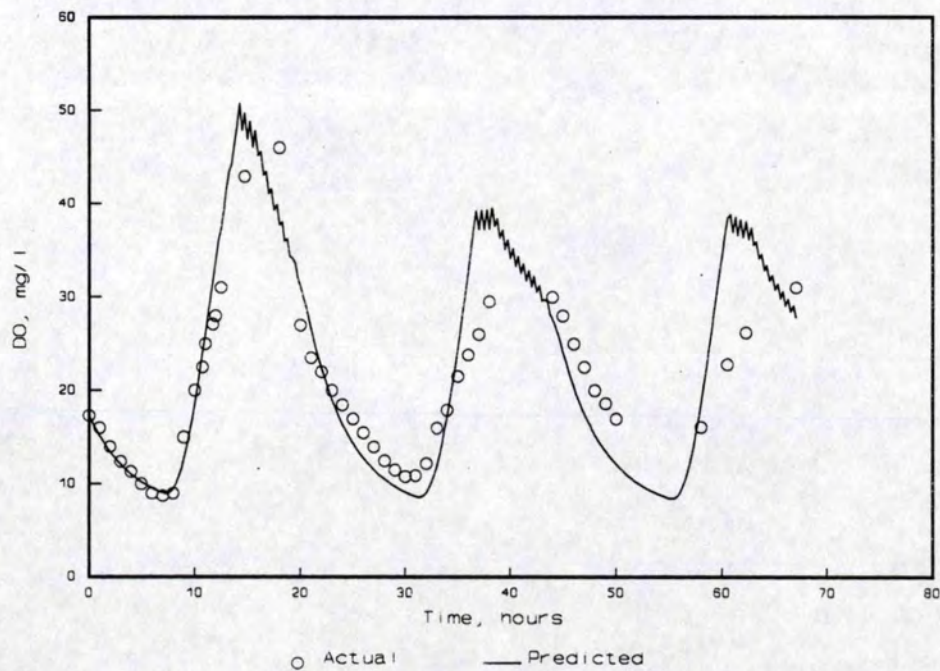
Figure 60. DO profile for Tank 1, 7/7/92. N ratio=0.04 mg N/mg TSS.

Figure 61. DO profile for Tank 1, 9/4/92. Water velocity=0.125 m/s, retention time=32 hr, water depth=0.64 m.

Figure 62. DO profile for Tank 2, 9/4/92. Water velocity=0.125 m/s, retention time=36 hr, water depth=0.68 m.

Figure 63. DO profile for Tank 3, 9/4/92. Water velocity=0.0313 m/s, retention time=40 hr, water depth=0.65 m.
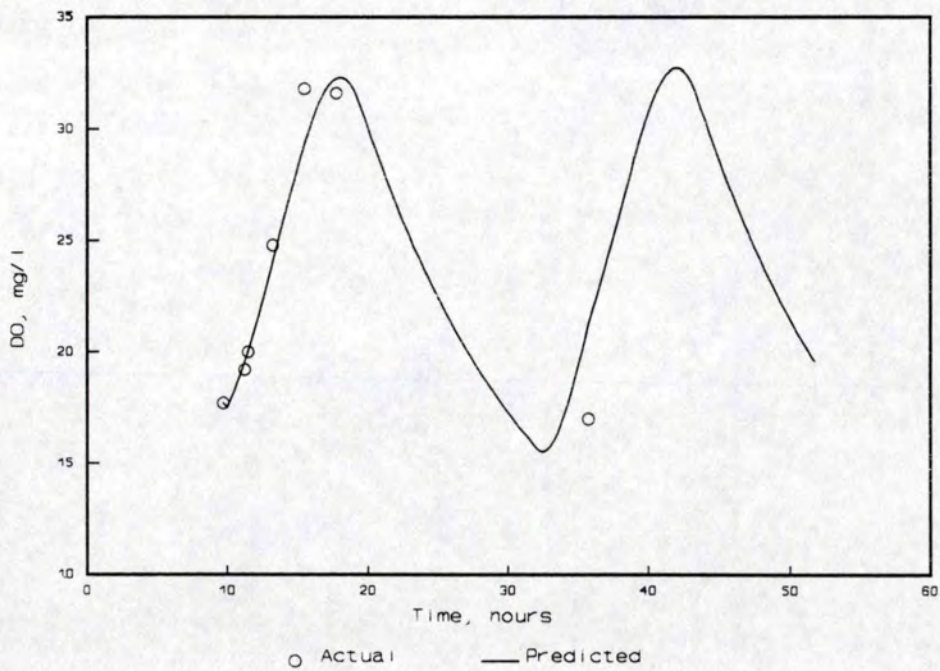
Figure 64. DO profile for Tank 4, 9/4/92. Water velocity=0.0313 m/s, retention time=38 hr, water depth=0.68 m.
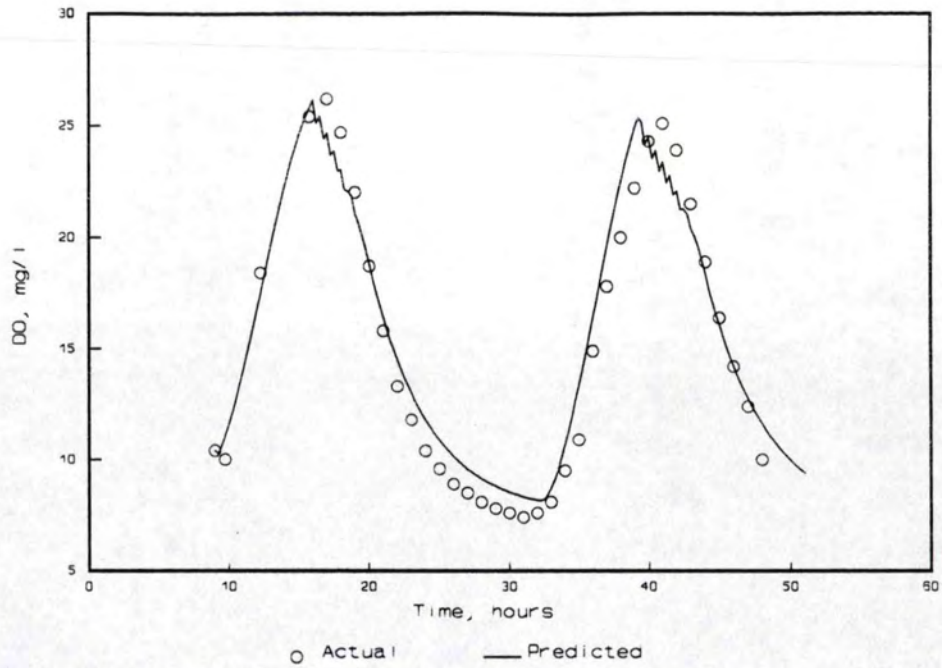
Figure 65. DO profile for Tank 2, 9/10/92. Water velocity=0.125 m/s, retention time 38 hr, water depth=0.68 m.

CHAPTER IX

MODEL SIMULATIONS

Simulations of the Partitioned Aquaculture System were made to predict the operating conditions which would optimize algal productivity and dissolved oxygen profiles to increase the fish carrying capacity. All simulations were made using a 0.6 m water depth, water temperature of 26°C, and standard solar radiation profile (Figure 66).
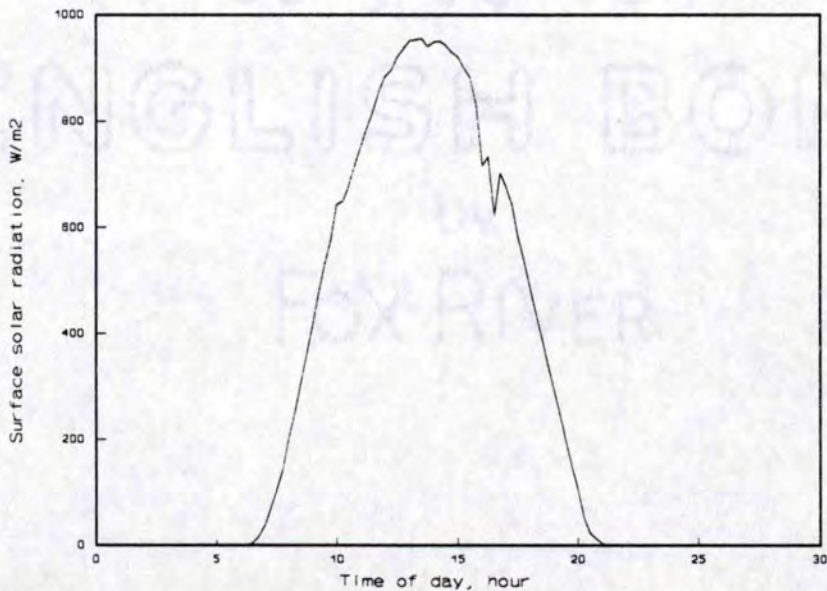

Figure 66. Surface solar radiation profile for 7/2/91.

Algal productivity was first simulated for light limited cultures as a function of retention time at three water velocities and a static condition (0 m/s velocity). The static water condition was simulated by setting the effective depth factor to 1, thereby

eliminating the effect of increased algal productivity with increased water velocity. Modelling the static condition in this manner does not include settling of the algal biomass which would most likely occur, so therefore is only an approximate prediction. Predicted algal productivity was greater for the 0.125 m/s water velocity than for the lower velocities at all retention times (Figure 67). This is a result of the decreased effective depth predicted for cultures mixed at the highest water velocity. Maximum productivity is predicted for a retention time of 20 - 24 hours for all mixed cultures. The simulations do not conform to the laboratory results for light limited cultures grown at low light levels in which productivity was constant as a function of retention time (Pipes and Koutsoyannis 1961). The static water condition simulation has a nearly flat slope, while all others show a distinct maximum near the 20 hour retention time. The shapes of the productivity curves match the results obtained by Shelef et al. (1968) for shallow light-limited cultures. The model predicts increased algal productivity at the highest water velocity, indicating that the cultures may not have been light saturated at the lower water velocities. Similarly, for the algal biomass vs retention time plot (Figure 68), the static (0 m/s) case conforms most closely to Pipes prediction of a linear increase in biomass with increasing retention time.

In the second set of simulations, algal productivity as a function of retention time for nitrogen limited cultures indicates that maximum productivity is predicted for the retention time period of 20 to 24 hours (Figure 69). The nitrogen-limited simulations, which were made using a constant influent nitrogen concentration of 5 mg/l, are actually a combination of light and nitrogen limitation because a natural diurnal light profile was used which limited growth for 12 - 20 hours depending on the retention time. This

combination of limitations is responsible for the non-uniform appearance of the algal biomass vs retention time curves (Figure 70).

Simulations of the maximum fish production that could be achieved at each retention time with light-limited algal cultures were produced by increasing the fish loading until the minimum DO value reached 3.0 mg/l (Figure 71). Maximum fish production was predicted to occur at water velocity of 0.0313 m/s and retention time of 20-24 hours. Although greater algal productivity and therefore greater oxygen production rates were predicted for the 0.125 m/s water velocity, greater losses of oxygen due to surface transfer were also predicted for the high mixing velocity. A maximum fish production of 10,000 kg/ha was predicted for the optimum conditions in the PAS of 20 - 24 hour retention time and 0.0313 m/s water velocity for the 0.6 m water depth.
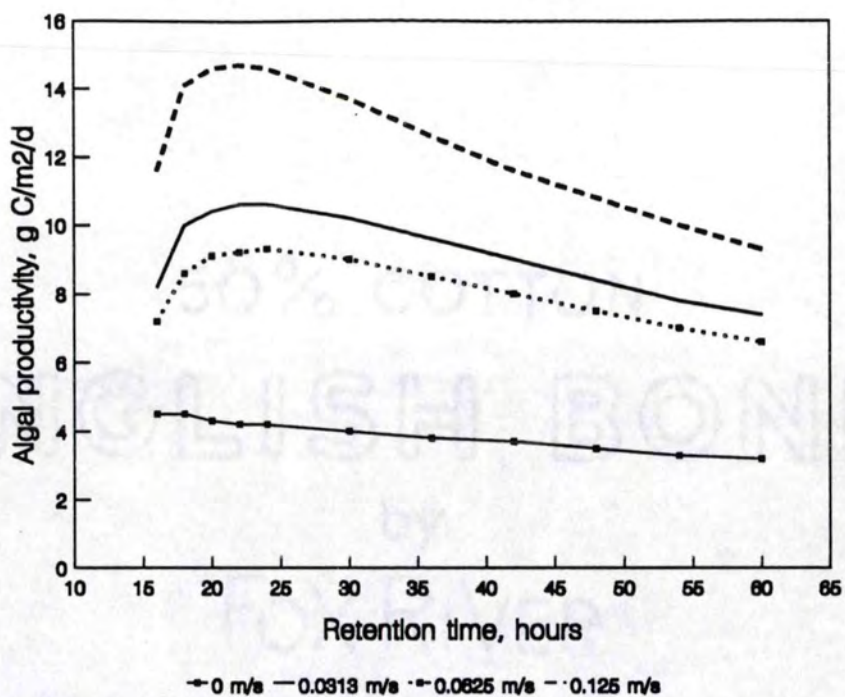
Figure 67. Predicted algal productivity for light-limited cultures.
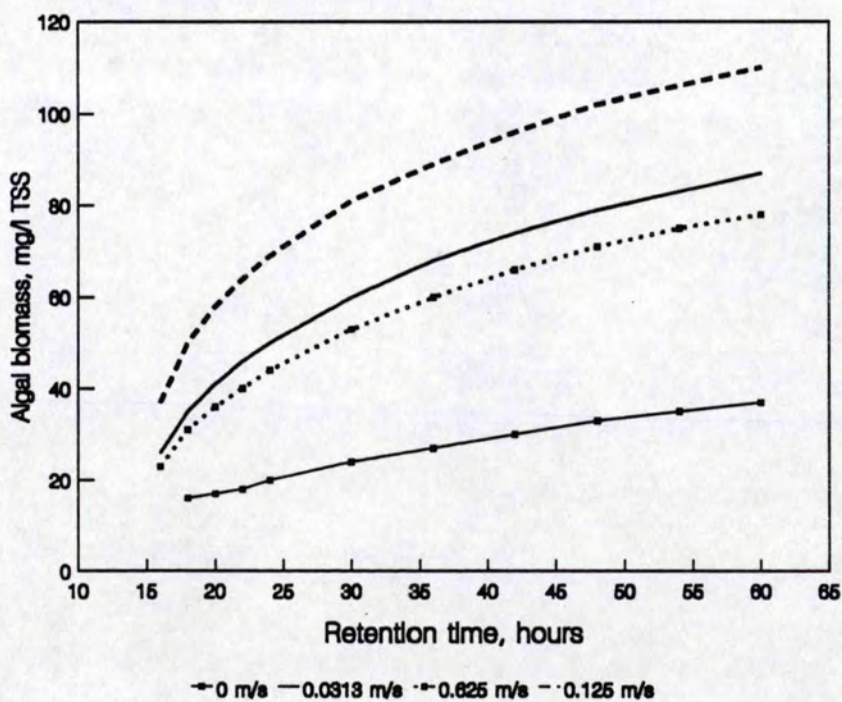

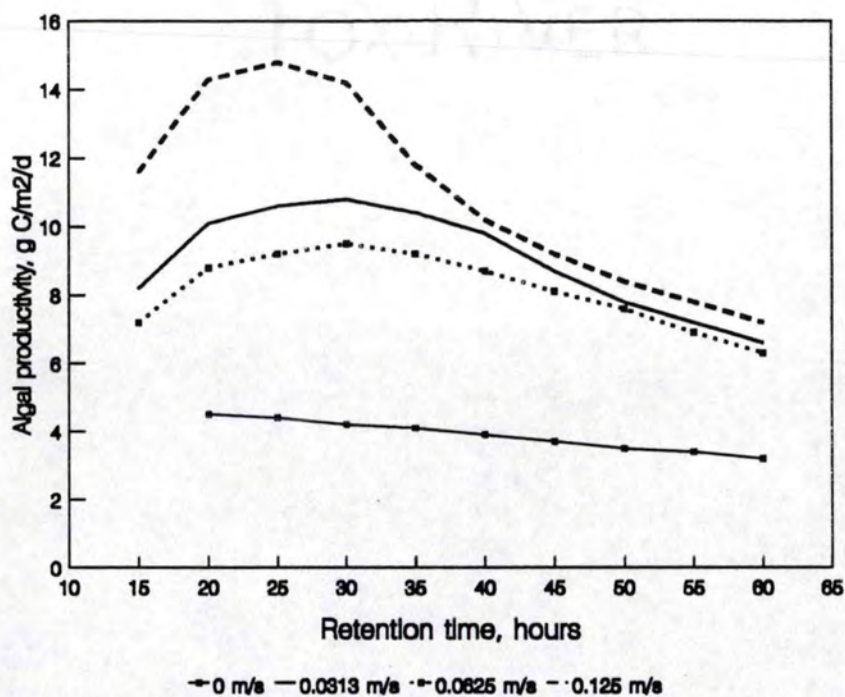Figure 68. Predicted algal biomass for light-limited cultures.

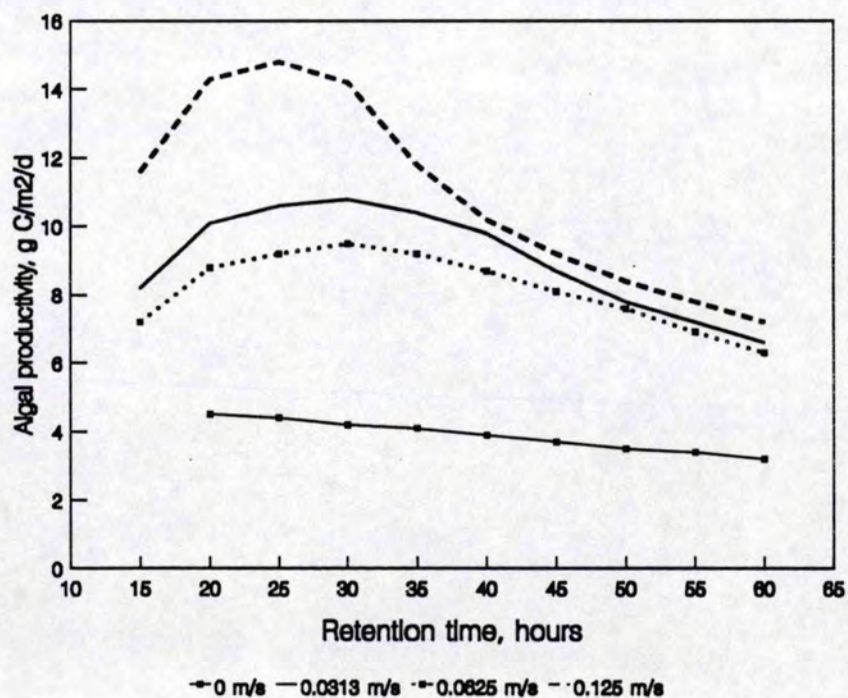Figure 69. Predicted algal productivity for nitrogen-limited cultures.

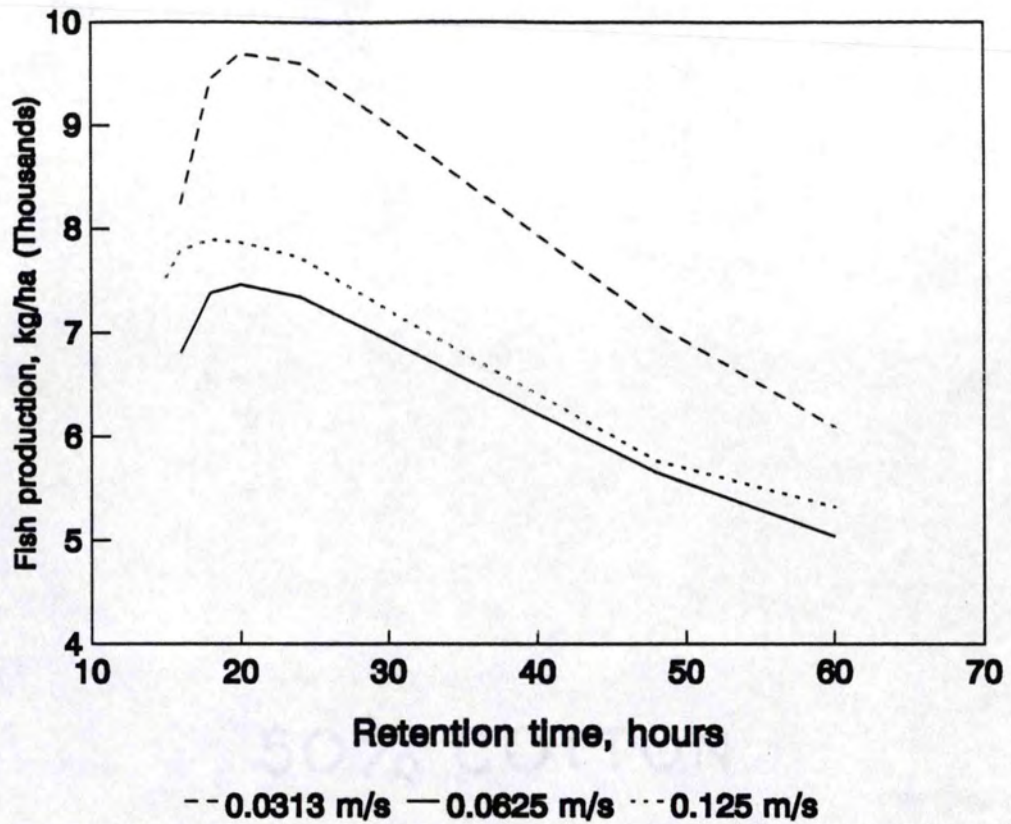Figure 70. Predicted algal biomass for nitrogen-limited cultures.

Figure 71. Predicted fish production for light-limited cultures in the PAS.

CHAPTER X

SUMMARY AND CONCLUSIONS

Summary

This research was undertaken to investigate the potential of using managed algal cultures to increase fish production in pond aquacultural systems by increasing the net oxygen production. Algal growth in conventional pond aquaculture systems exhibits characteristics typical of batch culture. This results in high respiration rates occurring at night when the cultures are in their stationary growth phase, and sudden declines in active algal biomass as the cultures reach the death phase. The impact on the dissolved oxygen (DO) diel response in a pond system is that the low DO values occurring at night during the stationary phase limit the total fish biomass that can be sustained in the pond. In addition, during the die-off phase, a sudden decline in DO concentration results as oxygen is consumed by the oxidation of the decaying algal biomass.

Management of the algal cell retention time can be used to control the algal growth rate. Decreasing the retention time increases the algal growth rate and therefore the oxygen production rate, and decreases the standing algal biomass in the pond which decreases the amount of oxygen consumed by algal respiration. Control of the algal cell retention time would be difficult in a conventional pond system; therefore, the Partitioned Aquaculture System was developed which utilizes separate algal culture and fish culture tanks. Algal cell retention time can be controlled through discharging or harvesting a portion of the culture continuously, by employing a cell separation technique and

returning the water flow back to the culture, or by utilizing filter-feeding organisms to graze the algal biomass. For this research work, algal cell retention time was controlled through discharging a portion of the culture continuously.

Algal biomass, measured as dry weight using 0.45 μm membrane filter technique, was modeled as a function of secchi disk visibility. The commonly-used filtering technique used by past researchers was found to be inadequate to measure the algal biomass because small algal cells were not retained on the filter.

Algal species composition was dependent on the inorganic carbon content of the culture water. The inorganic carbon concentration of the influent water averaged 0.8 mmol/l; therefore, the mass of inorganic carbon added averaged 0.7 mmol/l/d for the water flow rates used. Under these conditions, the genus *Merismopedia*, a member of the division Cyanophyta or blue-green algae, was observed to dominate. When inorganic carbon concentrations were increased to 1.1 - 1.8 mmol/l/d, the predominant algal genera were *Scenedesmus* and *Dictyospherium*, which are members of the division Chlorophyta or green algae. Since blue-green algae have been associated with off-flavor of catfish, inorganic carbon addition could be used to discourage the growth of blue-green algae in catfish culture system.

Inorganic carbon addition also increased algal productivity. The average carbon fixation rate (ACFIX) was 1.2 times greater for the high carbon addition rates (1.1 - 1.8 mmol/l/d) than the low rate (0.7 mmol/l/d). Mean algal biomass (TSS) and ACFIX were 44.8 mg/l TSS and 6.3 g C/m$_2$/d for the high carbon addition rates, respectively.

Algal productivity was 1.2 times greater at 0.34 m water depth than at 0.66 m depth. Mean TSS and ACFIX rates were 105 mg/l and 7.7 gC/m^2/d for the 0.34 m depth and 44 mg/l and 6.3 g C/m^2/d at the 0.66 m water depth.

Algal productivity was 1.5 times greater for the high water velocity (0.125 m/s) than the low water velocities (0.0313 and 0.0625 m/s). Mean algal TSS and ACFIX at the high velocity were 66 mg/l and 9.9 g C/m^2/d, and 48 mg/l and 6.5 g C/m^2/d at the low water velocity.

Algal TSS and ACFIX were greater at the 1.2 day retention time than the 2.5 day retention time, for cultures receiving inorganic carbon from the influent water flow only. Mean TSS and ACFIX were 44 mg/l and 4.1 g C/m^2/d for the 1.2 day retention time and 27 mg/l and 5.4 g C/m^2/d for the 2.5 day retention time. These results suggest carbon-limited conditions during these low inorganic carbon trials, especially in light of the fact that in laboratory studies of light-limited cultures, algal productivity was not found to vary with retention time.

Maximum photosynthetic oxygen production rates at 20°C were found to be 0.11 mg O$_2$/mg TSS/hr for the predominantly blue-green algal cultures and 0.12 mg O$_2$/mg TSS/hr for the predominantly green algal cultures. These values correspond to an maximum growth rate of 0.0887 - 0.0968/hr. The saturating or optimum light level was found to be twice as great for the blue-green algal cultures.

Algal respiration rates were not found to differ significantly as a function of culture conditions. The mean 24-hour respiration rate was found to be 0.00299 mg O$_2$/mg TSS/hr. The difference between the 12-hour day and night respiration rates was found

to be significant. Therefore, algal respiration rates for the PAS were modeled as 0.002 (day) and 0.004 (night) mg O_2/mg TSS/hr.

A dynamic model of algal biomass and productivity in the PAS was constructed to simulate the steady state and non-steady state growth of algae over a 2-day period. Calibration of the model to actual data was achieved by introducing an effective depth factor into the light extinction equation. An effective depth factor equation was formulated to predict the increased exposure of the algal cells to solar radiation at increased mixing levels.

The PAS model closely predicted the DO profiles and algal biomass density for cultures grown under light and nutrient limited conditions, water velocities of 0.0313 - 0.125 m/s, under naturally-occurring solar radiation profiles and water depth of 0.66 m. Predicted DO and algal TSS concentrations for the 0.34 m water depth were less than the observed values. Algal growth in the 0.34 m runs was predicted to be nitrogen limited; however, the measured DO profiles for these runs indicated primarily light limitation. Reducing the nitrogen/algal biomass ratio in the model improved the simulations, indicating that the nitrogen ratio may vary with culture conditions or that the ratio is less than the value predicted by the Redfield et al. (1963) ratio for algal cell composition.

Simulations of the PAS oxygen concentration were made to predict the operating conditions which would optimize algal productivity and dissolved oxygen profiles to increase the potential fish carrying capacity. For light-limited cultures (inorganic carbon and nitrogen supplied in excess) at 0.6 m water depth, maximum algal productivity was predicted for water velocity of 0.125 m/s and retention time of 20 - 24 hours. Algal biomass, and therefore algal respiration, was predicted to decrease with decreasing

detention time. However, the maximum fish production was predicted for a water velocity of 0.0313 m/s and retention time of 20 - 24 hours. This is the result of the greater loss of oxygen from the culture water due to surface oxygen transfer at increased water velocity when the DO concentration is supersaturated. Fish carrying capacity of 10,000 kg/ha was predicted for the 0.6 m water depth at 0.125 m/s water velocity, at 20-24 hour retention time.

Conclusions

The conclusions that can be drawn from this study are as follows:

1. A model developed to predict total daily solar radiation from weather data was superior to the existing weather models investigated for the data set analyzed.

2. The glass fiber filter technique for algal biomass determination may not retain up to 50% of the algal biomass present. The use of 0.45 μm filters will ensure better representation of the algal biomass.

3. At a low (0.8 mmol/l) concentration of naturally-occurring inorganic carbon in the supply water, addition of inorganic carbon shifted the predominant algal genera from Cyanophyta (blue-green) to Chlorophyta (green).

4. Algal productivity was increased (5.4 to 6.3 g $C/m^2/d$) by increasing inorganic carbon addition from 0.7 to 1.1 - 1.8 mmol/l/d. Productivity increased (6.3 to 7.7 g $C/m^2/d$) by decreasing water depth from 0.66 to 0.34 m. Algal productivity increased (6.5 to 9.9 g $C/m^2/d$) when water velocity was increased from 0.0313 - 0.0625 m/s to 0.125 m/s. Finally, productivity decreased (4.1 to 5.4 g $C/m^2/d$) when cell retention time was increased from 1.2 to 2.5 days.

5. Oxygen production rates as a function of effective light could be modeled using the inhibitory light model $P_{20} = P_{max20} (I/I_{opt}) e^{(1-(I/I_{opt}))}$.

6. Based on oxygen production rates, a maximum growth rate at 20°C of 0.0968 hr^{-1} was achieved.

7. The mean 24-hour algal respiration rate for the pooled 1991 and 1992 data was 0.003 mg O_2/mg TSS/hr. Based on the difference between the day and night respiration rates, algal respiration was modeled as 0.002 (day) and 0.004 (night) mg O_2/mg TSS/hr.

8. A model developed in this work can be used to predict the steady state and non-steady state diel response of algal productivity and dissolved oxygen concentration as a function of the environmental parameters of light and temperature (in the range of 15-35°C) and the operational parameters of inorganic carbon and nitrogen concentration, water velocity and cell retention time within the ranges tested.

9. At the 0.6 m water depth, projected maximum fish carrying capacity of 10,000 kg/ha was predicted for a 20 - 24 hour retention time and 0.0313 m/s water velocity. Maximum algal productivity for 0.6 m depth was predicted for the 0.125 m/s water velocity and 20 - 24 hour retention time.

APPENDICES

Appendix A

Titration Technique for DO > 20 mg/l

Sodium sulfite reacts with oxygen dissolved in water to form sulfate. Theoretically, 7.88 mg of sodium sulfite are required to react with 1 mg of oxygen. For example, if it is desired to lower the DO of a 300 ml water sample by 10 mg/l, 1 ml of a 23.6 g/l sodium sulfite solution would be needed. Cobalt is needed at a concentration of 0.1 to 0.5 mg/l to catalyze this reaction (ASCE, 1984). The procedure used is given below:

1. Prepare a sodium sulfite solution in the range of 12 to 24 g/l, depending on the expected DO values to be measured. Technical grade sodium sulfite (Ashland Chemical, Inc., Houston TX) was used. One ml of 11.8 g/l solution or 23.6 g/l solution added to a 300 ml sample should lower the DO by 5 mg/l or 10 mg/l respectively.

2. Prepare a 120 mg/l $CoCl_2 \cdot 6H_2O$ solution using reagent grade chemical.

3. Calibrate the sodium sulfite solution. Fill a minimum of three 300 ml BOD bottles with influent water and measure the initial DO. Add 1 ml of the cobalt chloride solution followed by 1 ml of the sodium sulfite solution. Stopper the bottles carefully to avoid trapping air bubbles, invert several times to mix, and wait at least 30 seconds for reaction to occur. Measure the final DO in each bottle and calculate the change in DO. Average the values to determine the oxygen equivalence per ml of sulfite solution. Recalibrate the solution every 3 to 4 hours.

4. For samples with DO level greater than 20 mg/l, add 1 ml each of the cobalt chloride and sodium sulfite solutions, stopper, invert and wait 30 seconds as described in step 3. Insert the DO probe into the bottle and record the DO value, if less than 20 mg/l, for each replicate. Average the values and then add the oxygen equivalence of the sulfite solution added. If the DO is still greater than 20 mg/l, add another ml of sulfite solution, mix and read sample again.

Appendix B

Residuals Analysis for Solar Radiation Models

Residuals analysis is a technique used to determine the appropriateness of a certain model to represent a data set. The studentized residual, e_i^*, is calculated as the difference between the actual and predicted value, divided by the standard error of the residual. The expected value of e_i^* is zero; therefore, a plot of the studentized residuals vs one of the independent variables in the model should appear randomly distributed around zero if the model is correctly specified. A plot of e_i^* vs the dependent variable should also appear randomly distributed around zero. A discernable trend in this plot indicates that a variable or interaction between variables may be missing from the model.

Figure B-1 shows a plot of the studentized residuals vs EVAP (evaporation, cm) for the Jenson-Haise model. A clear downward trend is evident indicating that this model is not adequate to represent the solar radiation data set.

A plot of e_i^* vs DAIRT (maximum and minimum dry-bulb air temperature difference, °C) for the linear model reveals that the residuals appear randomly distributed, indicating that the model is correctly specified (Figure B-2). However, the plot of e_i^* vs solar radiation (Figure B-3) shows a slight upward trend indicating that some variable may be missing from the model.

Similarly, the residuals obtained from the hyperbolic model show that the e_i^* appear randomly distributed around zero when plotted against the variable SQDAIRT (the square of DAIRT), indicating a good fit of the model (Figure B-4). A slight upward trend

is detectable in the plot of e_i^* vs solar radiation, which may indicate that a variable is still missing from the model (Figure B-5).
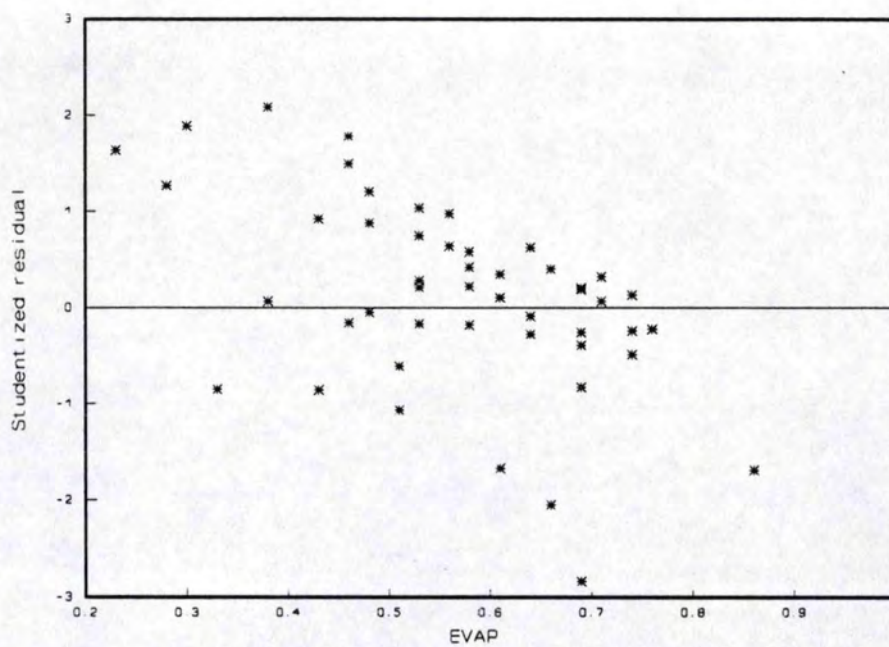

Figure B-1. Studentized residuals vs EVAP (evaporation, cm) for Jenson-Haise model.
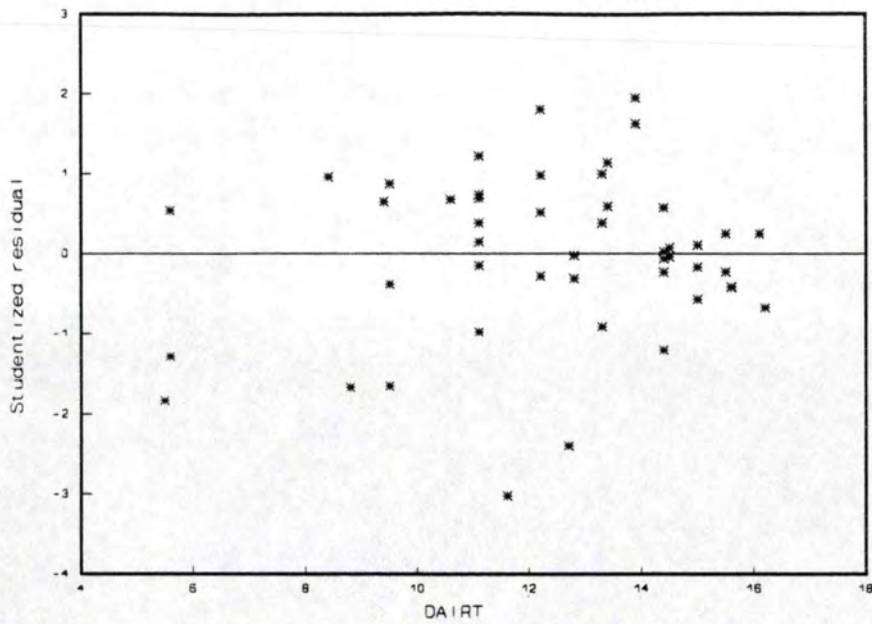
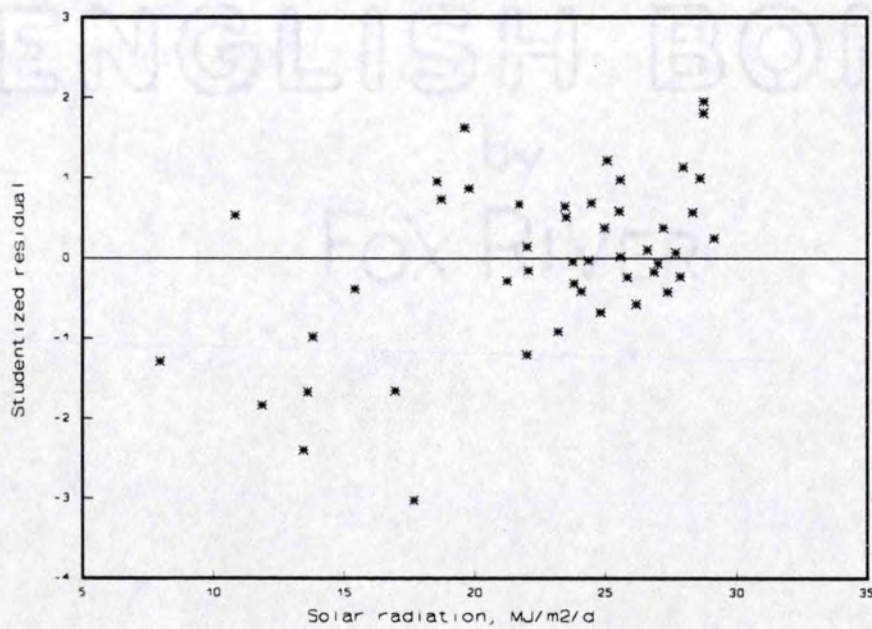Figure B-2. Studentized residuals vs DAIRT (difference in air temperature, °C) for linear model.

Figure B-3. Studentized residuals vs solar radiation for linear model.
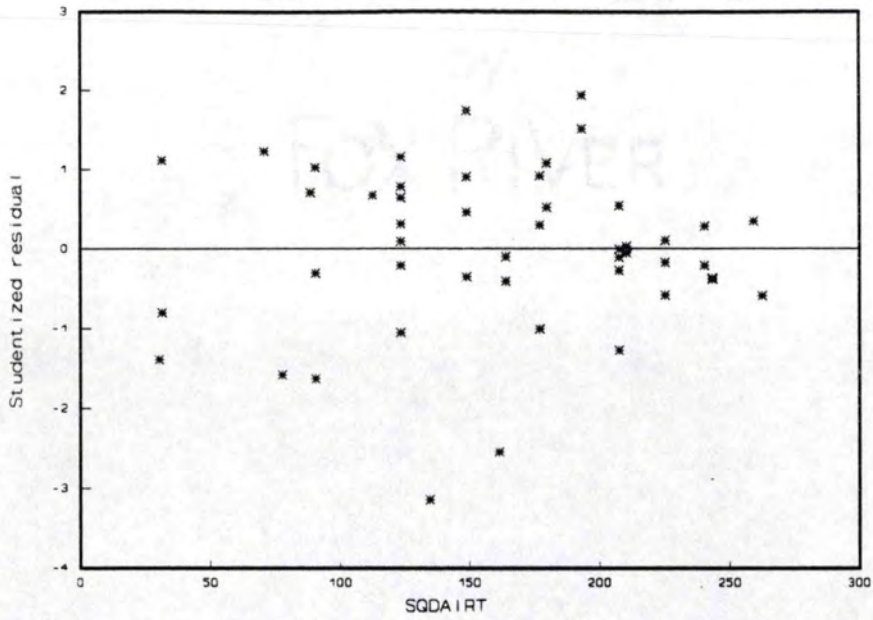
Figure B-4. Studentized residuals vs SQDAIRT (square of difference in air temperature) for hyperbolic model.
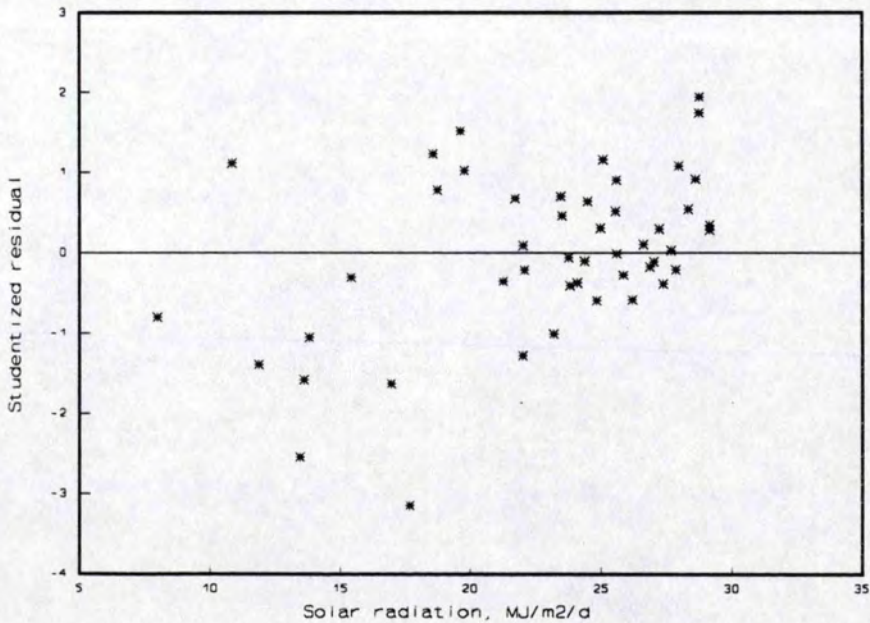

Figure B-5. Studentized residuals vs solar radiation for hyperbolic model.

Appendix C

Scatter Plots Used in Solar Radiation Model Development

Plots of solar radiation (R_s) vs the variables DAIRT (daily rise in dry-bulb air temperature °C), SUNMIN (sunshine duration in minutes), PERCENT (percent of possible sunshine), RHTMAX2 (inverse of relative humidity at the maximum air temperature), RHTAVE2 (inverse of relative humidity at the average air temperature) and SQDAIRT (square of DAIRT) are given below. Linear relationships are evident in the plots of R_s vs DAIRT, SUNMIN, PERCENT, RHTMAX2 and RHTAVE2 (Figures C-1 through C-5). A slight non-linear trend was evident in the plot of R_s vs SQDAIRT (Figure C-6).
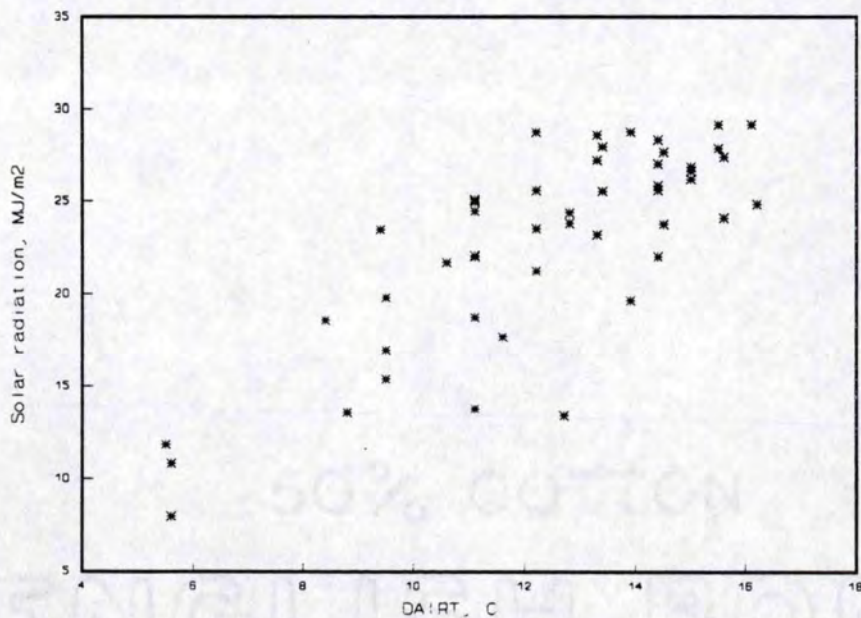
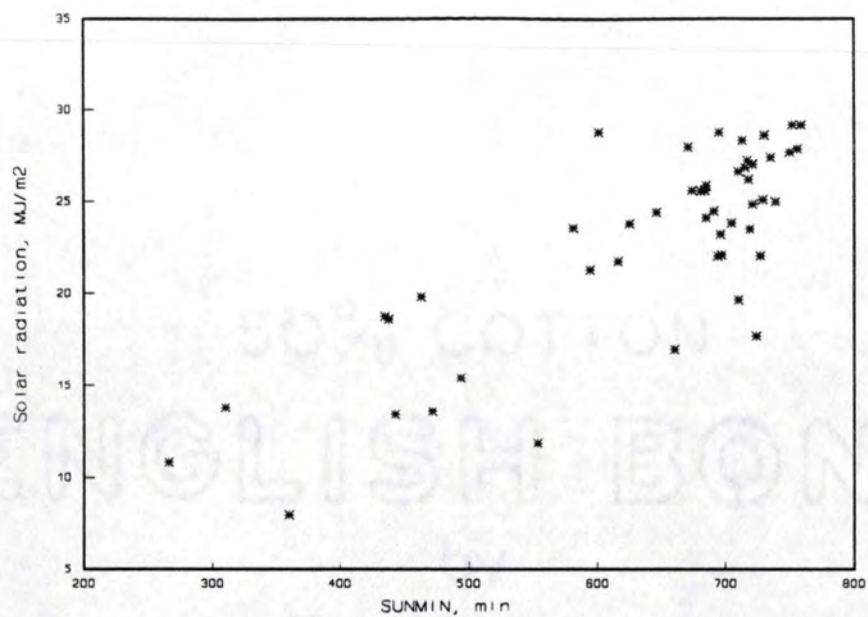

Figure C-1. Solar radiation vs DAIRT.
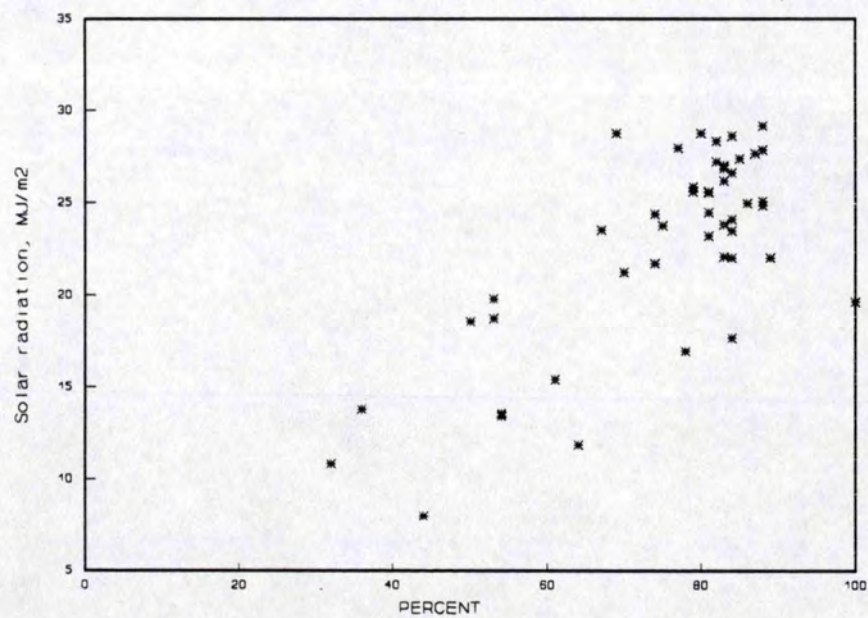
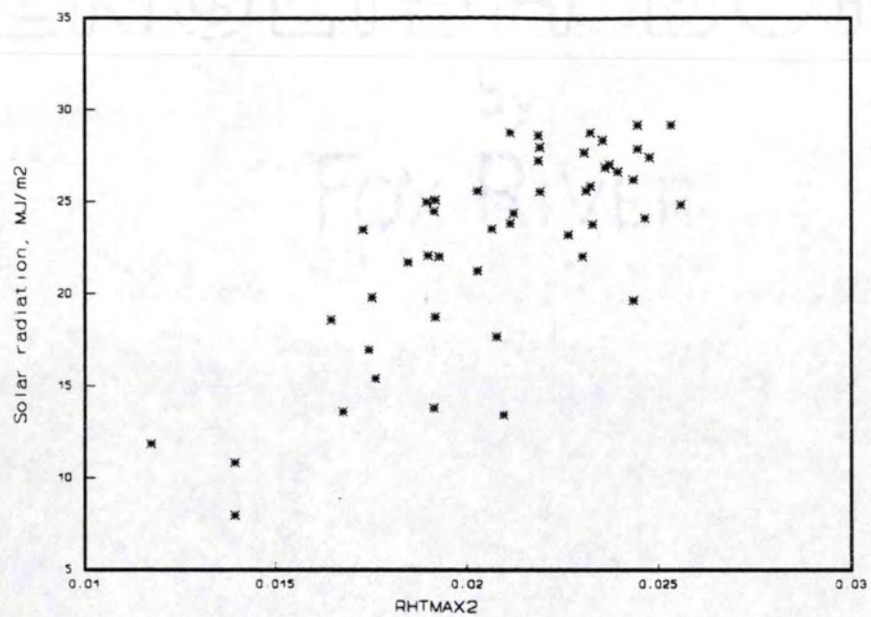Figure C-2. Solar radiation vs SUNMIN.

Figure C-3. Solar radiation vs PERCENT.

Figure C-4. Solar radiation vs RHTMAX2.

Figure C-5. Solar radiation vs RHTAVE2.
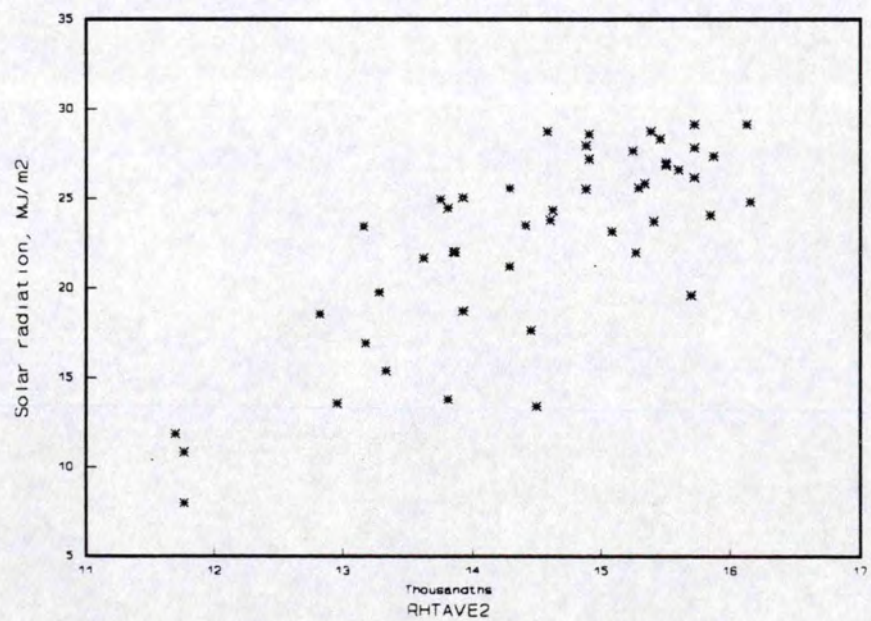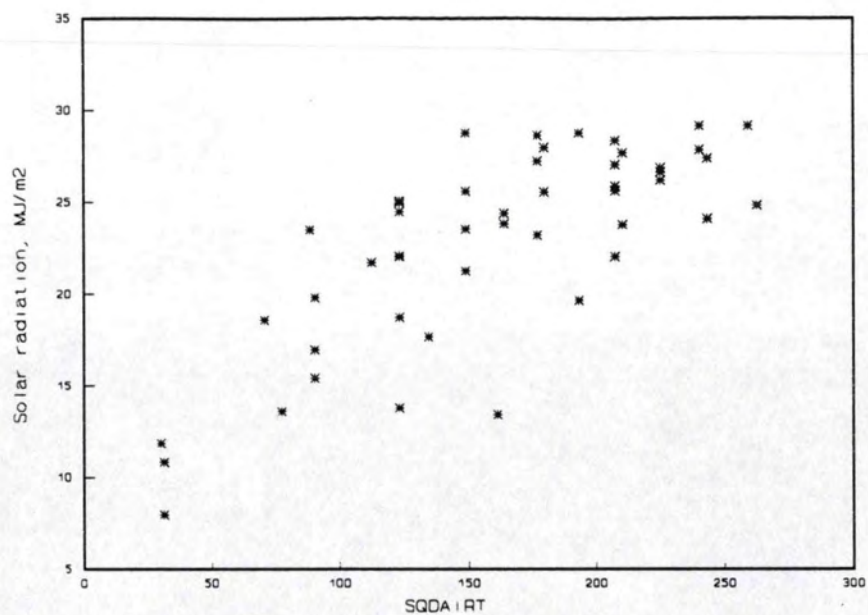
Figure C-6. Solar radiation vs SQDAIRT.

Appendix D

Carbonate Equilibria Equations

The concentration of total inorganic carbon and the equilibrium concentration of species present in a closed aqueous carbonate system can be calculated using pH and alkalinity data using the following equations (Stumm and Morgan, 1981).

$$\alpha_o = (1 + \frac{K_1}{[H^+]} + \frac{K_1 * K_2}{[H^+]^2})^{-1} \tag{D-1}$$

$$\alpha_1 = (\frac{[H^+]}{K_1} + 1 + \frac{K_2}{[H^+]})^{-1} \tag{D-2}$$

$$\alpha_2 = (\frac{[H^+]^2}{K_1 * K_2} + \frac{[H^+]}{K_2} + 1)^{-1} \tag{D-3}$$

$$C_T = \frac{[ALK] - [OH^-] + [H^+]}{\alpha_1 + 2\alpha_2} \tag{D-4}$$

$$[H_2CO_3^*] = C_T\alpha_o \tag{D-5}$$

$$[HCO_3^-] = C_T\alpha_1 \tag{D-6}$$

$$[CO_3^{2-}] = C_T\alpha_2 \tag{D-7}$$

where

K_1, K_2 = first and second acidity constants for carbonic acid;

[H^+] = hydrogen ion concentration, mol/l;

[ALK] = alkalinity, mol equivalence/l;

[OH^-] = hydroxyl ion concentration, mol/l;

C_T = total carbon concentration, mol/l;

[$H_2CO_3^*$] = total dissolved CO_2 and carbonic acid concentration, mol/l;

[HCO_3^-] = bicarbonate concentration, mol/l; and

[CO_3^{2-}] = carbonate concentration, mol/l.

The values of K_1 and K_2 are $10^{-6.3}$ and $10^{-10.25}$, respectively, at 25 C and 1 atm

pressure. [OH^-] can be calculated from the following equation.

$$[OH^-] = \frac{K_w}{[H^+]}$$
(D-8)

where K_w = ion product of water, equal to 10^{-14} at 25°C.

Appendix E

Computer Hardware and Software Requirements

Model written in Lotus 123 Release 3 for DOS.

DOS Version 5.00.

IBM PC compatible 486 computer with 3 MB extended memory.

16 color monitor recommended.

Appendix F

Model Statements

Cell Inputs

The following input values are entered in cells in Rows 1 - 25 in Columns A - Y of the model.

Oxygen Transfer Information

1. ELEV Elevation, m. [F4]
2. WINDD Wind velocity (day), m/s; needed only if rpm=0. [F6]
3. WINDN Wind velocity (night), m/s; needed only if rpm=0. [F7]
4. RADIUS Circulator blade radius, m. [F8]
5. RPMD Circulator rotational speed (day), rpm. [F9]
6. RPMN Circulator rotational speed (night), rpm. [F10]

Description of Algal Culture System

1. TAU Detention time, hrs. [L2]
2. DEPTH Water depth, m. [L3]
3. AREA Tank area, m^2. [L4]
4. DOI DO concentration in influent, mg/l. [L5]

Algal Respiration Rates

1. ARD Respiration (day), mg DO/mg TSS/hr. [L10]
2. ARN Respiration (night), mg DO/mg TSS/hr. [L11]

Algal Growth Parameters

1. UMAX Maximum gowth rate @ 20°C, /hr. [L14]
2. KSN Ks value for N, mg/l. [L15]
3. KSC Ks value for C, mg/l. [L16]
4. PMAX Maximum photosynthetic rate, mg DO/mg TSS/hr. [L17]
5. IOPT Optimum light level, W/m^2. [L18]
6. ALGAE Algal species code; 1=green algae, 0=bluegreen algae. [L19]

Fish Loading

1. FISHLOAD Fish loading, kg/ha. [R2]
2. FISHWT Fish weight, g. [R3]

Nutrient Inputs

1. NFISH Nitrogen excreted from fish, g N/kg fish/hr. [S12]
2. NADDED N addition rate, mg/min. [S14]
3. ALGALN N content in algal cells, mgN/mgTSS. [S16]
4. CADDED NaHCO$_3$ added per tank, kg/day. [S17]
5. CWATER Inorganic carbon concentration in supply water, mg/l. [S18]
6. ALGALC C content in algal cells, mgC/mgTSS. [S20]

The following calculations are performed in the model input section.

Oxygen Transfer Information

1. EF Elevation factor. [F4]
   EF={100-(0.0115*EL)}/100
2. WVD Water velocity (day), m/s. [F11]
   WVD=RPMD*2*pi*RADIUS/60*0.6224
3. WVN Water velocity (night), m/s. [F12]
   WVN=RPMN*2*pi*RADIUS/60*0.6224

Calculated Oxygen Transfer, K @ 20°C

1. K20WD K20 due to wind (day), m/hr. [F16]
   IF RPMD=0,
       THEN K20WD=0.0036(8.43*WINDD$^{0.5}$-3.67*WINDD+0.43*WINDD^2
       ELSE K20WD=0
2. K20WN K20 due to wind (night), m/hr. [F17]
   IF RPMN=0,
       THEN K20N=0.0036(8.43*WINDN$^{0.5}$-3.67*WINDN+0.43*WINDN^2,
       ELSE K20WN=0
3. K20D K20 due to water velocity (day), m/hr. [F18]
   K20D=WVD*0.9003
4. K20N K20 due to water velocity (night), m/hr. [F19]
   K20N=WVN*0.9003

Description of Algal Culture System

1. FLOW Required water flow rate for set TAU, lpm. [L5]
   FLOW=VOL/(60*TAU)

2. VOL Tank volume, l. [L6]
VOL=1000*AREA*DEPTH

Calculation of Effective Depth

1. EFFDEPTH Effective depth. [L20]
IF ALGAE=0, THEN EFFDEPTH=0.52
ELSE IF 0.0313<WVD<=0.0625,
THEN EFFDEPTH=1.60*WVD+0.51
ELSE EFFDEPTH=-2.56*WVD+0.77

Fish Loading

1. FEEDRATE Feed rate, g feed/g fish/d. [R4]
If FISHWT<27, THEN FEEDRATE=0.035,
ELSE IF FISHWT>450,
THEN FEEDRATE=0.0175,
ELSE FEEDRATE=0.035-3.889×10^{-5}*FISHWT

Oxygen Demand due to Fish

1. rFRD Rate of fish respiration (day),mg/l/hr @26°C. [S7]
RFRD=(1.761*FISHWT^(-0.2108))*FISHLOAD/(10,000*DEPTH)
2. FRN Rate of fish respiration (night), mg/l/hr @26@°C. [S8]
RFRN=(1.263*FISHWT^(-0.2294))*FISHLOAD/(10,000*DEPTH)
3. rWOD Rate of fish waste oxygen demand, mg/l/hr. [S9]
RWOD=0.83*FEEDRATE*1000*FISHLOAD/(10,000*24*DEPTH)

Nutrient Load

1. r_{NE} Rate of nitrogen excretion by fish, mg/l/hr. [S13]
r_{NE}=NFISH*FISHLOAD/(10,000*DEPTH)
2. NIN Total nitrogen in influent flow, mg/l. [S15]
NIN=[(r_{NE}*VOL/60)+NADDED]/FLOW
3. CIN Total carbon in influent flow, mg/l. [S19]
CIN=CWATER+(CADDED*10^6*12/84)/(1440*FLOW)

Daily Oxygen Balance

1. ARESP, Algal respiration, g O_2/d. [X2]
AVG(AA103..AA199)*VOL*24/1000
2. FOD, Fish oxygen demand, g O_2/d. [X3]
[RWOD+(RFRD+RFRN)/2]*VOL*24/1000
3. Surface reaeration, g O_2/d. [X4]
AVG(H103..H199)*VOL*24/1000

4. DOPROD, Algal DO production, g O_2/d. [X5]
    AVG(Y103..Y199)*VOL*24/1000
5. DOE, DO in effluent, g O_2/d. [X6]
    (AVEDO*VOL*24)/(1000*TAU)
6. DOINF, DO in influent, g O_2/d. [X7]
    (DOI*VOL*24)/(1000*TAU)
7. Net DO production, g O_2/d. [X8]
    (DOPROD+DOINF-ARESP-FOD+REAER-DOE)

Daily Summary

1. DOMIN, DO minimum, mg/l. [X11]
    MIN(V103..V199)
2. DOMAX, DO maximum, mg/l. [X12]
    MAX(V103..V199)
3. DOAVE, DO average, mg/l. [X13]
    AVE(V103..V199)
4. TSSMIN, Minimum TSS, mg/l. [X14]
    MIN(W103..W199)
5. TSSMAX, Maximum TSS, mg/l. [X15]
    MAX(W103..W199)
6. TSSAVE, Average TSS, mg/l. [X16]
    AVE(W103..W199)
7. CFIX, Carbon fixation rate, g C/m^2/d. [X17]
    (TSSAVE*DEPTH*24)/(2.79*TAU)
8. SSGR, Steady state growth rate, /hr. [Y19]
    (1/TAU)
9. DGR, Diel-averaged growth rate, /hr. [Y20]
    (AVG(U92..U187)
10. Adjust initial algal TSS? [Y21]
    IF SSGR=DGR
        THEN 'NO, AT STEADY STATE'
        ELSE IF SSGR>DGR
            THEN 'YES, DECREASE'
            ELSE 'YES, INCREASE'

Range Inputs

1. Water temp, °C. [D31..D199)
2. Actual DO, mg/l if available. [C31..C199]
3. Surface solar radiation, W/m2 (full spectrum values). [I31..I199]

<u>Range Calculations</u>

1. Range [A] HOUR
2. Range [B] Day/night code
   @IF(($A31>=8#AND#$A31<20)#OR#($A31>=32#AND#$A31<44)#OR#
   ($A31>=56#AND#$A31<68),1,0)
3. Range [C] Actual DO, mg/l.
4. Range [D] Water temperature, °C.
5. Range [E] Water temperature, K
   ($D31+273.15)
6. Range [F] Oxygen transfer coefficient, m/hr.
   @IF($B31=1,($K20WD+$K20D)*(1.024^($D31-20)),
   ($K20WN+$K20N)*(1.024^($D31-20)))
7. Range [G] Calculated Cs, saturation oxygen concentration, mg/l.
   @EXP(-139.344+(157570/$E31)-(66423080/$E31^2)+
   (12438000000/$E31^3)-(862194900000/$E31^4))*$EF
8. Range [H] rOT Rate of oxygen transfer, mg/l/hr.
   ($G31-$V31)*$F31/$DEPTH
9. Range [I] Surface solar radiation, W/m2
10. Range [J] Effective light, W/m2
    @IF($I31>0,$I31*@EXP(-(1.7/$X31)*$EFFDEPTH*$DEPTH),0)
11. Range [K] DO produced @20°C, mg DO/mgTSS/hr.
    ($PMAX/$IOPT)*($J30*@EXP(1-($J30/$IOPT)))
12. Range [L] DO produced @T,°C.
    (@EXP(($D31-20)*0.7707/10))*$K31
13. Range [M] Light-limited growth rate @ T, /hr.
    (L31/1.24)
14. Range [N] Total inorganic carbon, mg/l.
    ($CIN/$TAU)*12 for [N31]
    @IF((N31+(A32-A31)*(($CIN-N31)/$TAU-P31))>0,
    (N31+(A32-A31)*(($CIN-N31)/$TAU-P31)),0)
15. Range [O] Carbon-limited growth rate @T, /hr.
    ($Q31*$N31)/($KSC+$N31)
16. Range [P] rCU Rate of carbon uptake, mg/l/hr.
    ($U31*$W31*$ALGALC)
17. Range [Q] $\mu_{max,T}$, /hr.
    $UMAX*@EXP(($D31-20)*0.7707/10)
18. Range [R] Nitrogen, mg/l.
    ($NIN/$TAU)*12 for [R31]
    @IF((R31+(A32-A31)*(($NIN-R31)/$TAU-T31))>0,
    (R31+(A32-A31)*(($NIN-R31)/$TAU-T31)),0)
19. Range [S] Nitrogen-limited growth rate @T, /hr.
    (Q31*R31/($KSN+R31))
20. Range [T] rNU Rate of nitrogen uptake, mg/l/hr.
    ($U31*$W31*$ALGALN)

21. Range [U] Minimum μ, /hr.
    MIN($M31,$O31,$S31)
22. Range [V] Predicted DO, mg/l.
    $DOMIN for [V31]
    @IF($B31=1,
    (V31+(A32-A31)*(($DOI-V31)/$TAU+H31+Y31-AA31-$RFRD-$RWOD)),
    (V31+(A32-A31)*(($DOI-V31)/$TAU+H31+Y31-AA31-$RFRN-$RWOD)))
23. Range [W] Algal TSS, mg/l.
    Initial value for [W31]
    (W31+(A32-A31)*(W31*(U31-(1/$TAU))))
24. Range [X] Predicted SDV, m.
    @IF(W31<11.66,1.5,@IF(W31>=309,0.0001,
    @LN((W31-11.659)/297.33)/-8.2212))
25. Range [Y] Carbon fixation rate, gC/m²/d.
    ($W31*$U31*1.24)
26. Range [Z] DO produced, mg/l/hr.
    (W31*$U31*24*$DEPTH/2.79)
27. Range [AA] Algal respiration, mg/l/hr.
    @IF($B31=1,$ARD*W31,$ARN*W31)

Appendix G

Product References

American Optical
Buffalo NY 14215

AREA (Aquaculture Research/Environmental Associates, Inc)
PO Box 1303, Homestead FL 33090
305-248-4205

Ashland Chemical, Inc.
Houston TX
1-800-437-3378

Aquatic Eco-Systems, Inc.
P.O. Box 1446, Apopka, FL 32704-1446

Cole-Parmer Instrument Company
7425 North Oak Park Avenue, Chicago IL 60648
1-800-323-4340

Dayton Electric Manufacturing Co.
5959 West Howard Street
Chicago, IL 60648

Engineered Systems & Designs
119A Sandy Drive, Newark DE 19713
302-456-0446

Fisher Scientific International
50 Fadem Road, Springfield NJ 07081
201-467-6400

FMC Corporation
Alkali Chemical Division
Philadelphia, PA 19103

Grainger, a Division of W.W. Grainger, Inc.
730 Congaree Road, Greenville SC 29607
803-288-0110

Kent Meters, Inc.
P.O. Box 1852, Ocala FL   32678-1852
904-732-4670

Miller Chemical & Fertilizer Corporation
Hanover, PA   17331

Nitram, Inc.
Tampa FL   33601
1-800-237-6956

Omega Engineering, Inc.
P.O. Box 2669, Stamford CT 06906
1-800-622-2378

Piedmont Plastics
1200 Woodruff Road, Greenville SC 29607
803-288-7201

Reef Industries
P.O. Box 750245, Houston TX   77275-0245
1-800-231-2417

Solar Components Corporation
Manchester, NH   03103
1-800-258-3072

Yellow Springs Instrument Company
Yellow Springs, OH   45387
513-767-7241

LITERATURE CITED

Almazan, G. and Boyd, C.E. 1978 An evaluation of secchi disk visibility for estimating plankton density in fish ponds. Hydrobiologia 61(3):205-208.

Andrews, J.W. and Matsuda, Y. 1975 The influence of various culture conditions on the oxygen consumption of channel catfish. Transactions of the American Fisheries Society 2:322-327.

Banks, R.B. and Herrera, F.F. 1977 Effect of wind and rain on surface reaeration. Journal of Environmental Engineering Division, ASCE 103(EE3):489-503.

Bosca, C., Dauta, A. and Marvalin, O. 1991 Intensive outdoor algal cultures: How mixing enhances the photsynthetic production rate. Bioresource Technology 38(2/3):185-188.

Boyd, C.E. 1991 Empirical modeling of phytoplankton growth and oxygen production in aquaculture ponds. Pages 363-395 *in* D.E. Brune and J.R. Tomasso, editors. Aquaculture and Water Quality. The World Aquaculture Society, Baton Rouge, LA.

Boyd, C.E. 1985 Chemical budgets for channel catfish ponds. Transactions of the American Fisheries Society 114:291-298.

Boyd, C.E. 1979 Water quality in warmwater fish ponds. Auburn University Agricultural Experiment Station, Auburn, AL.

Brune, D.E. 1994 Phytoplankton species succession in eutrophic aquatic ecosystems; Cell detention time as a design and management strategy for aquaculture. Journal of World Aquaculture Society (submitted).

Brune, D.E. 1981 Carbon and light limitation in mass algal culture. Pages 99-126 *in* D.L. Klass, and G.H. Emert, editors. Fuels From Biomass and Wastes. Ann Arbor Science, MI.

Brune, D.E. 1978 The growth kinetics of freshwater algae. Ph.D. dissertation. University of Missouri, Columbus, MO.

Brune, D.E., Drapcho, C.M. and Piedrahita, R. 1992 Pond oxygen dynamics; design and management strategies. Paper No. Aqua92-101. Presented at 1992 International Conference of World Aquaculture Society, Orlando, FL.

Cook, N.J. 1985 Design wind speed data. Pages 202-210. The Designer's Guide to Wind Loading of Building Structures, Part I. Butterworths, London.

Conrad, V. and Pollack, L.W. 1950 Methods in Climatology. Harvard University Press, Cambridge, MA.

Davis, S.A., Drapcho, C.M. and Brune, D.E. Algal populations in outdoor continuous cultures. Journal of World Aquaculture Society (submitted).

Dunlap, J.L. Jr, Young, R.E., and Hale, S.A. 1988 Instrumentation improvements in the Clemson SPAR system. American Society of Agricultural Engineers Paper No. 88-3550, ASAE, St. Joseph, MI.

Goldman, J.C. and Carpenter, E.J. 1975 A kinetic approach to the effect of temperature on algal growth. Limnology and Oceanography 19(5):756-766.

Goldman, J.C. and Ryther, J.H. 1975 Nutrient transformations in mass cultures of marine algae. Journal Environmental Engineering Division, ASCE 101(EE3):351-364.

Jewell, W.J. and McCarty, P.L. 1971 Aerobic decompostion of algae. Environmental Science and Technology 5(10):1023-1031.

King, D.L. 1970 The role of carbon in eutrophication. Journal of Water Pollution Control Technology 42:2035-2051.

Larsen, D.P., Mercier, H.T., and Malueg, K.W. 1973 Modeling algal growth dynamics in Shagawa lake, Minnesota with comments concerning projected restoration of the lake. Pages 15-31. in Modeling the Eutrophication Process. Proceedings of a workshop held at Utah State University, Logan, September, 1973. Published by the Utah Water Research Laboratory, Utah State University, Logan, UT.

Lehman, J.T., Botkin, D.B. and Likens, G.E. 1975 The assumptions and rationales of a computer model of phytoplankton population dynamics. Limnology and Oceanography 20(3):343-364.

Lovell, R.T. 1977 Feeding practices. Pages 50-55. in R.T. Lovell, and R.R. Stickney, editors. Nutrition and feeding practices of channel catfish. Southern Cooperative Series bulletin #218. Alabama Agricultural Experiment Station, Auburn AL.

McCutcheon, S.C. 1989 Water quality modeling, Volume I: Transport and surface exchange in rivers. CRC Press, Inc., Boca Raton, FL.

Parsons, T.R., Takahashi, M. and Hargrave, B. 1984 Biological oceanographic processes. Pergamon Press, New York, NY.

Moriarty, C.M. and Moriarty, D.J.W. 1973 Quantitative estimation of the daily ingestion of phytoplankton by Tilapia nilotica and Haplochromis nigripinnis in Lake George, Uganda. Journal of Zoology, London, 171:15-23.

Newbold, J.D. and Liggett, J.A. 1974 Oxygen depletion model for Cayuga Lake. Journal of the Environmental Engineering Division, ASCE 100(EE1):41-59.

Piedrahita, R.H. 1991 Modeling water quality in aquaculture ecosystems. *in* D.E. Brune and J.R. Tomasso, editors. Aquaculture and water quality. World Aquaculture Society, Baton Rouge, LA.

Redfield, A.C., Ketchum, B.H. and Richards, F.A. 1963 The influence of organisms on the composition of sea-water. Pages 26-77. *in* M.N. Hill, editor. The Sea. Vol 2. New York, NY.

Rosenberg, N.J., Blad, B.L. and Verma, S.B. 1983 Microclimate, the biological environment. John Wiley & Sons, New York, NY.

Schroeder, G.L. 1987 Carbon and nitrogen budgets in manured fish ponds on Israel's coastal plain. Aquaculture, 62:259-279.

Schwab, G.O., Frevert, R.K., Edminster, T.W., and Barnes, K.K. 1981 Soil and water conservation engineering, 3rd edition. John Wiley & Sons, New York, NY.

Schwab, G.O. and Frevert, R.K. 1985 Elementary soil and water engineering, 3rd edition. John Wiley & Sons, New York, NY.

Shelef, G., Oswald, W.J. and Golueke, C.G. 1968 Kinetics of algaly systems in waste treatment: light intensity and nitrogen concentration as growth-limiting factors. Sanitary Engineering Research Laboratory Report No. 68-4.

Shelef, G. Schwartz, M. and Schechter, H. 1973 Prediction of photosynthetic biomass production in accelerated algal-bacterial wastwater treatment systems. Pages 181-189. *in* S.H. Jenkins, editor. Advances in water pollution research. Pergamon Press, Oxford, Great Britain.

Sill, B.L. 1988 Turbulent boundary layer profiles over uniform rough surfaces. Journal of Wind Engineering and Industrial Aerodynamics 31:147-163.

Smith, D.W. and Piedrahita, R.H. 1988 The relation between phytoplankton and dissolved oxygen in fish ponds. Aquaculture 68:249-265.

Standard methods for the examination of water and wastewater. 1989. 17th Edition, American Public Health Association, Washington, DC.

Steele, J.H. 1962 Environmental control of photosynthesis in the sea. Limnology and Oceanography 7:137-150.

Stickney, R.R. editor. 1986 Culture of non-salmonid freshwater fishes. CRC Press, Boca Raton, FL.

Stumm, W. and Morgan, J.J. 1981 Aquatic chemistry, 2nd edition. John Wiley & Sons, New York, NY.

Stumm, W. and Morgan J.J. 1962 Pages 16-26. *in* Stream pollution by algal nutrients. Transactions of the 12th Annual Conference on Sanitary Engineering, University of Kansas, Topeka, KS.

Tucker, C.S. and Lloyd, S.W. 1984 Phytoplankton communities in channel catfish ponds. Hydrobiologia 112:137-141.

Weissman, J.C., Goebel, R.P. and Benemann, J.R. 1988 Photobioreactor design: Mixing, carbon utilization, and oxygen accumulation. Biotechnology and Bioengineering 31:336-344.

Welch, E.B. 1980 Ecological effects of waste water. Cambridge University Press, Cambridge, Great Britain.